ABSTRACT

PACKET DATA COMMUNICATIONS OVER CODED CDMA WITH HYBRID TYPE-II ARQ

by

Seokhyun Yoon

This dissertation presents in-depth investigation of turbo-coded CDMA systems in packet data communication terminology. It is divided into three parts; (1) CDMA with hybrid FEC/ARQ in deterministic environment, (2) CDMA with hybrid FEC/ARQ in random access environment and (3) an implementation issue on turbo decoding.

As a preliminary, the performance of CDMA with hybrid FEC/ARQ is investigated in deterministic environment. It highlights the practically achievable spectral efficiency of CDMA system with turbo codes and the effect of code rates on the performance of systems with MF and LMMSE receivers, respectively. For given ensemble distance spectra of punctured turbo codes, an improved union bound is used to evaluate the error probability of ML turbo decoder with MF receiver and with LMMSE receiver front-end and, then, the corresponding spectral efficiency is computed as a function of system load.

In the second part, a generalized analytical framework is first provided to analyze hybrid type-II ARQ in random access environment. When applying hybrid type-II ARQ, probability of packet success and packet length is generally different from attempt to attempt. Since the conventional analytical model, customarily employed for ALOHA system with pure or hybrid type-I ARQ, cannot be applied for this case, an expanded analytical model is introduced. It can be regarded as a network of queues and Jackson and Burke's theorems can be applied to simplify the analysis. The second part is further divided into two sub topics, i.e. CDMA slotted ALOHA with hybrid type-II ARQ using packet combining and CDMA unslotted ALOHA with hybrid type-II ARQ using code combining. For code combining, the rate compatible punctured turbo (RCPT) codes are examined.

In the third part, noticing that the decoding delay is crucial to the fast ARQ, a parallel MAP algorithm is proposed to reduce the computational decoding delay of turbo codes. It utilizes the forward and backward variables computed in the previous iteration to provide boundary distributions for each sub-block MAP decoder. It has at least two advantages over the existing parallel scheme; No performance degradation and No additional computation.

PACKET DATA COMMUNICATIONS OVER CODED CDMA WITH HYBRID TYPE-II ARQ

by
Seokhyun Yoon

A Dissertation
Submitted to the Faculty of
New Jersey Institute of Technology
In Partial Fulfillment of the Requirements for the Degree of
Doctor of Philosophy in Electrical Engineering

Department of Electrical and Computer Engineering, NJIT

January 2003

APPROVAL PAGE

PACKET DATA COMMUNICATIONS OVER CODED CDMA WITH HYBRID TYPE-II ARQ

Seokhyun Yoon

Dr. Yeheskel Bar-Ness, Dissertation Advisor — Date
Distinguished Professor of Electrical and Computer Engineering, NJIT

Dr. Alexander M. Haimovich, Committee Member — Date
Professor of Electrical and Computer Engineering, NJIT

Dr. Hongya Ge, Committee Member — Date
Associate Professor of Electrical and Computer Engineering, NJIT

Dr. Ali Abdi, Committee Member — Date
Assistant Professor of Electrical and Computer Engineering, NJIT

Dr. Stephan ten Brink, Committee Member — Date
Bell Laboratories, Lucent Technology

BIOGRAPHICAL SKETCH

Author: Seokhyun Yoon

Degree: Doctor of Philosophy

Date: January 2003

Undergraduate and Graduate Education

- Doctor of Philosophy in Electrical Engineering,
  New Jersey Institute of Technology, Newark, NJ, 2003

- Master of Science in Electronics Engineering,
  Sung Kyun Kwan University, Suwon, Korea, 1996

- Bachelor of Science in Electronics Engineering,
  Sung Kyun Kwan University, Suwon, Korea, 1992

Major: Electrical Engineering

Publications (Journal):

S. Yoon and Y. Bar-Ness, "Packet Data Communications over Coded CDMA Part I: Achievable Spectral Efficiency of CDMA Systems with Turbo Codes and Linear Multiuser Detections", submitted to *IEEE Trans. on Wireless Communications.*

S. Yoon and Y. Bar-Ness, "Packet Data Communications over Coded CDMA Part II: Throughput Bound of CDMA Unslotted ALOHA with Hybrid Type-II ARQ using Rate Compatible Punctured Turbo Codes", submitted to *IEEE Trans. on Wireless Communications.*

S. Yoon and Y. Bar-Ness, "Analysis of CDMA Slotted ALOHA with Packet Combining using Queuing Network Model", submitted to *IEEE Comm. Letters.*

S. Yoon and Y. Bar-Ness, "A Parallel MAP Algorithm for Low Latency Turbo Decoding", *IEEE Communications Letters*. Vol. 6 No.7, pp. 288-290, July 2002.

S. Yoon and Y. Bar-Ness, "Performance Analysis of Linear Multiuser Detectors for Randomly Spread CDMA Using Gaussian Approximation" *IEEE Journal on Selected Areas in Communications*, Vol. 20 No.2, pp. 409-418, Feb. 2002.

Publications (Conference Papers):

S. Yoon and Y. Bar-Ness, "Throughput Bound of CDMA Unslotted ALOHA with Hybrid Type-II ARQ using Rate Compatible Punctured Turbo Codes", submitted to ICC'2003.

S. Yoon and Y. Bar-Ness, "Throughput Analysis of Turbo-Coded CDMA Communication Systems", *Proc. of VTC* 2002 Spring pp. 1462-1466, May.6-9, Birmingham, AL.

S. Yoon and Y. Bar-Ness, "Low Latency Turbo Decoding: Blocked Belief Propagation Algorithm", *Proc. of 39th Allerton Conference,* 2001, Oct.3-5, Monticello, IL.

S. Yoon and Y. Bar-Ness, "Linear Multiuser Receivers in Random Spreading with Rake Combining: Turbo Coded System Performance", *Proc. of 36th Asilomar Conference on Signal, System and Computers* 2001, Nov.5-7, Pacific Grove, CA.

S. Yoon and Y. Bar-Ness, "An Approximate performance of Linear Decorrelating Detector for Dynamic CDMA" *Proc. of ISSSTA'00*, Sep.5-8, 2000.

To my family, Yunjeong and Emily (HeeSoo)

ACKNOWLEDGMENT

I wish to express my sincere gratitude to those who have inspired me to imagine, learn and create, including the colleagues and Faculty members in the Center for Communications and Signal Processing Research.

Special thanks to Dr. Haimovich and Dr. Ge, whose lectures were, to some extent, the bases of my research, and to Dr. Fang, who has left the school, for teaching me Queuing theory, which provided valuable input for my dissertation.

To Dr. Abdi and Dr. ten Brink, I would like to thank for serving as members of dissertation committee and for their comments.

Most of all, I owe heartfelt thanks to Dr. Bar-Ness, my advisor, who provided constant supervision, many suggestions and encourage throughout the course of study. It has been a great privilege to work with you these past years. Your every support, in both the substance and spirit, has been invaluable to my study at New Jersey Institute of Technology and has helped, immeasuarably, to guide me through the trials of research.

I also would like to express deep gratitude to Marlene, who have supported me in every respect and, sometime, made corrections for my journal submissions.

TABLE OF CONTENTS

TABLE OF CONTENTS
(Continued)

TABLE OF CONTENTS
(Continued)

LIST OF FIGURES

LIST OF FIGURES
(Continued)

LIST OF FIGURES
(Continued)

Figure **Page**

CHAPTER 1

INTRODUCTION

With the successful application to second generation (2G) wireless telephony [1], CDMA has been employed to most major standards of third generation (3G) wireless multiple access system [2-6] and also become a strongest candidate for future wireless packet communication system. While 2G wireless systems mainly carried voice streams, 3G systems intend to multimedia plus data services [7]. And now demand for data in wireless/mobile environments, which requires more reliability while allows some transmission delay, are growing fast. Although 3G wireless systems provide data service, it is basically connection oriented to efficiently provide multimedia services, such as voice and video. For data services, it is still inconvenient and inefficient since their resource management and allocation are devoted to connection-oriented services. This doubt raises some question regarding CDMA systems as a packet switched data communication systems; i.e. how efficient are they for packet data transmission and what can be done to improve the performance of CDMA systems. These questions motivate in-depth reinvestigation of CDMA systems in terms of packet data communications terminology.

1.1 System Overview and Performance Criterion

In this dissertation, a cellular CDMA system consisting of a single base station and a number of active users is considered. In particular, the author focuses on the performance of uplink transmission, where the users simultaneously send (but not necessarily synchronized to each other) their data to the base-station over a common wireless channel. The analytical approach provided in this dissertation, however, is not limited only to cellular based CDMA system. It can also be applied to other wireless network configurations, such as CDMA based packet radio and Ad hoc networks. Nevertheless,

the performance analysis will be restricted to a traditional cellular CDMA system with only one hop communication, as in 3G Wireless or in IEEE 802.11a.

Figure 1.1 shows a simplified uplink signal path of a coded CDMA system to be analyzed in this dissertation. First, the information bits are encoded with outer error detection code, of which the primary purpose is to detect errors in the receiver side and request a copy if an error detected. Then, it again encoded with forward error correction code, of which the code rate is much lower than that of outer error detection code. The primary purpose of inner FEC code is to provide high coding gain so that the packet error probability after FEC is low enough to obtain reasonable packet throughput. Finally, the coded data packet is modulated with spreading sequences for simultaneous use of a common channel. Attention will be paid on the system performance with various configuration of hybrid FEC/ARQ in deterministic/random access environment.

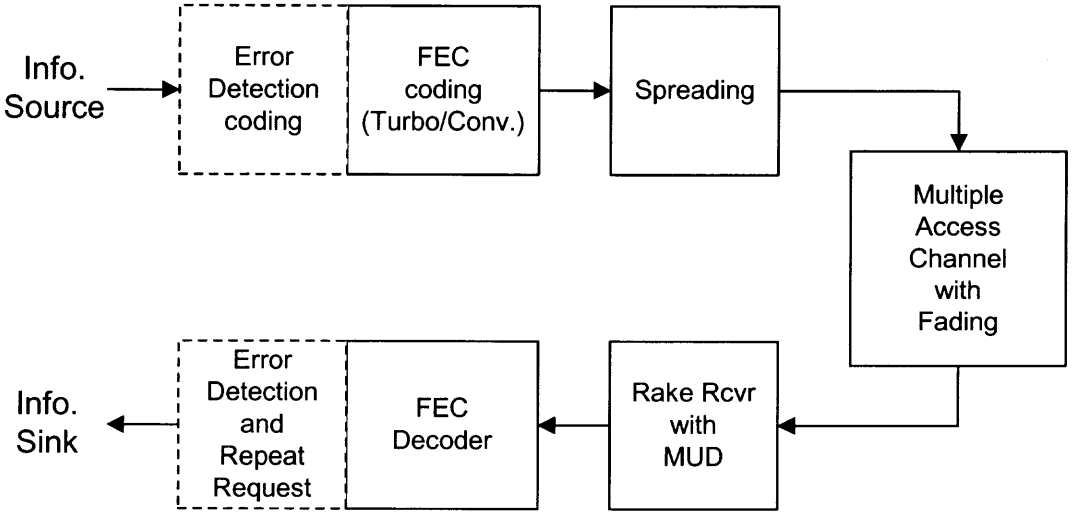

Figure 1.1 A simplified block diagram of Coded DS/CDMA System.

FEC Coding

The reason that CDMA system was so successful for wireless/cellular systems is the anti multipath fading capability of rake receiver and inherent immunity to interference (soft collision) [8, 9]. Moreover, the latter allows cell design with frequency utilization

factor of 1, even though there would be capacity degradation to some extent due to inter-cell interference. When applying to cellular packet radio network, CDMA can provide uncoordinated channel access with relatively small delay [10] and seamless hand-over when a terminal moves to a nearby cell. On the other hand, despite these advantages, it still suffers from inter and intra cell interference, which are generally called multiple access interference (MAI). When considering only single cell scenario, due to this MAI, the net bandwidth utilization of CDMA based random multiple access system has shown to be rather poorer than or, at best, similar to traditional ALOHA systems unless a strong channel coding (of low code rate) is used to suppress the harsh effect of the MAI from other active terminals [11,12]. This is why CDMA system heavily relies on channel coding.

Since the first introduction of turbo code by Berrou *et al.* [13, 14], it has received considerable attention and prompted many related researches, to the extent that it has been accepted by most of the 3G standards as a coding option. Most major 3G wireless standards [2-6] provide several coding options to support various quality and delay demands. Some of typical configurations are convolutional codes, concatenated convolutional-Reed Solomon codes and turbo codes. First two options are suitable for real time applications, such as voice or video, which need certain delay requirement. While, the last option is more suitable for data communications since it shows very good error performance even if the decoding delay can be much larger than the first two. Hence, in this dissertation, only the turbo coding option will be considered.

Hybrid Type-II ARQ

A concern in data communication system is how to control the transmission errors caused by the channel noise so that error free data can be delivered to the users. In wireless communication systems, hybrid FEC/ARQ (Forward Error Correction and Automatic Repeat Request) schemes are usually considered to exploit both the high coding gain of FEC codes and the rate flexibility of ARQ protocol [15]. While a high rate

error detection code is enough for proper operation of ARQ scheme, the primary purpose of FEC code is to achieve high coding gain so that error probability after FEC is low enough for the ARQ scheme to work properly.

The hybrid ARQ schemes are classified into two types; type-I and type-II [16]. In type-I ARQ, the same copy of a packet, which is encoded with a fixed rate FEC coding, is transmitted at each retransmission attempt. While, in type-II the previously received packets are combined together in some way, to accomplish enhanced throughput performance. Two well-known forms of hybrid type-II ARQ are packet combining and code combining scheme [16]. In packet combining scheme, while the packet contents at each attempt are the same as in pure or hybrid type-I ARQ, it effectively combines the soft decision values of these noisy copies so that better probability of packet success can be accomplished as it combines more of noisy copies. On the other hand, Code combining scheme employs a type of incremental redundancy retransmission, which will be described later in more detail. Generally speaking, hybrid type-II ARQ has different probability of packet success and packet service time from attempt to attempt. In this dissertation, the author investigates how much throughput improvement can be achieved hybrid Type II ARQ in a CDMA based random access environment.

CDMA based ALOHA system

Although ALOHA is the simplest random multiple access schemes, it is particularly interesting because CDMA slotted and unslotted ALOHA are the two limiting case of the random access in WCDMA system. In WCDMA, the random access is a type of slotted-offset ALOHA [17,18], where a packet can be transmitted at a periodic time instances. When the time offset is equal to the packet duration, the system resembles slotted ALOHA, while when the offset goes to zero, it corresponds to unslotted ALOHA. Thus, the same procedure as will be described here can also be applied to the analysis of those slotted offset ALOHA systems. Another reason of considering ALOHA system in preference to carrier sense multi access (CSMA) is that ALOHA type random

access is more practical for medium to large coverage area, where carrier sensing is almost impractical especially when large amount of MAI exists. While for small coverage area, which is the main target coverage for WLAN, CSMA is practically feasible and is more attractive than ALOHA type random access scheme.

Performance Criterion: Throughput

A fundamental figure of merit of the packet data communication system would be the throughput performance, while in connection oriented systems, such as circuit based telephone system, the user capacity would be of primary interest. The system throughput can be defined in various ways. In this dissertation, we will use two different types of throughput, each of which is named as Spectral Efficiency and Normalized throughput. As will be discussed later, however, these two are the same measure, even though they are defined in different way. They differ only in that the former is for deterministic environment while the latter for random access environment.

1.2 Dissertation Overview

The dissertation can be roughly divided into three parts as follows

1) CDMA with Hybrid FEC/ARQ in Deterministic environment (Ch.2)
2) CDMA with Hybrid FEC/ARQ in Random Access Environment (Ch.3 and 4)
3) An implementation issue on Turbo Decoding. (Ch.5)

"Deterministic" stands for that the system load does NOT change during a packet transmission time, including both the original and retransmission. This assumption, though impractical, makes the analysis simple while gives insightful results on the system performance. More practical cases for random access environment are then analyzed in the second part using a Queuing Network Model. The second part is further divided into

two sub topics, i.e. CDMA Slotted ALOHA with Hybrid type-II ARQ using Packet Combining and CDMA Unslotted ALOHA with Hybrid type-II ARQ using Code Combining. For code combining, the rate compatible punctured turbo (RCPT) codes are examined.

In the third part, an implementation issue on low latency turbo decoding is considered. Decoding latency may be one of the critical factors in ARQ protocol in the sense that it can be a primary cause of large transmission delay, which in turn affects the window size of Selective-Repeat ARQ. When turbo codes are used, it is especially the case due to the computational complexity of the turbo decoding.

CHAPTER 2

CDMA WITH HYBRID FEC/ARQ IN DETERMINISTIC ENVIRONMENT

As a preliminary, the performance of CDMA with Hybrid FEC/ARQ is investigated in deterministic environment. Especially, it highlights the practically achievable spectral efficiency of CDMA system with turbo codes and multiuser detection, assuming the use of hybrid type-I ARQ. The effect of code rates on the performance of systems is also investigated with matched filter and linear MMSE receivers front-end, respectively. For given ensemble distance spectra of punctured turbo codes, an improved union bound is employed to evaluate the error probability of maximum likelihood turbo decoder and compute the corresponding spectral efficiency as a function of system load.

2.1 System Description and Definitions

Consider a CDMA system consisting of a single base station and K active users who simultaneously send (but not necessarily synchronized to each other) their data packets to the base-station over a common wireless channel. The scenario is similar to the code division packet scheduling [7] in WCDMA system. Each user is assigned a dedicated channel, over which the packet stream is transmitted. With this scenario, the spectral efficiency of uplink transmission is evaluated, assuming the number of users does not change until the entire packet stream is successfully transmitted. Although practical analysis will need a well-defined packet generation model, this scenario can give useful insight into the packet transmission over the dedicated channels in 3G wireless systems and provide a preliminary result for random access scenarios. The analysis for random access environment, where the number of active users may change during a packet period, will be provided in Chapter 3 and 4. A detailed description of modulation/demodulation and encoding/decoding is in Figure 1.1.

A fundamental figure of merit of the system with hybrid ARQ would be the throughput. For simplicity and analytical compactness, the author considers an idealized system in which packet overheads, transmission and decoding delay can be ignored. Throughput degradation due to these factors can be minimized by use of well-designed protocols, such as selective repeat ARQ. The objective here is rather to examine spectral efficiency that can be achieved by given rate of punctured turbo codes in CDMA channel. For the idealized ARQ scheme, the per-user throughput can be expressed as a function of the packet length and the probability of packet failure. Let $r_{inner,eff}$ be the effective code rate of the inner FEC code and r_{outer} the code rate of the outer error detection code. Then, the per-user throughput of CDMA system with hybrid FEC/ARQ can be expressed as

$$t_u = r_{outer} \cdot r_{inner,eff} = r_{outer} \cdot \frac{M}{m_{ave}} \qquad \text{[Bits/symbol]} \tag{2.1}$$

where M is the number of information bits that has been successfully transmitted without errors and m_{ave} is the average number of total bits that actually transmitted, including parities and retransmissions. Since r_{outer} is usually close to one, the rate reduction due to this factor can be ignored. m_{ave} can be related to the probability of packet failure, which in turn depends on the system parameters, such as the number of users, processing gain, effective number of multi-path and so on. Let $P_f^{(j)}$ be the probability of packet failure at j^{th} trial such that the probability of packet success after i transmissions is given by

$$P_s^{(i)} = [1 - P_f^{(i)}] \cdot \prod_{j=1}^{i-1} P_f^{(j)} \tag{2.2}$$

Then, the average number of bits m_{ave} that has to be transmitted to deliver M information bits (without errors) can be expressed as

$$m_{ave} = \sum_{i=1}^{\infty} m^{(i)} \cdot P_s^{(i)} = \sum_{i=1}^{\infty} \left(\sum_{j=1}^{i} l^{(j)} \right) \cdot P_s^{(i)} \tag{2.3}$$

where $m^{(i)}$ is the total number of bits transmitted up to i^{th} trial and $l^{(j)}$ is the number of bits transmitted at j^{th} trial. Consider hybrid type-I ARQ scheme, in which a fixed rate (r_{inner}) FEC code is used and a copy of the packet is retransmitted if any error is detected. In this case, $P_f^{(i)} = P_f$ and $l^{(j)} = l = M/r_{inner}$ $\forall j$, by taking the code rate into consideration, and $m^{(i)} = i \cdot l$. Then, the per-user throughput is reduced to

$$t_u = r_{outer} \cdot \frac{M}{(M / r_{inner})(1 - P_f) \sum_{i=1}^{\infty} i \cdot P_f^{i-1}} = r_{outer} \cdot r_{inner} \cdot (1 - P_f) \tag{2.4}$$

As a measure of the normalized throughput, the spectral efficiency is defined as

$$t = \frac{K \cdot t_u}{N} \tag{2.5}$$

where N is the processing gain and K the number of users in the system. Note that the unit of the spectral efficiency is bits/chip, hence, assuming the bandwidth is roughly equal to the chip rate, bits/chip equals to bits/Hz/sec.

Since in CDMA system $P_f^{(i)}$ depends on the number of active users, one can find the spectral efficiency t as a function of the number of users in the system given the processing gain N. In practical situation, the system load may change during the message exchange in ARQ so that the SNIR at the output of a receiver may also change. However, deferring the analysis for random access environment to Ch.3 and 4, we assume here for analytical simplicity that the system load does not change until a packet is successfully transmitted.

2.2 Analytical Procedure

2.2.1 Decision Statistics with Random Spreading

There are two philosophies in CDMA system; Deterministic CDMA and Random CDMA [19]. Random CDMA uses long codes, of which the period is much larger than the bit interval so that the local cross-correlation between any two spreading codes varies randomly from symbol to symbol. Existing commercialized CDMA systems, such as IS-95, are random-CDMA [1]. One of the reasons of using long codes is to avoid being trapped in a bad situation in which some of active users have high correlation to each other for a long time. In practice, such random interference can be regarded as Gaussian noise, making it more suitable to use channel codes with appropriate interleaver than to use multiuser detection technique [20]. In fact, the communication quality of IS-95 relies heavily on the coding gain to mitigate the effect of the interference, while it uses a simple correlation (matched filter) receiver, which does not have interference suppression capability. On the other hand, deterministic-CDMA employs short codes of which the period is the same as the bit interval. The primary purpose of using short codes is to enable using multiuser detection with reasonable complexity [21-30]. These multiuser detectors utilize the cross-correlation between the spreading codes, to suppress the multiple access interference. By employing short codes, one can use adaptive schemes and/or pilot signals making multiuser detection implementable in less complex hardware.

Although a reasonable assumption requires long codes for conventional correlation receivers and short codes for multiuser receivers, the use of latter does not necessarily imply that the cross-correlation matrix is fixed and deterministic [31, 32]. Even for deterministic CDMA system, the cross-correlation has random nature due to the random assignment of spreading codes, and/or the time variation of channel delay, where one chip delay of a spreading sequence can make the cross-correlation structure quite different. Taking the randomness into account, we will perform our analysis based on the random spreading assumption, regardless whether it results from the use of long code or

from the random assignment of spreading codes or from the random variation of time delays.

With this random spreading assumption, three cases are considered; matched filter receiver in AWGN channel, matched filter receiver – rake combining in L-path Rayleigh fading channel and MMSE receiver in AWGN channel.

Matched Filter Receiver in AWGN Channel: Consider BPSK modulated, asynchronous CDMA system with K active users. Usually, for the analysis of matched filter receiver with random spreading, the standard Gaussian approximation (SGA) [33, 34] is used for simplicity. Here the interference power is obtained by averaging the conditional variance over the time delays and the carrier phase shift. When applying this SGA to perfectly power-controlled CDMA signals in AWGN, the SNIR of a matched filter receiver is given by

$$\gamma_{MF,AWGN} = \frac{1}{\beta^{-1} + (K-1)/3N} \tag{2.6}$$

where β is the signal to background noise ratio for each user and N is the processing gain. One may employ improved Gaussian approximation in [35] for more accurate results, but SGA gives quite accurate results, especially for heavily loaded system, which is our main concern.

Matched Filter/Rake Combiner in Fading Channel: For L-path Rayleigh fading channel, a maximal ratio combiner (MRC) is used with L matched filter receivers (finger) each for a path. Assuming every user have the same number of paths, L, each of which has identical Rayleigh distribution with the same average power, the pdf of the SNIR at the output of a rake finger, $\gamma_{MF,Fading}$, can be expressed as; (See Appendix A)

$$f_{\gamma_{MF,Fading}}(\gamma)=\frac{L}{B}\cdot\left(1+\frac{B(KL+1)}{L}(3N/\Omega+\gamma)^{-1}\right)\cdot e^{-\frac{L}{B}\gamma}\cdot\left(\frac{3N}{3N+\Omega\gamma}\right)^{KL-1} \tag{2.7}$$

Let γ_l denote the SNIR at the output of l^{th} rake finger, then the PDF of MRC output SNIR can be expressed as an L-fold convolution of the PDF of rake finger output SNIR, $f_{\gamma_1}(\gamma)$, i.e.

$$f_{\zeta}(\gamma)=f_{\gamma_1}(\gamma)*f_{\gamma_2}(\gamma)*\cdots*f_{\gamma_L}(\gamma) \tag{2.8}$$

Since (2.8) has no closed form expression, the PDF $f_{\zeta}(\gamma)$ should be evaluated numerically.

Linear MMSE Receiver in AWGN Channel: The SNIR of MMSE receiver is not as simple to analyze as that of matched filter receiver. In [31], an approximate PDF of the output SNIR of linear MMSE receiver has been derived. Unfortunately, this approximation is valid only when the system load is less than half the processing gain. On the other hand, asymptotic average SNIR of MMSE receiver has been derived in [36-38], showing its convergence to a deterministic limit as the number of users and the processing gain go to infinity while their ratio remains fixed. Since asynchronous CDMA is being considered here, the author employs the results of [39], which is an extension of [37] to asynchronous CDMA. The following theorem is the essence of the results in [39].

<Theorem 4.2> *In a symbol asynchronous (but chip synchronous) CDMA system, if the relative delay distribution $G(\tau)$ satisfies the condition $G(\tau) = 1 - G(1-\tau)$ and the observation window is an odd integer $T \geq 1$, symmetric about the symbol to be demodulated, then the asymptotic SNIR, χ of linear MMSE receiver is lower bounded by γ_{MMSE}, which is the unique solution of the equation*

$$\gamma_{MMSE} = \frac{P_1}{\sigma^2 + (K/N)T^{-1}E_{P,\tau}[I(\tau P, P_1, \gamma_{MMSE}) + (T-1)I(P, P_1, \gamma_{MMSE}) + I((1-\tau)P, P_1, \gamma_{MMSE})]} \tag{2.9}$$

$I(P,P_1,\gamma)$ is defined as the effective interference of a user of power P at SNIR γ

$$I(P, P_1, \gamma) = \frac{PP_1}{P_1 + P\gamma}.$$

where σ^2 is the noise power and P_1 is the signal power of the first user (desired user). As stated in [39], for complete asynchronous system, the interference power P from a user is replaced with $P/3$, taking into account the chip and phase asynchronism, which reduces the effective interference power by a factor of 1/3. Assuming uniform time and phase delay distribution, perfect power control and complete asynchronous system, the equation (2.9) reduces to

$$\gamma_{MMSE} = \frac{P}{\sigma^2 + \frac{2K}{3N}\frac{T-1}{T}\left(\frac{P}{1+r_{MMSE}}\right) + \frac{KP}{3NT \cdot r_{MMSE}}\left(1 - \frac{\ln(1+r_{MMSE})}{r_{MMSE}}\right)}$$

Moreover, when the observation window goes to infinity, one can obtain a closed form solution of the above equation, given by

$$\gamma_{MMSE} = \frac{P}{2\sigma^2}(1 - AK/N) - \frac{1}{2} + \sqrt{\frac{P^2}{4\sigma^4}(1 - AK/N)^2 + \frac{P}{2\sigma^2}(1 + AK/N) + \frac{1}{4}} \tag{2.10}$$

where A = 1/3 for asynchronous system and 1 for synchronous system. (2.10) will be used to evaluate the throughput performance and spectral efficiency of the system with linear MMSE receiver, especially for heavily loaded system.

2.2.2 Theoretical System Capacity

Once the output SNIR is given, the theoretical capacity limit can be easily computed. In [36], such capacity limit has been found for unconstrained signal constellation. However, in this dissertation the signal constellation is restricted to BPSK only. Hence, assuming the noise plus interference at the output of a demodulator is Gaussian, the theoretical capacity limit can be computed as

$$C_{K,N} = \begin{cases} K \cdot C_{BICO}(\gamma)/N & \text{for AWGN channel} \\ K \cdot E_{\gamma}[C_{BICO}(\gamma)]/N & \text{for fading channel} \end{cases} \tag{2.11}$$

where the mutual information of binary-input continuous-output channel $C_{BICO}(\gamma)$ is given by [41]

$$C_{BICO}(\gamma) = \frac{1}{2} \cdot \sum_{x=+1,-1} \int_{-\infty}^{\infty} p(y \mid x, \gamma) \cdot \log_2 \left(\frac{2 \cdot p(y \mid x, \gamma)}{p(y \mid +1, \gamma) + p(y \mid -1, \gamma)} \right) \cdot dy \tag{2.12}$$

with

$$p(y \mid x, \gamma) = \exp\left[-\left(y - x\sqrt{\gamma}\right)^2 / 2 \right] / \sqrt{2\pi} \, .$$

2.2.3 Turbo Code Performance and Improved Union Bound

Compared to convolutional codes [42], turbo codes perform very well even at low SNR region [13, 14]. They show the so called 'turbo cliff' near the Shannon limit provided the codeword length is large enough. The better performance of turbo code results from the combination of the recursive systematic encoding and its parallel concatenation with appropriate interleavers. For a low weight input sequence, the parity weight of non-

recursive convolutional code does not change much as the position of ones changes. That is, for example, with a weight one input sequence, wherever the one is located, non-recursive systematic encoder produces the same parity weight. On the other hand, recursive convolutional encoder can generate for low weight input sequences (say weight 1 or 2) parity sequences with quite large weight, which may differ according the position of ones in the input information sequence. In addition to this property, parallel concatenation provides a type of transmit diversity. That is, when one of the parity sequences has low weight, the other, which is produced by a permutated version of the same input sequence, may have large weight making overall weight of the codeword large in probability. These two features make the turbo code work well, especially at low SNR region.

Since the exact analysis is very difficult, the error performance of a code is, in general, evaluated numerically via union bound, which is based on the pair-wise error probability [1]. Let C be a binary linear block code of length N and $|C|$ be the alphabet size of C. Let $\mathbf{x}_j=[x_{j0}, x_{j1},.., x_{j(N-1)}]$ be the j^{th} codeword in C and $\mathbf{y}=[y_0, y_1,.., y_{N-1}]$ be the noise observation. Assuming that $\mathbf{x}_0$, which is conventionally taken to be the all zero sequence, is transmitted and $E_0(\mathbf{x}_j)$ be the event that the received noisy observation is decided to $\mathbf{x}_j$ in favor of $\mathbf{x}_0$. The union bound on the codeword error probability can be expressed as

$$P_{e0} = \Pr\left\{\bigcup_{j\neq 0} E_0(\mathbf{x}_j)\right\} \leq \sum_{j\neq 0} \Pr\{E_0(\mathbf{x}_j)\} \tag{2.13}$$

The evaluation of the pair-wise error event $\Pr\{E_0(\mathbf{x}_j)\}$ in (2.13) is trivial, and so is its right hand side, if the distance spectrum of the code is given. Unfortunately, even though this shows good matches in turbo codes at medium to high SNR region, it leads to computational cutoff in error performance well above the actual cutoff in low SNR region.

Many papers have recently dealt with improved union bounds [43-47], most of which are based on the Gallager's bounding technique in [48] or in [49], and obtained tighter results than the conventional union bounds. Particularly, these bounds predict the turbo cliff quite precisely for low rate turbo codes. Therefore, in this paper, we use one of the improved union bound described in [47] to evaluate the probability of packet failure. In the following, we will briefly overview this improved union bound and extend it to the case of fading channel.

Note that most of the improved union bounds recently re-investigated employ partitioning C into a set of sub-code C_d whose codeword have Hamming weight d. Assuming $\mathbf{x}_0$ has been sent, let $E_0(C_d)$ be the event that the received noisy observation $\mathbf{y}$ is decided as $\mathbf{x}_j$ in C_d instead of $\mathbf{x}_0$. A tighter union bound on the error probability of ML decoder can be obtained using

$$P_{e0} = \Pr\left\{\bigcup_{d=1}^{N} E_0(C_d)\right\} \le \sum_{d=1}^{N} \Pr\{E_0(C_d)\} \tag{2.14}$$

Since the evaluation of $\Pr\{E_0(C_d)\}$ is not as easy as that of the pair-wise error probability, it is suggested to employ a bounding technique. In this dissertation, the author employs the technique devised by Gallager in [48], which will be described in the sequel.

Let $D(\mathbf{y},\mathbf{x}_j)$ be the metric value of the noisy codeword $\mathbf{y}$ for the codeword $\mathbf{x}_j$. Then, for any arbitrary real number t, we get an upper bound on $\Pr\{E_0(C_d)\}$ as

$$\Pr\{E_0(C_d)\} = \Pr\{E_0(C_d), D(\mathbf{y},\mathbf{x}_0) < t\} + \Pr\{E_0(C_d), D(\mathbf{y},\mathbf{x}_0) \ge t\} \tag{2.15.a}$$

$$\le \Pr\{E_0(C_d), D(\mathbf{y},\mathbf{x}_0) < t\} + \Pr\{D(\mathbf{y},\mathbf{x}_0) \ge t\} \tag{2.15.b}$$

$$\le \sum_{j=0}^{K_d-1} \Pr\{E_0(\mathbf{x}_j^d), D(\mathbf{y},\mathbf{x}_0) < t\} + \Pr\{D(\mathbf{y},\mathbf{x}_0) \ge t\} \tag{2.15.c}$$

where K_d is the number of codeword belonging to C_d. Introducing an arbitrary function, $\psi(y)$, a distance measure $D(\mathbf{y},\mathbf{x}_j)$ is defined as

$$D(\mathbf{y},\mathbf{x}_j)=\ln\left(\prod_{n=0}^{N-1}\frac{\psi(y_n)}{p(y_n\mid x_{jn})}\right) \tag{2.16}$$

which is in fact equivalent to weighted Euclidian distance for Gaussian noise channel. The function $\psi(y)$ will be chosen such that the bound in (2.15) becomes as tight as possible. For more compact notation, let us define $p_0(y)=p(y\mid x=0)$ and $p_1(y)=p(y\mid x=1)$. Then, assuming binary antipodal signaling, $p_0(-y)=p_1(y)$. Using Chernoff bound for each term in right hand side of (2.15.c), the followings hold for any real number $r\le 0$ and $s\ge 0$; (See Appendix B.1)

$$\Pr\{D(\mathbf{y},\mathbf{x}_0)\ge t\}\le e^{-st}\cdot[g(s)]^N \tag{2.17.a}$$

$$\sum_{j=0}^{K_d-1}\Pr\{E_0(\mathbf{x}_j^d),D(\mathbf{y},\mathbf{x}_0)<t\}\le K_d\cdot[g(r)]^{N-d}\cdot[h(r,w)]^d\cdot e^{-rt} \tag{2.17.b}$$

where $$g(r)=\int_{-\infty}^{\infty}\psi(y)^r\cdot p_0(y)^{1-r}dy \tag{2.18.a}$$

$$h(r,w)=\int_{-\infty}^{\infty}\psi(y)^r\cdot[p_0^{1-r+w}(y)p_1^{-w}(y)]dy \tag{2.18.b}$$

Substituting (2.17.a) and (2.17.b) into (2.15.c) and minimizing with respect to t, then, after certain manipulation, one can obtain

$$\Pr\{E_0(C_d)\}\le\exp\left(H\left(\frac{s}{s-r}\right)-NE(s,r,w)\right) \tag{2.19}$$

with $$E(s,r,w)=-\frac{s}{s-r}\cdot\left(M(\delta)+\delta\ln h(r,w)+(1-\delta)\ln g(r)\right)+\frac{r}{s-r}\cdot\ln g(s) \tag{2.20}$$

$$H(\lambda)=-\lambda\cdot\ln\lambda-(1-\lambda)\cdot\ln(1-\lambda) \tag{2.21}$$

$$M(\delta) = (\ln K_d)/N$$

where $\delta = d/N$ and the relation $(-r/s)^{r/(s-r)} + (-r/s)^{s/(s-r)} = \exp(H(s/(s-r)))$ was used. The tightest bound of (2.19) is obtained by minimizing with respect to s, r, w and $\psi(y)$. Resorting to calculus of variation, one can obtain (See Appendix B.2) the optimal $\psi(y)$, which minimize (2.19) for given s, r and w of the form,

$$\psi(y) = k \cdot p_0(y)\left(1+\alpha\left(\frac{p_1(y)}{p_0(y)}\right)^{-w}\right)^{\frac{1}{s-r}} \tag{2.22}$$

Since the constant, k, is cancelled out in (2.20), we set $k = 1$ for convenience. It is also shown in Appendix C that, with the expression of $\psi(y)$ of (2.22),

$$g(s) = g(r) + \alpha\, h(r,w)\,. \tag{2.23}$$

which leads to the fact that the constant α can be determined by solving

$$\frac{\int_{-\infty}^{\infty} p_0(y)\cdot\left(1+\alpha(p_1(y)/p_0(y))^{-w}\right)^{1-\rho} dy}{\int_{-\infty}^{\infty} p_0(y)\cdot\left(1+\alpha(p_1(y)/p_0(y))^{-w}\right)^{\rho} dy} = 1-\delta \tag{2.24}$$

in which we set $\rho = s/(s-r)$.

This argument can be easily extended to a fully interleaved fading channel. Let $\varsigma = [\varsigma_0, \varsigma_1, ..., \varsigma_{N-1}]$ be an $N\times 1$ random vector, of which each element is independent and identically distributed with the PDF, $f_\varsigma(\varsigma)$. Assume the perfect knowledge about ς at the receiver so that the detection algorithm can utilize it. Usually, $p(\mathbf{y},\varsigma|\mathbf{x}_j)$ is evaluted,

instead of $p(\mathbf{x}_j|\mathbf{y},\varsigma)$, as the former make things simpler. With $p(\mathbf{y},\varsigma|\mathbf{x}_j)$, the distance metric $D(\mathbf{y},\mathbf{x}_j)$ can be defined as

$$D(\mathbf{y},\mathbf{x}_j) = \ln\left(\prod_{n=0}^{N-1} \frac{\psi(y_n,\varsigma_n)}{p(y_n,\varsigma_n \mid x_{jn})}\right) \tag{2.25}$$

And, as before, the following notations make the expression more compact

$$p_0(y,\varsigma) = p(y,\varsigma \mid x=0) \text{ and } p_1(y,\varsigma) = p(y,\varsigma \mid x=1). \tag{2.26}$$

Using the Chernoff bound on each term in (2.15.c) with (2.25) and (2.26), one can obtain the same bound as those in (2.17.a) and (2.17.b), except that, now, with

$$g(r) = \int_{\varsigma}\int_{-\infty}^{\infty} \psi(y,\varsigma)^r \cdot p_0(y,\varsigma)^{1-r}\, dy d\varsigma \tag{2.27.a}$$

$$h(r,w) = \int_{\varsigma}\int_{-\infty}^{\infty} \psi(y,\varsigma)^r \cdot [p_0^{1-r+w}(y,\varsigma) p_1^{-w}(y,\varsigma)] dy d\varsigma \tag{2.27.b}$$

The rest of the derivation is exactly the same and the improved union bound for fading environment is expressed in the same form as those in (2.19), (2.20) and (2.21), but with $g(r)$ and $h(r,w)$ given by (2.27.a) and (2.27.b), respectively. The function $\psi(y,\varsigma)$ which minimize the bound is given by

$$\psi(y,\varsigma) = k \cdot p_0(y,\varsigma)\left(1+\alpha\left(\frac{p_1(y,\varsigma)}{p_0(y,\varsigma)}\right)^{-w}\right)^{\frac{1}{s-r}} \tag{2.28}$$

where α is computed by solving

$$\frac{\int_{\varsigma}\int_{-\infty}^{\infty} p_0(y,\varsigma)\cdot\left(1+\alpha\left(p_1(y,\varsigma)/p_0(y,\varsigma)\right)^{-w}\right)^{1-\rho} dyd\varsigma}{\int_{\varsigma}\int_{-\infty}^{\infty} p_0(y,\varsigma)\cdot\left(1+\alpha\left(p_1(y,\varsigma)/p_0(y,\varsigma)\right)^{-w}\right)^{\rho} dyd\varsigma} = 1-\delta \tag{2.29}$$

2.2.4 Distance Spectrum

From (2.19) together with (2.20) and (2.21), the problem of finding the upper bound is reduced to finding the distance spectrum K_d of a turbo code. For convolutional codes, computing the distance spectrum is well defined in the sense that it gives exact number of codeword that have a given Hamming weight. For turbo codes, in which several constituent codes are concatenated with interleavers, the situation is not as simple as with convolutional codes. As described in [50,51], for a specific interleaver, a state path of a turbo code is defined in hyper trellis, which represents all the combinations of the trellis paths for each constituent convolutional code. For large block sized code, the number of the combination is innumerable, making the whole search in the hyper trellis impossible. For computational simplicity, the notion of the uniform interleaver, which is a conceptual interleaver that averages all the possible permutations, has been introduced in [50]. Although it does not give the exact weight enumerating function for a specific interleaver, it does give at least the averaged weight enumerating function over all possible interleavers. In this dissertation, the same approach as in [50] is used to find the ensemble distance spectrum of turbo codes and also [52] and [53.Ch.6] to compute the weight enumerating function of the constituent convolutional codes.

2.3 Numerical Results

In this section, some numerical results on the throughput performance of CDMA system with idealized hybrid type-I ARQ scheme using punctured turbo codes are shown for both the AWGN and multipath fading channels.

Table 2.1 Distance Spectrum of The Punctured Turbo Code Used

Weight	4/5	2/3	4/7	1/2	4/9	2/5	4/11	1/3
1	0	0	0	0	0	0	0	0
2	1.45E+00	1.18E-01	0	0	0	0	0	0
3	6.54E+00	9.50E-01	0	0	0	0	0	0
4	2.11E+01	2.68E+00	1.20E-01	0	0	0	0	0
5	8.31E+01	4.92E+00	1.08E+00	0	0	0	0	0
6	3.38E+02	1.23E+01	2.81E+00	4.86E-01	3.04E-02	5.61E-06	0	0
7	1.44E+03	2.74E+01	2.79E+00	1.93E+00	3.63E-01	4.49E-05	0	0
8	6.47E+03	6.45E+01	6.47E+00	1.94E+00	1.27E+00	1.22E-01	3.46E-05	0
9	3.00E+04	1.61E+02	8.43E+00	2.01E+00	1.35E+00	7.29E-01	1.96E-04	0
10	1.44E+05	4.03E+02	1.63E+01	6.07E+00	2.07E+00	1.58E+00	7.59E-01	9.12E-05
11	7.18E+05	1.03E+03	3.32E+01	4.95E+00	2.87E+00	1.73E+00	9.22E-01	5.43E-04
12	3.67E+06	2.67E+03	5.93E+01	6.79E+00	3.23E+00	1.79E+00	1.20E+00	1.96E+00
13	1.93E+07	7.08E+03	1.16E+02	1.76E+01	4.83E+00	2.38E+00	1.26E+00	1.04E-01
14	1.04E+08	1.91E+04	2.17E+02	2.45E+01	6.35E+00	2.72E+00	1.95E+00	2.31E-02
15	5.77E+08	5.22E+04	4.14E+02	3.81E+01	9.53E+00	3.46E+00	1.96E+00	3.93E+00
16	3.27E+09	1.45E+05	8.07E+02	7.06E+01	1.64E+01	4.63E+00	2.84E+00	3.41E-01

(for the first 16 Hamming Weights)

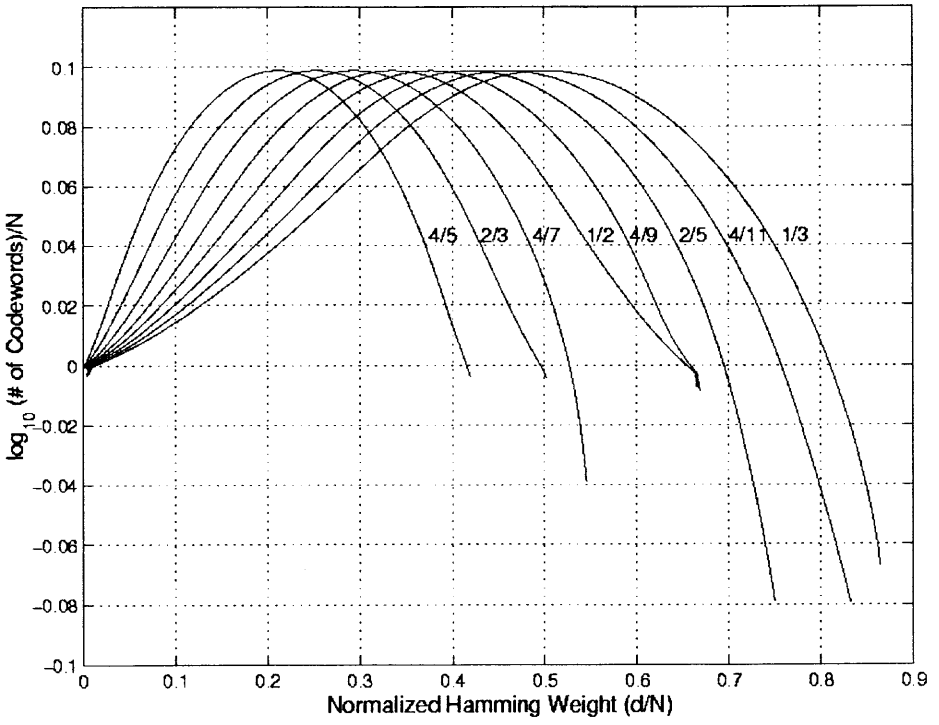

Figure 2.1 The Distance Spectrum of punctured Turbo codes. Mother turbo code with (1,23/35) constituent RSC code.

2.3.1 Punctured Turbo Codes

The punctured turbo codes to be used are derived from a 1/3-rate mother turbo code of input block length 512, which consists of two identical 16-state recursive systematic convolutional code with generator polynomial (1, 23/35). Surely, the code performance depends on the puncturing pattern and its period as presented in [53], where some optimal puncturing patterns were provided. However, according to the procedures described in [53.Ch.6], since the multiplication of state transition matrix is permutative the puncturing pattern itself is not required in the ensemble distance spectrum computation of the punctured turbo codes, as it depends only on the puncturing rate. In this work, puncturing period of 8 is used to obtain a set of punctured code of rate 4/5, 2/3, 4/7, 1/2, 4/9, 2/5, 4/11, and 1/3, without considering their specific puncturing patterns.

Figure 2.1 shows the distance spectrum of the set of punctured turbo codes and Table.1 shows some detailed values for first 20 Hamming weights. These values have been used for the computation of the codeword error probability, which is equivalent to the probability of packet failure.

2.3.2 Spectral Efficiency of Turbo Coded CDMA

Consider hybrid type-I ARQ scheme with a fixed rate turbo code, where a copy of the original packet is retransmitted if error occurred. For matched filter receiver, Figure 2.2 and 3 shows the codeword error probability and the corresponding throughput, respectively, in AWGN channel separately for all the puncture turbo codes of rate 4/5, 2/3, 4/7, 1/2, 4/9, 2/5, 4/11 and 1/3. Perfect power control and BPSK modulation were assumed and the signal to background noise ratio, Es/No, was set to 10 dB for all the users in the system. For comparison, the theoretical bound that is defined in (2.11) was also plotted. In Figure 2.3, the throughput reduction caused by outer error detection code was ignored, so that the nominal throughput is equal to the code rate of inner FEC code.

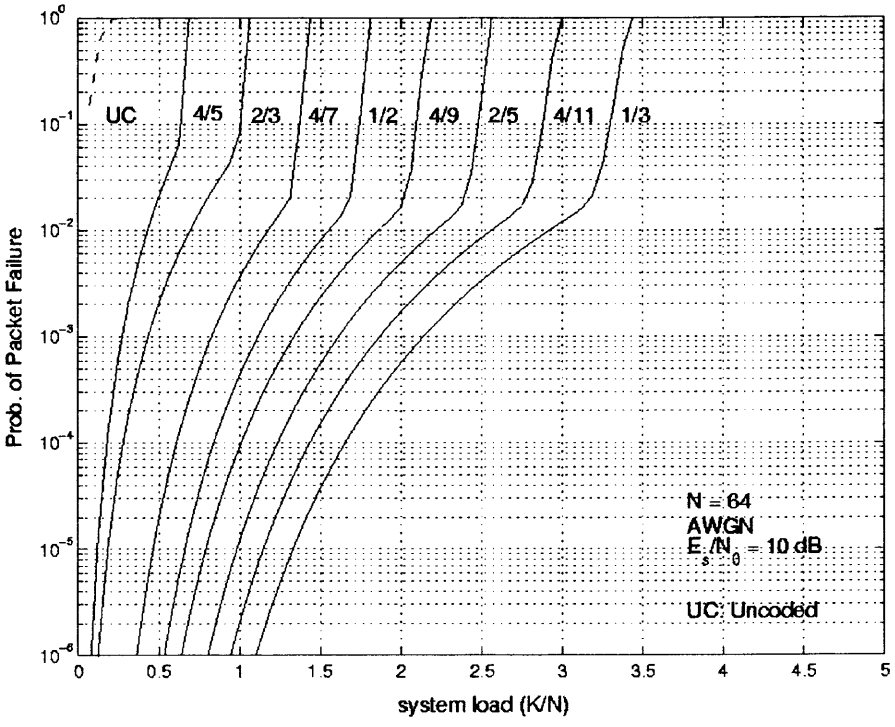

Figure 2.2 Codeword Error Probability of turbo coded CDMA system in AWGN channel. Es/No = 10 dB, BPSK modulation.

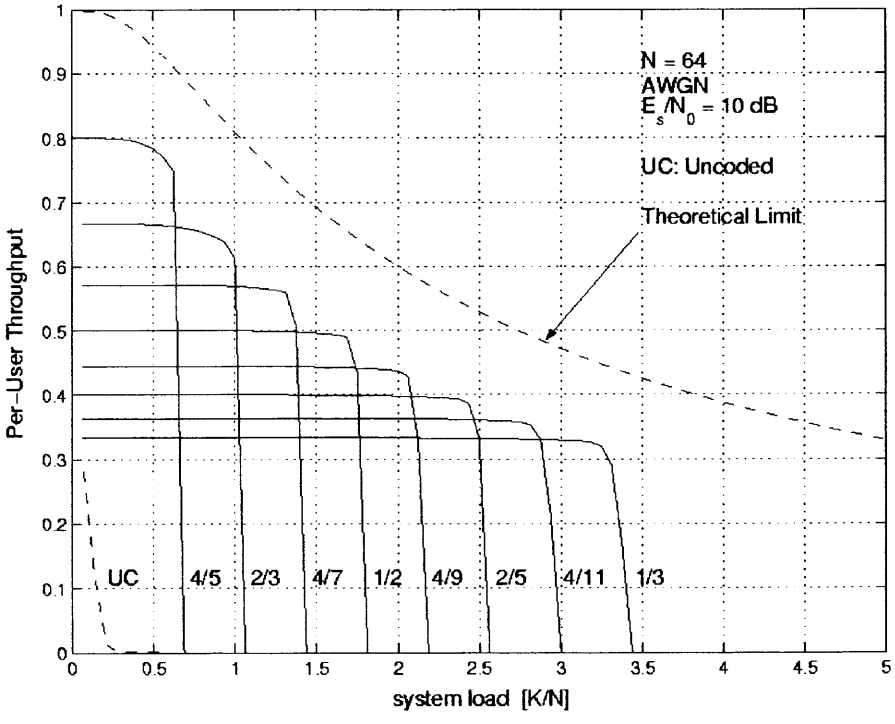

Figure 2.3 Per-user throughput of turbo coded CDMA system in AWGN channel. Es/No = 10 dB, BPSK modulation.

The spectral efficiencies are plotted in Figure 2.4 and 2.5 for both AWGN channel and a 4-path, equal average power, Rayleigh fading channel, respectively. For a given rate of punctured turbo code, the spectral efficiency increases almost linearly with the system load, but the system breaks down at a certain point, where the turbo code does not support the SNIR. From these figures, one can find the system capacity (the maximum number of users that can be supported by given rate of punctured turbo codes) and the corresponding spectral efficiencies that can be maximally achieved. Figure 2.6 depicts the achievable spectral efficiencies versus the code rate. Apparently, with matched filter receiver, the CDMA system is useless without channel coding. When employing channel coding, one can obtain higher spectral efficiency with lower rate code. For given rate of turbo codes, it is desirable to keep the nominal operating point fixed such that one can obtain as high spectral efficiency as possible without system break down.

Next, the performance improvement that can be obtained by the use of linear MMSE multiuser receiver is evaluated. Using the same coding options, the spectral efficiency is compared with that of matched filter receiver. The overall computation procedure is the same as that for matched filter receiver, except that for the SNIR (2.10) is used instead of (2.6). Figure 2.7 depicts the spectral efficiency with the linear MMSE receiver for the coded CDMA system with Hybrid type-I ARQ and Figure 2.8 shows the achievable spectral efficiency as a function of code rate with and without linear MMSE receiver. Note that the former saturates at a code rate around 4/5. This means that the linear MMSE receiver achieves maximum spectral efficiency with moderate channel coding, while the spectral efficiency of matched filter receiver depends heavily on channel coding. As mentioned in [20] and other literature, however, theoretically the performance of MMSE converge to that of matched filter receiver as the system load goes infinity. Accordingly, it is expected that the performance difference between matched filter and linear MMSE receiver will be smaller, if one employs a lower rate mother code for matched filter receiver, and a well-designed channel codes can be an alternative to linear multiuser receivers when comparing hardware complexity.

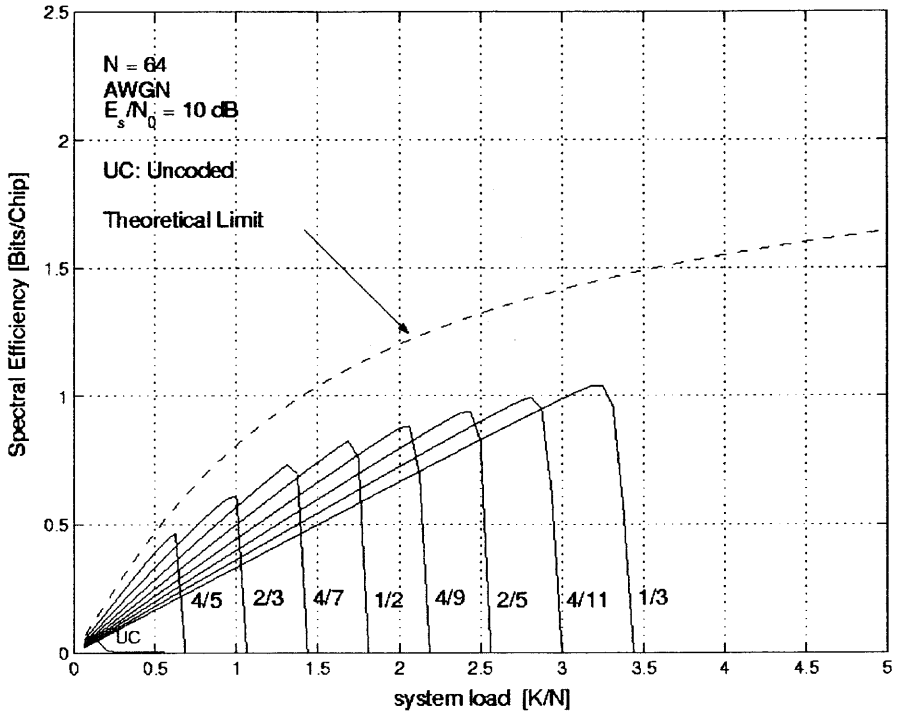

Figure 2.4 Spectral Efficiency of turbo coded CDMA system in AWGN channel. Es/No = 10 dB, BPSK modulation.

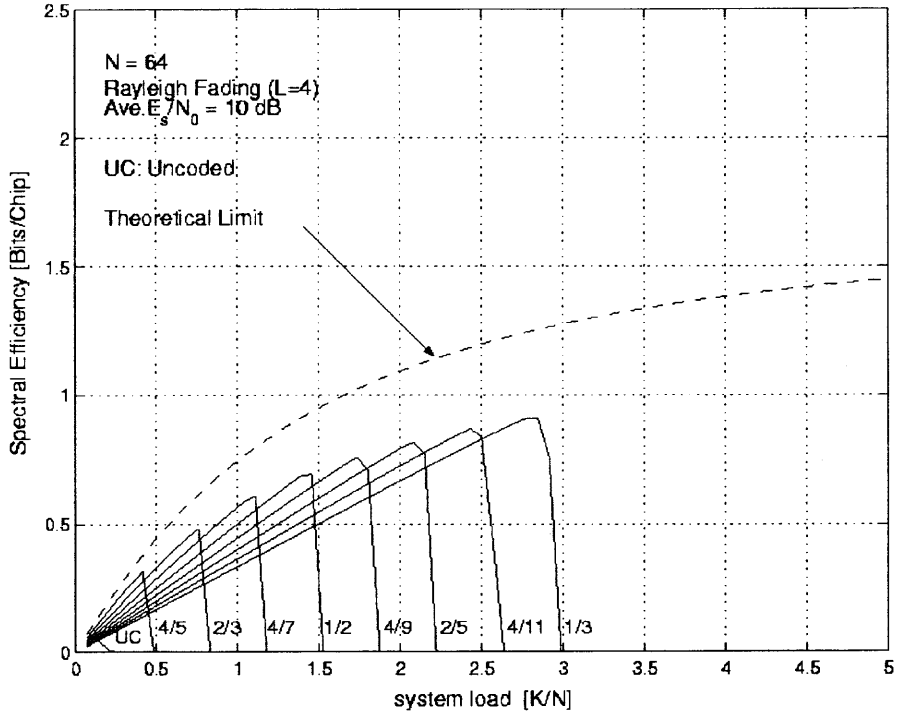

Figure 2.5 Spectral Efficiency of turbo coded CDMA system in fading channel. L=4, Ave. Es/No = 10 dB, BPSK modulation.

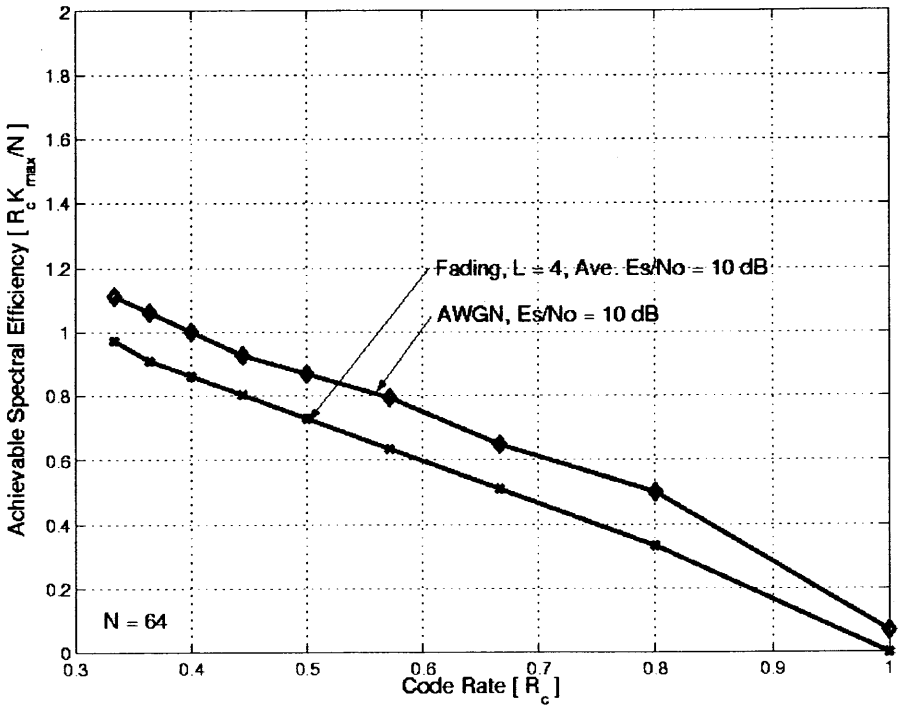

Figure 2.6 Achievable Spectral Efficiency of turbo coded CDMA system in AWGN and 4-path Rayleigh Fading Channel.

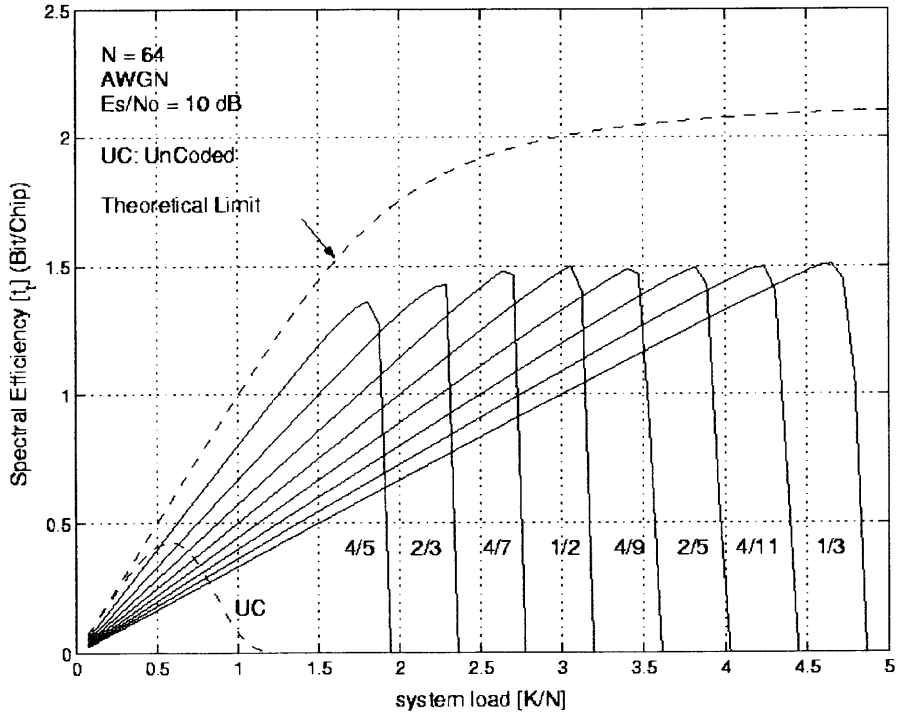

Figure 2.7 Spectral Efficiency of turbo coded CDMA with linear MMSE receiver. Es/No = 10 dB, BPSK modulation.

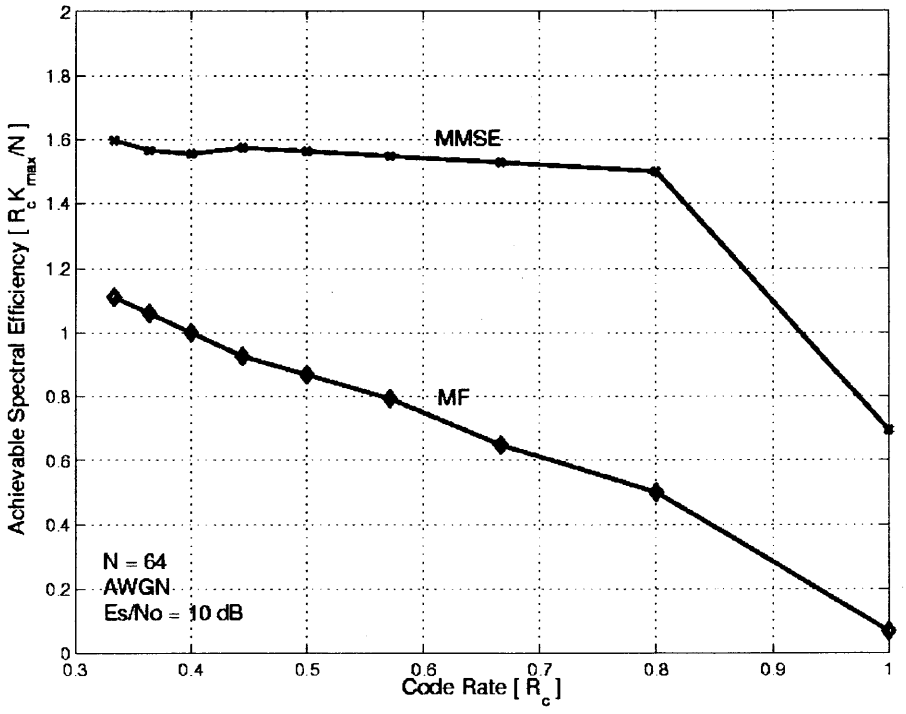

Figure 2.8 Achievable Spectral Efficiency of turbo coded CDMA system with MF and linear MMSE receiver front-end.

2.4 Chapter Summary

Apparently, due to the multiple access interferences, CDMA system with only matched filter receiver is useless without coding. As shown numerically, when using lower rate turbo codes than 1/3, one can obtain more spectral efficiency than 1.1 bits/Hz/sec. On the other hand, by employing multiuser detection, the spectral efficiency could be even higher than 1.6 bits/Hz/sec. Multiuser detections can improve the system capacity for given rate of coding options, but the efficiency can also be improved with lower rate channel coding, even without multiuser detection. As the number of users $K \rightarrow \infty$, the spectral efficiency of MMSE receiver converges to that of the conventional matched filter receiver. Hence we may consider lower rate turbo coding in favor of multiuser detection if the latter requires more complicated hardware than that needed for implementing lower rate channel coding/decoding. Although the improved union bound still shows gap

between the actual cutoff and the computational cutoff, especially for high rate punctured codes, the results in this work can give useful insights into the network level protocol design in CDMA based random access systems.

CHAPTER 3

QUEUING NETWORK MODELS AND THEIR APPLICATION TO THE ANALYSIS OF CDMA SLOTTED ALOHA WITH PACKET COMBINING

In this chapter, to analyze hybrid type-II ARQ in random access environment, a generalized analytical framework is introduced. When applying hybrid type-II ARQ, probability of packet success and packet length is generally different from attempt to attempt. Since the conventional analytical model, customarily employed for ALOHA system with pure or hybrid type-I ARQ, cannot be applied for this case, we introduce an expanded analytical model, which can be regarded as a network of queues, and apply Jackson and Burke's theorems to simplify the analysis. Then, the analytical model is applied to a simple example, a CDMA slotted ALOHA with packet combining. The effectiveness of the model is verified by comparing with some simulation results. The results show that the packet combining hybrid type-II ARQ automatically adjusts the spreading factor according to the traffic situation.

3.1 CDMA Slotted ALOHA with Packet Combining

Throughout the last decades, many papers have dealt with the subject of CDMA based ALOHA system, either slotted [54, 11, 12] or unslotted [55-58], as a candidate for packet radio network [59]. Most of these papers, however, implicitly assumed pure or hybrid type-I ARQ, for which a single queue model with feedback has generally been used. Unlike pure or hybrid type-I ARQ, hybrid type-II scheme combines the recent retransmission with the previously received signals to accomplish enhanced channel utilization. Packet combining and code combining are the two well-known forms of hybrid type-II ARQ. When applying hybrid type-II ARQ to ALOHA system, the probability of packet success and packet length is generally assumed to be different from attempt to attempt, making the analysis complicated and conventional single queue model

not applicable. Recently, some efforts have been made to analyze CDMA based ALOHA system with hybrid type-II ARQ. In particular, CDMA slotted ALOHA with packet combining has been analyzed in [60], [61] and [62].

In this work, an expanded analytical model is introduced as a general analytical framework for CDMA based random access system with hybrid type-II ARQ. It shows a graphical description of equilibrium traffic flow for ALOHA system with hybrid type-II ARQ. As discussed in detail later, the model can be regarded as a network of queue so that Jackson and Burke's theorem [63] can be applied to simplify the analysis. Then, as a simple example, the expanded model is applied to CDMA slotted ALOHA system with packet combining. The effectiveness of the queuing network model is verifed by comparing to simulation results. As will be discussed later, the queuing network model approach provides a unified methodology for analyzing CDMA based ALOHA with hybrid type-II ARQ in various scenarios and the work in [62] is a special example of our generalized framework for CDMA slotted ALOHA with packet combining.

It is also shown that the hybrid type-II ARQ with maximal ratio packet combining can be regarded as a decentralized automatic spreading factor adaptation, where the spreading factor automatically adjusted according to the traffic and/or the channel status. It is comparable to the hybrid type-II ARQ with code combining, which is an automatic code rate adjustment employing incremental parity retransmission.

3.1.1 System Operation

The system consists of a single base station and many nodes, each tries to access the base station receiver with some probability at a predefined periodic time offset. Throughout this chapter, the following assumptions are held.

1) The new message arrival is modeled as Poisson process with an arrival rate λ_I and every message has fixed, L_o bits of source information.

2) When a message is arrived at a terminal, it is encoded first by a cyclic redundancy check (CRC) code and then by a forward error correction code of rate r. The rate reduction caused by the outer CRC code will be ignored.
3) To share a common channel, each packet is spread with a sequence from a set of predefined spreading codes. Assuming the number of predefined spreading codes is very large, the probability that two or more users choose the same spreading code is not counted.
4) AWGN channel with perfect power control.
5) Newly received packet is maximal ratio combined with the previously received packets. Then, the signal to noise plus interference ratio (SNIR) of the combined signal up to ith attempt, $\gamma^{(i)}$, is expressed as

$$\gamma^{(i)} = \sum_{j=1}^{i} \gamma_j = \sum_{j=1}^{i} \frac{1}{\beta^{-1} + K_j / 3N} \tag{3.1}$$

where γ_j and K_j are SNIR and the number of interfering users (not including the desired user) at the jth attempt, respectively, and N is the spreading factor and β the signal to background noise ratio.
6) When any error occurred, a terminal waits for random time (random number of slots) before retransmission.

3.2 Analytical Framework

As mentioned before, when applying hybrid type-II ARQ to ALOHA system, the probability of packet success and packet length is generally assumed to be different from attempt to attempt. In such case, one can group terminals into multiple classes according to their transmission attempts (1^{st}, 2^{nd},..., i^{th},..) whose average packet success probability and packet length are the same, respectively. Then, considering the traffic dependency between these groups, one can construct a queuing network model to analyze the steady-

state system behavior. This section presents the queuing network models and a simplified analytical methodology for them.

Figure 3.1(a) shows a conventional analytical model for ALOHA system. λ_o denotes arrival rate of new packets and λ_r that of retransmissions. p_s is the average probability that a packet is successfully received. Usually, the composite arrival $\lambda_T = \lambda_o + \lambda_r$ is modeled as Poisson process [55]. The model in Figure 3.1(a) implicitly assumes the use of pure or hybrid type-I ARQ, where an exact copy of an original packet is retransmitted if any error is detected at the receiver and the retransmitted copy is decoded as a new one, independently of the previously received packet. This means that the packet length at each attempt, regardless whether it is retransmission or original one, has the same length, $T_p = L_p \cdot T_b$, where L_p is the number of bits contained in a packet and T_b the time duration of a bit. Therefore, the average packet service time (packet length) is also T_p and the composite offered traffic is simply given by $G_T = (\lambda_o + \lambda_r) \cdot T_p$. (Note that fixed packet length system is being condidered.) Moreover, since the original and the retransmitted packets are identical and decoded independently of the others, the average probabilities of packet success at each attempt is the same at every attempts, as well. In this case, the steady state analysis (equilibrium analysis) is simple.

3.2.1 Expanded Analytical Model – Network of Queues

When hybrid type-II ARQ scheme is used, both the packet length and the probability of packet success may be different from attempt to attempt and the model in Figure 3.1(a) cannot be applied to this case. Instead, Figure 3.1(b) shows an expanded model, which takes this situation into account. In the figure, λ_i denote the arrival rate of the packets in the i^{th} attempt, λ_1 the arrival rate of newly arriving packets, p_s^i explicitly denotes the probability of packet success. This model can be regarded as a series of network links or a series of queues, where packets are coming into the network through the first node and going out at different nodes. Some of the incoming packets can be routed to go out right

away if no error is detected and some routed to the next node if there is any error in the packet. The random event whether a packet is erroneous or not, decides which route a packet passed through. In this system, the random event is governed by the composite arrival rate λ_T and the average departure rate μ of the system. With this resemblance to the queuing network in mind, Burke's theorem [63] can be applied to safely model each of the arrivals at a node as a Poisson process. Moreover, by applying Jackson's theorem [63] with the help of the random delay assumption, each node can also be regarded as an independent queue so that one can easily obtain a set of equations, with which the throughput of the system can be uniquely determined.

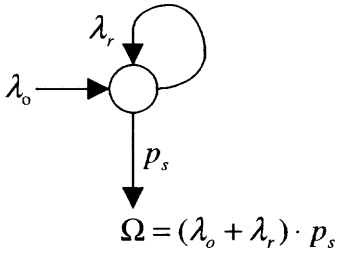

(a) Conventional Model

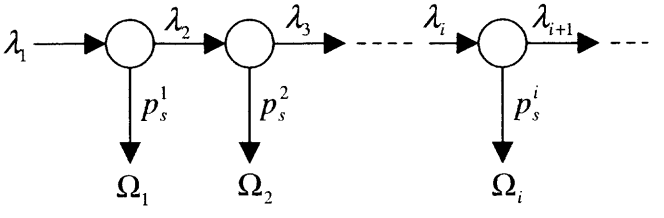

(b) Expanded Model with infinite number of retransmissions

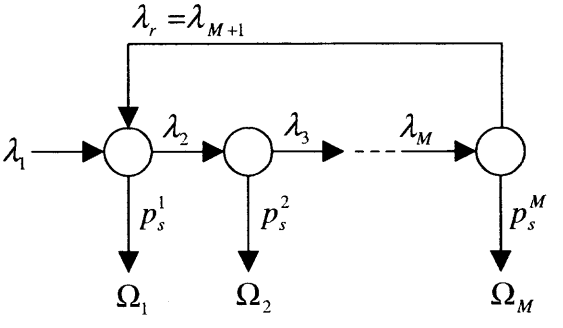

(c) Expanded Model with finite number of retransmissions

Figure 3.1 Analytical Models for ALOHA systems.

In Figure 3.1(b), the model implicitly assumes infinite retransmission for erroneous packet. More realistically, however, the base station receiver would reset the erroneous transmission when the number of retransmissions exceeds a certain number, saying *M*. That is, the reset transmission will try again as new message (with systematic bits only). In Figure 3.1(c), a more general analytical model is shown with finite number of retransmissions. This case will be investigated in Chapter 4 for a more complicated example; CDMA unslotted ALOHA with code combining.

3.2.2 Equilibrium Analysis

Now, the author briefly discusses on the equilibrium analysis (mean value analysis [63]), which assumes that $p_s^{(i)}$'s are given. At equilibrium, the conventional model in Figure 3.1(a) gives

$$\lambda_r = (\lambda_o + \lambda_r) \cdot (1 - p_s)$$

and since the inflow rate and the outflow rate should be the same at equilibrium, it also gives for the outflow rate

$$\Omega = (\lambda_o + \lambda_r) \cdot p_s = \lambda_o.$$

Note that the throughput is a percentage of the offered traffic that has been successfully transmitted. It can be expressed as a product of the average rate of successful packets and the information contents of the successful transmission measured in time. For an inner FEC code of rate *r*, the throughput is defined by

$$S = r \cdot \Omega \cdot T_p = r \cdot G_T \cdot p_s . \qquad (3.2)$$

The average probability of packet success, p_s, can be expressed as

$$p_s = \sum_{k=0}^{\infty} m_k \cdot p_s(k)$$

where $p_s(k)$ is the conditional probability of packet success given that the number of interfering users is k and m_k the probability mass function of the number of interfering users. Since the composite arrival is modeled as Poisson process of rate $(\lambda_o+\lambda_r)$, m_k is given by Poisson density function defined as

$$m_k = G_T^k \exp(-G_T)/k! \tag{3.3}$$

with $G_T = (\lambda_o+\lambda_r)\cdot T_p$. Therefore, the throughput in (3.2) is expressed as

$$S = r \cdot G_T \cdot \sum_{k=0}^{\infty} m_k \cdot p_s(k) \tag{3.4}$$

This result is comparable to that of Raychaudhuri [54], where the throughput is given by

$$S = r \cdot \sum_{k=0}^{\infty} k \cdot m_k \cdot p_s(k) \tag{3.5}$$

Comparing (3.4) with (3.5), the result from equilibrium analysis replaces the variable k with its mean value, G_T. These two are appeared to perfectly match when the offered traffic is less than a point after which the throughput decreases with offered traffic. Beyond that point, they show slightly difference in throughput. However, even in this region, they match well if the processing gain N is large enough (i.e. greater than 64).

3.3 Analysis of CDMA slotted ALOHA with Packet Combining

Using the model in Figure 3.1(b), the CDMA slotted ALOHA with packet combining described in Section 3.1 is now analyzed. As mentioned before, with the random time delay assumption (6), the analysis is simplified by applying Jackson's and Burke's theorem [63], to treat each node as an independent queue with independent Poisson arrival. For fixed message length traffic, each node in Figure 3.1 acts like $M/D/\infty$ queue. Denoting the time span of a packet as T_p, the composite offered traffic is given by

$$G_T = T_p \cdot \sum_{i=1}^{\infty} \lambda_i = T_p \cdot \lambda_T \tag{3.6}$$

where $\Sigma_i \lambda_i = \lambda_T$. From Figure 3.1(b), since $1-p_s^{(i-1)}$ percentage out of λ_{i-1} is routed to the next ith node, we establish the following set of equations for equilibrium conditions.

$$\lambda_i = \lambda_{i-1} \cdot (1 - p_s^{(i-1)}) \quad \text{for } i = 2,3,4,\ldots \tag{3.7}$$

Substituting (3.7) into (3.6) and arranging terms, we obtain

$$\lambda_1 = G_T \cdot [T_p \cdot \sum_{i=1}^{\infty} \prod_{j=1}^{i-1} (1 - p_s^{(j)})]^{-1} \tag{3.8}$$

for given G_T. Once λ_1 is found, the throughput and the average number of transmissions required are easy to find.

Since the total inflow to the queuing network and the total outflow should be the same at equilibrium, the sum of outflow rate $\Sigma_i \Omega_i$ should be equal to λ_1. Therefore, the throughput S is given by

$$S = r \cdot T_p \cdot \sum_{i=1}^{\infty} \Omega_i = r \cdot T_p \cdot \lambda_1 = r \cdot G_T \cdot [\sum_{i=1}^{\infty} \prod_{j=1}^{i-1} (1 - p_s^{(j)})]^{-1} \tag{3.9}$$

where r is the code rate of inner FEC code. Note that by setting $p_s^{(i)} = p_s$(constant) for all i in Figure 3.1(b) one can obtain the same equation as that of (3.4). Knowing $p_s^{(i)}$ for i = 2,3,..., and with (3.7) and (3.8), the average number of transmissions needed, N_{TX}, (including the original one) is given by

$$N_{TX} = \frac{\sum_{j=1}^{\infty} j \cdot \Omega_j}{\sum_{j=1}^{\infty} \Omega_j} = \frac{\sum_{j=1}^{\infty} j \cdot p_s^{(j)} \lambda_j}{\lambda_1} \tag{3.10}$$

3.3.1 Packet Success Probability

Now, the problem is reduced to finding $p_s^{(i)}$'s. In CDMA system, the probability of error can be expressed as a function of the number of active interfering users. In random access environment, it fluctuates with time or from slot to slot, where in most practical situation these fluctuations can be modeled as Markov process. This means that we need to solve multi dimensional Markov chain model to obtain $p_s^{(i)}$'s. Fortunately, a simple solution can be obtained with fixed message length and random time delay assumptions. Note the following observations.

1) With the assumption (6), one can treat each traffic flow λ_i as independent Poisson process.
2) Since the SIR in (3.1) is governed by the total traffic of the average rate λ_T, it is not needed to handle each node separately to evaluate SIR fluctuation, so that only one Markov chain model is required.
3) With the fixed packet length and random time delay assumption, the number of active terminals at each time slot is independent (or at least uncorrelated) to each other.

These three observations lead to the fact that K_j's in (3.1) are independent and identically distributed random variables with Poisson distribution, m_k, given by

$$K_j \sim m_k = \frac{G_T^k}{\Gamma(k+1)}\exp(-G_T) \tag{3.11}$$

where $k!$ was replaced with the gamma function $\Gamma(k+1)$ defined as $\Gamma(a) = \int_0^\infty t^{a-1}e^{-t}dt$.

For the system with packet combining described by (3.1), by treating k as a continuous variable one can obtain the average probability of packet success as

$$\begin{aligned} p_s^{(i)} &= E_{K_1,K_2,\ldots,K_i}\left(1 - p_{we}\left(\sum_{j=1}^{i}[\beta^{-1} + K_j/3N]^{-1}\right)\right) \\ &= 1 - \int p_{we}(v)\cdot f_V(v)\cdot dv \end{aligned} \tag{3.12}$$

where the random variable V is defined as

$$V \equiv \sum_{j=1}^{i}[\beta^{-1} + K_j/3N]^{-1}$$

whose PDF is i-fold convolution of the PDF of $[\beta^1+2K_j/3N]^{-1}$ given by

$$f_V(v) = \frac{1.5\cdot v^{-2}\cdot G_T^{1.5(v^{-1}-\beta^{-1})}}{\Gamma(1.5(v^{-1}-\beta^{-1})+1)}\exp(-G_T) \tag{3.13}$$

$p_{we}(\cdot)$ is the word error probability. Without packet combining, $p_s^{(j)} = p_s(\text{const})$ given by

$$\begin{aligned} p_s^{(i)} &= E_K\left(1 - p_{we}\left([\beta^{-1} + K/3N]^{-1}\right)\right) \\ &= 1 - \sum_{k=0}^{\infty} p_{we}\left([\beta^{-1} + k/3N]^{-1}\right)\cdot m_k \end{aligned} \tag{3.14}$$

For uncoded system, $p_{we}(\gamma) = [1\text{-}Q(\gamma^{1/2})]^{Lo}$, while, for coded system, one can use the results in Chapter 2 (Figure 2.2).

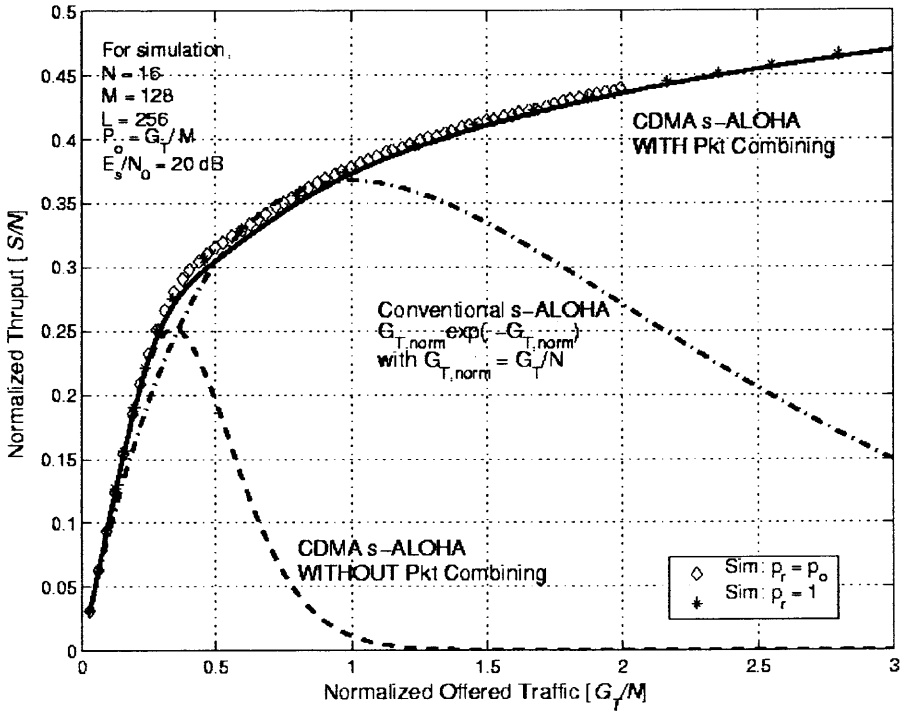

Figure 3.2 Throughput performance of CDMA Slotted ALOHA with Packet Combining. No FEC coding, Es/No = 20 dB.

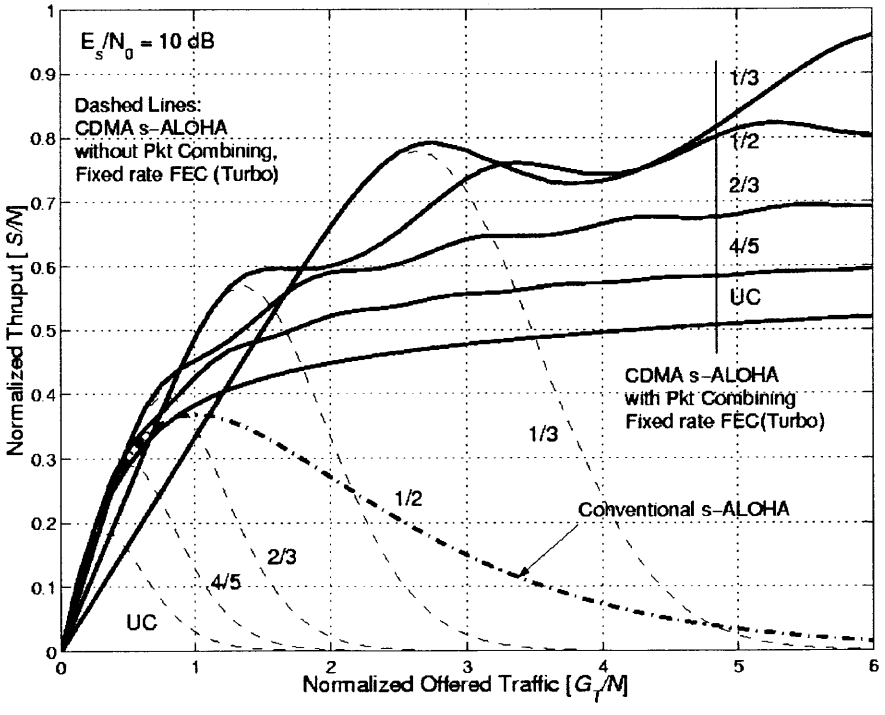

Figure 3.3 Throughput performance of CDMA Slotted ALOHA with Packet combining and FEC (Turbo) coding, Es/No = 10 dB.

3.4 Numerical Results

For uncoded system, Figure 3.2 shows the normalized throughput (S/N) versus normalized offered traffic (G_T/N) of CDMA slotted ALOHA with and without packet combining and of conventional slotted ALOHA without spreading. To verify the effectiveness of the proposed approach, the simulation results are also plotted for CDMA slotted ALOHA with packet combining, for which the spreading factor N was set to 16, the number of terminals in the system M to 128, packet length L_o = 256 and E_s/N_0 to 20 dB. First, the probability of original packet generation, p_o, and that of retransmission, p_r, were set equally to $G_T/M = (G_T/N)\cdot(N/M)$ (diamond marks) for each terminal. Then, in another simulation, p_r was changed to 1 (* marks), meaning immediate retransmission when error occurred, while p_o remained the same. The result shows that for packet combining CDMA slotted ALOHA the proposed analytical approach is valid even with immediate retransmission. Figure 3.3 shows the same plot, but now with FEC coding. A set of punctured turbo codes defined in the previous chapter of rate 4/5, 2/3, ½ and 1/3 were used. Figure 3.4 shows limiting throughput performance when offered traffic gets large and Figure 3.5 compares the system performance with different signal to background noise ratio, E_s/N_0, of 10 dB and 20 dB, respectively.

Packet Combining ARQ as an Automatic Spreading Factor Adaptation

Without packet combining, it should be noted [55] that immediate retransmission leads to instability causing, as offered traffic increases, sharper dropdown in throughput than retransmission with random delay. With packet combining, however, there is no dropdown in throughput, even with immediate retransmission making the system always stable. The reason is that; packet combining scheme can be regarded as automatic spreading factor adaptation such that combining n signals is equivalent to the effective spreading factor of n times the nominal spreading factor N. Hence, as offered traffic

increases, the probability of packet success decreases causing each terminal to require more retransmissions on the average, which result in increased effective spreading factor to fit the current traffic situation. Therefore, with packet combining the throughput is retained for wide range of offered traffic. Note however that an increased spreading factor results in n time larger delay since per terminal data rate reduces by $1/n$. This argument is clearer in Figure 3.6. When offered traffic load is small enough, the system throughput increases linearly with a slope of 1/3, which is the rate of FEC codes. However, once the offered traffic gets larger than a certain point most of the packets will be unsuccessful at first attempt, since the offered traffic can not be supported. Now, most of the backlogged terminal will try again (the second attempt) and make the effective spreading factor of 2, which in turn makes the effective rate reduced to 1/6. This effective rate reduction will continue until the system settles down to a stable point.

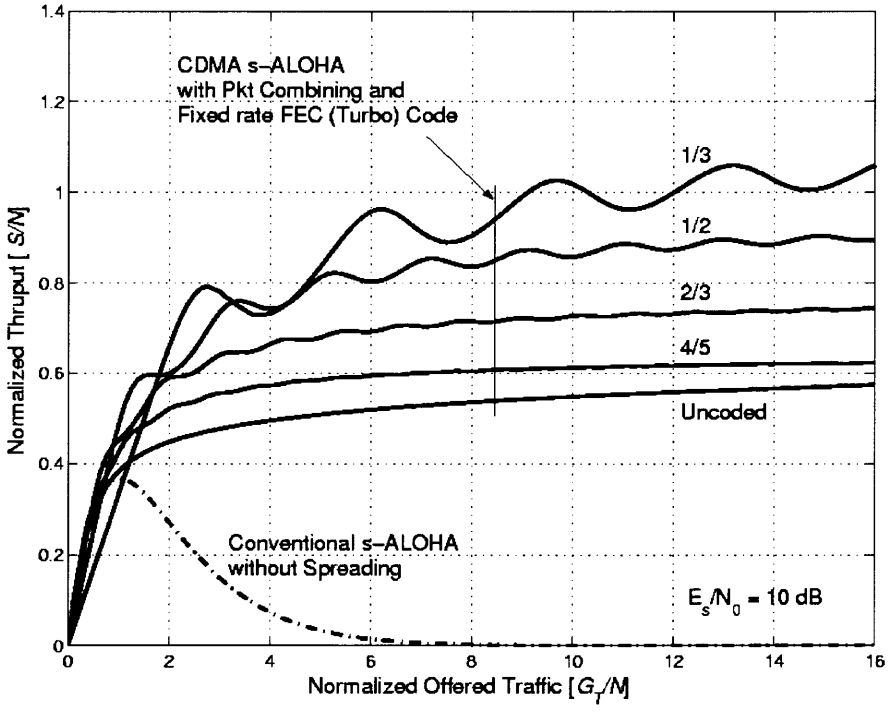

Figure 3.4 Throughput performance of CDMA Slotted ALOHA with Packet combining and FEC (Turbo) coding, Es/No = 10 dB.

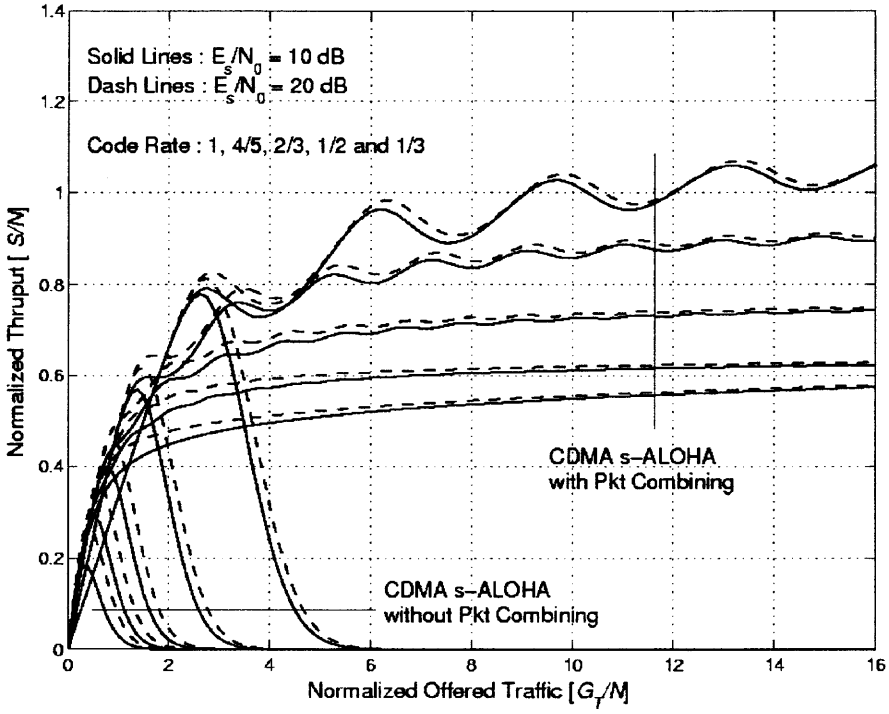

Figure 3.5 Throughput performance of CDMA Slotted ALOHA with Packet combining and FEC (Turbo) coding, Es/No = 10 and 20 dB.

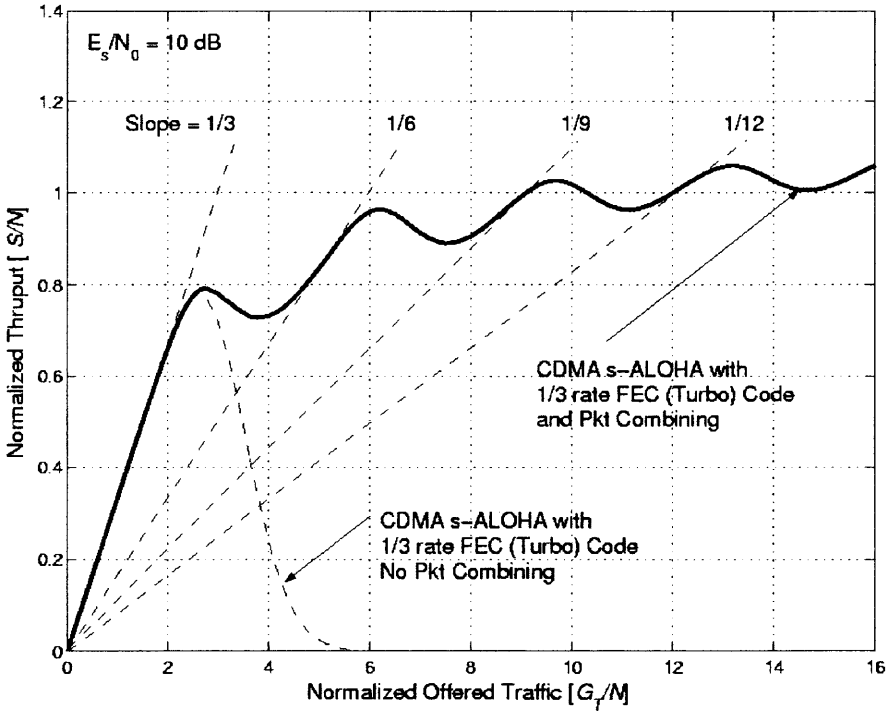

Figure 3.6 Packet combining automatically adjusts the effective spreading factor according to the traffic condition.

Packet Delay Consideration

Figure 3.7 depicts the average number of transmissions versus offered traffic curves for uncoded system and compares it with simulation results. Figure 3.8 plots the same curves, but now with FEC coding. With Figure 3.8, one can obtain the actual average delay as the product of the average number of transmissions, the average retransmission delay and N/r, which is the nominal rate reduction of coded CDMA system; i.e.

$$D = N_{TX} \cdot T_d \cdot N / r \tag{3.15}$$

where T_d is the average time delay between successive attempts. Apparently, due to the large rate reduction of $1/N$, CDMA system might have much larger delay than conventional slotted ALOHA and in some cases the delay is not acceptable for the service requirements. In this case, one may be required to use multiple codes (multiple channels) to meet the data rate requirement.

3.5 Chapter Summary

As a generalized analytical framework for CDMA ALOHA with hybrid type-II ARQ, the expanded queuing network model was introduced and applied to a CDMA slotted ALOHA system with packet combining. The effectiveness of the model was verified by comparing with some simulation results. Comparing to the code combining ARQ scheme, which provides a natural mean of code rate adaptation, the hybrid type-II ARQ with packet combining can be regarded as a decentralized spreading factor adaptation. Packet combining itself, however, does not increase the system throughput (or the spectral efficiency) of the system. What improves the limiting performance of the CDMA based ALOHA system is well-designed FEC code. While this paper focuses only on fixed packet length traffic, further study can be extended to variable length traffic.

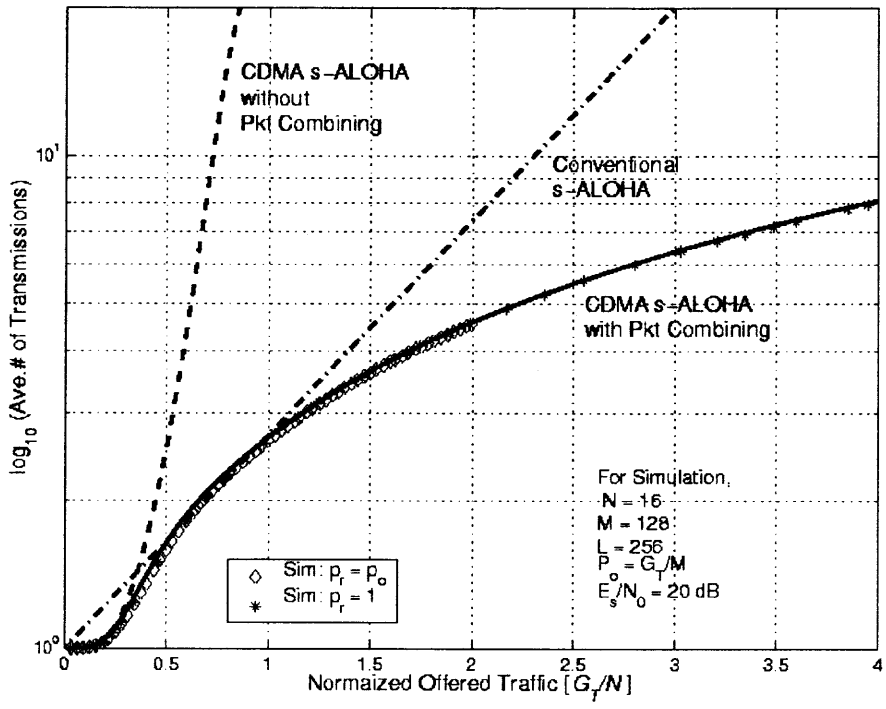

Figure 3.7 Average number of transmissions versus Throughput Curves, No FEC coding Es/No = 20 dB.

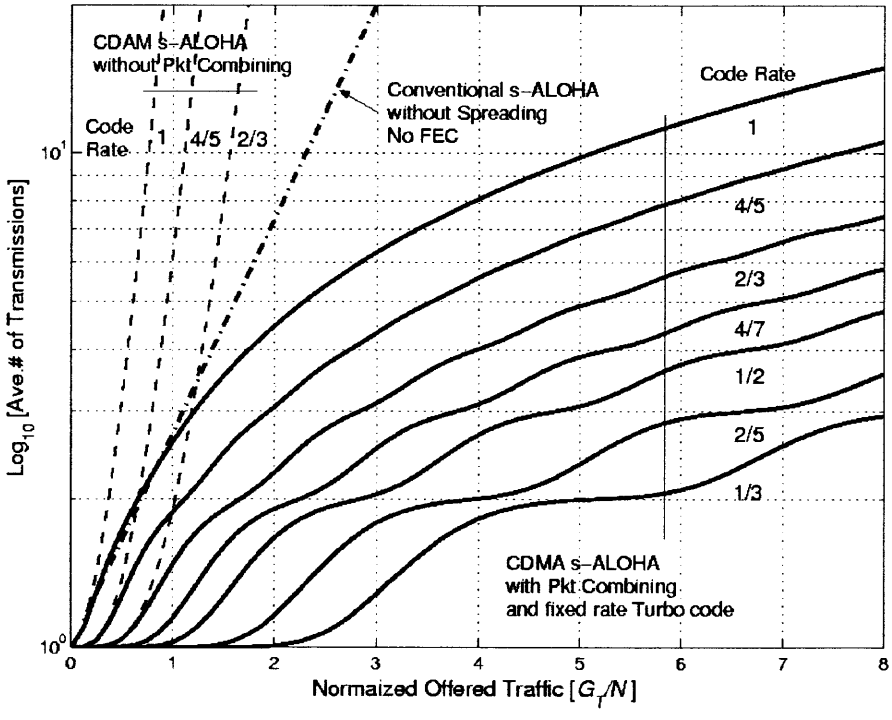

Figure 3.8 Average number of transmissions versus Throughput Curves with FEC (Turbo) coding. Es/No = 10 dB.

CHAPTER 4

CDMA UNSLOTTED ALOHA WITH HYBRID TYPE II ARQ USING RATE COMPATIBLE PUNCTURED TURBO CODES

As a sequel of the previous chapter, we apply the expanded analytical model to a more general case; CDMA unslotted ALOHA with Hybrid Type-II ARQ that uses rate compatible punctured turbo codes. As mentioned before, CDMA unslotted ALOHA is especially interesting because its operation is quite similar to that of the random access channel in WCDMA standards. When using code combining, soft-decision decoding is usually considered, in which case it is very difficult to find the actual probability of packet success, especially when the number of terminals changes during a packet time duration. Hence, instead of finding the actual probability of packet success, a lower and an upper bound are evaluated. Then, together with the expanded model and the packet success probability bound, the corresponding throughput bounds are obtained by iteratively searching the steady-state arrival rate, λ, and the average departure rate, μ, for given composite offered traffic, $G = \lambda/\mu$.

4.1 Hybrid Type II ARQ using RCPT Codes - SYSTEM DESCRIPTION

Since the first introduction of turbo code by Berrou *et al.* [13, 14], its application to hybrid ARQ schemes using rate compatible punctured turbo (RCPT) code [64-71] has been investigated in many papers to improve throughput performance of communication systems. Originally, the rate compatible punctured code was first introduced by Hagenauer in [72] using convolutional codes and subsequently studied in [73,74]. The scheme employs the notion of incremental redundancy retransmission, which is inherent in punctured convolutional codes. In rate compatible punctured turbo (RCPT) code, the convolutional codes in rate compatible punctured convolutional (RCPC) codes are replaced with the turbo codes. In particular, rate compatible codes are useful when the

channel state and/or the traffic change with time, and where fixed rate FEC can be inefficient. This motivates the application of RCPT code to random access systems, such as ALOHA system, where the number of active terminal varies with time according to the random arrival of messages. In such a system, by employing incremental redundancy retransmission we can expect to some extent improvement in throughput.

In the Rate Compatible Punctured Convolutional/Turbo Codes, a low rate $1/n$ code is punctured periodically with period P to obtain a family of codes of rate $P/(P+l)$ with l an integer satisfying $0 \leq l \leq (n\text{-}1)\cdot P$ [72] ($l = 0$ corresponds to the uncoded frame). This type of code can be used for incremental redundancy transmission.

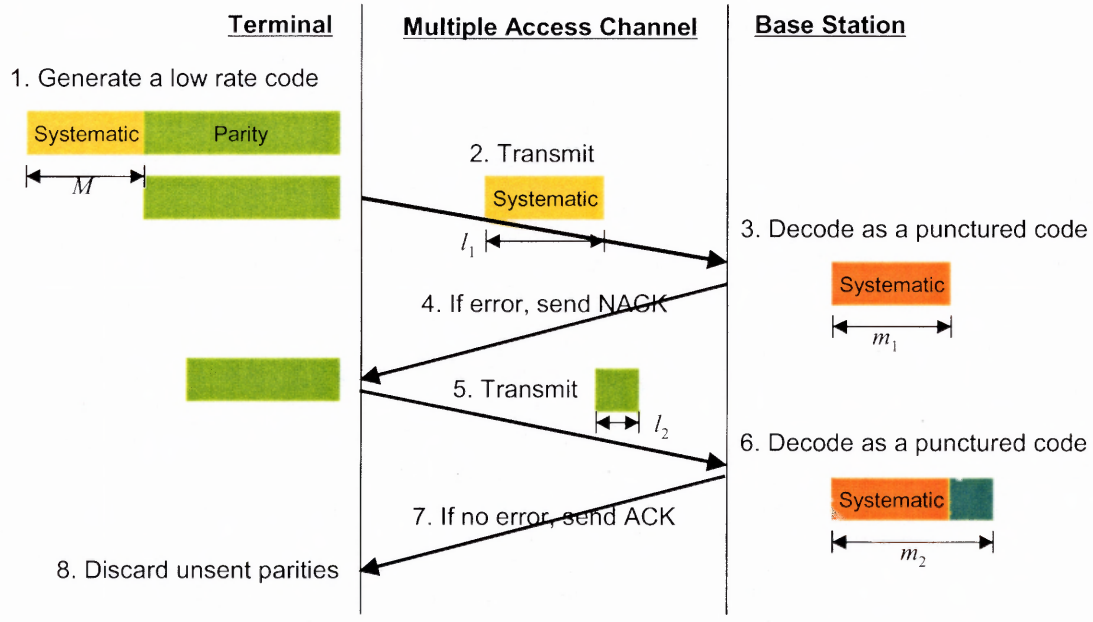

Figure 4.1 Operation of Hybrid type-II ARQ using Rate Compatible Punctured Codes.

This idea of using rate compatible punctured code for incremental transmission of redundancies is depicted in Figure 4.1. At a terminal node, when a message is arrived, turbo encoder encodes the message and generates a codeword of rate $1/n$. At first attempt,

however, it sends only a part of them as a punctured codeword. The rest of the parities are stored in memory for further use. At base station receiver, a turbo decoder is used to recover the information bits only with the (punctured) partial codeword. If any error is detected, then the receiver requests the terminal node to send more parity bits. After receiving the parity bits, the base station receiver combines them with the previous (punctured) codeword and decodes the combined codeword as a lower rate punctured code. If there is no error, it sends an ACK message and the terminal node discards the stored parities.

4.1.1 System Operation

The packet radio system we are dealing with consists of a single base station and many terminal nodes, each of which tries to access the base station receiver with some probability. Throughout this chapter, the following assumptions are held.

1) The new message arrival is modeled as Poisson process with an arrival rate λ_o and every message has source information of the same length of L_o bits.
2) When a message is arrived at a terminal, it is first encoded by a cyclic redundancy check (CRC) code for error detection and then by a forward error correction (turbo) code of rate $1/n$ before being transmitted. The CRC code is assumed to be able to detect all the possible errors. As in Chapter 3, the rate reduction caused by the outer CRC code is ignored.
3) Hybrid type-II ARQ scheme described in the previous sub-section (Figure 4.1) is used with mother FEC code of rate r_M. At first attempt, it sends only the systematic part. Later on if any error occurs, it incrementally sends L_r extra bits of parities out of the stored in memory after a random time delay. As mentioned in Section 3.3, the random time delay makes the queues in the model of Figure 3.1(b) and 3.1(c) virtually independent.

4) For analytical purpose, the maximum number of attempts is restricted to an integer M, after which the packet transmission is reset and restarted as a new arrival. M is selected to such a value that r_M be the code rate without puncturing.
5) Let L_i be the number of bits transmitted at each attempt. Then, $L_1 = L_o$ and $L_i = L_r$, for $i = 2, 3, \ldots, M$. The effective code rate at i^{th} attempt can be expressed as

$$r_i = \frac{L_o}{L_o + (i-1)L_r} \tag{4.1}$$

6) To share a common channel, each packet is spread using one of the sequence from a set of predefined spreading codes and transmitted at any time. Assuming the number of predefined spreading codes is very large, the probability that two or more users choose the same spreading code is ignored.
7) Perfect power control is assumed, so that every packet is received with equal power.
8) Soft decision decoding at the base station receiver.
9) The packet overhead is assumed to be much smaller than an entire packet size and is ignored in the packet service time.

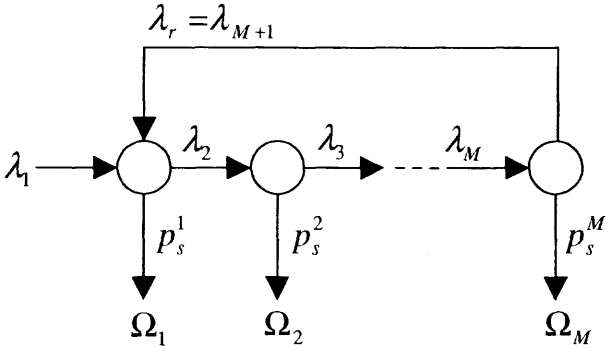

Figure 4.2 Analytical Models for CDMA unslotted ALOHA with Code Combining.

4.2 Analytical Model and Equilibrium (Mean Value) Analysis

Consider the model in Figure 3.1(c), which is replotted in Figure 4.2 for convenience. The equilibrium analysis is almost the same as in Section 3.2 and 3.3. Let the time span of the first attempts and the retransmission be $T_o = L_o T_b$ and $T_r = L_r T_b$, respectively. Then, the composite offered traffic is given by

$$G_T = (\lambda_1 + \lambda_{M+1}) \cdot T_o + \sum_{i=2}^{M} \lambda_i \cdot T_r \tag{4.2}$$

Also using Figure 4.2, the following M equations can be established at equilibrium.

$$\lambda_2 = (\lambda_1 + \lambda_{M+1}) \cdot (1 - p_s^{(1)}) \tag{4.3}$$

$$\lambda_i = \lambda_{i-1} \cdot (1 - p_s^{(i-1)}) \quad \text{for } i = 3,4,\ldots,M+1 \tag{4.4}$$

and

$$\lambda_T = \sum_{i=1}^{M+1} \lambda_i \tag{4.5}$$

When hybrid type-II ARQ is used, the throughput cannot simply be expressed as in (3.2). As noted before, the throughput can be expressed as a product of the average rate of successful packets and the information contents of the successful transmission measured in time. In Figure 4.2, the sum of outflow rates is the average rate of total successful packets and the information content of each successful transmission is T_o (The time duration of the systematic part). Hence, the throughput of the system is given by

$$S = T_o \cdot \sum_{i=1}^{M} \Omega_i \,, \tag{4.6}$$

where, from Figure 4.2, the sum of outflow rate is given by

$$\sum_{i=1}^{M} \Omega_i = (\lambda_1 + \lambda_{M+1}) \cdot p_s^{(1)} + \sum_{i=2}^{M} \lambda_i \cdot p_s^{(i)} \tag{4.7}$$

Since at equilibrium the total inflow to the queuing network and the total outflow should be the same, (4.7) also should be equal to λ_1.

For given $p_s^{(i)}$s, one can easily solve M+1 equations given by (4.2), (4.3) and (4.4) to find λ_i's in terms of G_T. And then, using (4.6) and (4.7), one can obtain the throughput S versus offered traffic G_T curve, provided $p_s^{(i)}$ is available. However, there is a dilemma in obtaining S-G curve. As noted in [11], the average probability of packet success for CDMA unslotted ALOHA can be expressed as a function of the composite arrival rate, λ_T, and the average departure rate, $\underline{\mu}$; i.e. $p_s^{(i)} = p_s^{(i)}(\lambda_T, \underline{\mu})$. The dilemma is that λ_T cannot be found without the solution of the set of equations (4.3) to (4.5), which in turn can be solved only when $p_s^{(i)}(\lambda_T, \underline{\mu})$'s are given. For slotted ALOHA, packet length is a constant T_p such that $\underline{\mu} = 1/T_p$. Hence, the composite arrival rate is expressed as $\lambda_T = G_T/T_p$ for given G_T and, then, $p_s^{(i)}$ is a function of G_T only; i.e. $p_s^{(i)} = p_s^{(i)}(G_T/T_p, 1/T_p) = p_s^{(i)}(G_T)$. Thus, by finding the average probability of packet success, $p_s^{(i)}(G_T)$, for given G_T and plugging it in (3.2), the throughput versus offered traffic (S-G) curve that specifies the system equilibrium behavior could be easily obtained. However, in the case here, the packet length at each attempt is different from others and the average departure rate is not $1/T_p$ any more. Hence, even for given G_T, $p_s(\lambda_T, \underline{\mu})$ cannot be reduced to $p_s(G_T)$ and λ_T can never be known until the set of equations given by (4.2) to (4.4) is solved in terms of G_T. Instead, λ_T can be found by trial and error as follows.

a) For given G_T, select a value for $\underline{T_p}$ between T_o and T_r.

b) Set $\lambda_T = G_T/\underline{T_p}$.

c) Compute $p_s^{(i)}$ for given $\underline{\mu} = 1/\underline{T}_p$ and λ_T following the procedure in the next subsection.[1]

d) Solve the set of equations (4.2) to (4.4)

e) Obtain the right hand side of (4.5) and compare it with λ_T set in (b).

f) If they are equal or the absolute value of the difference is less than a small value ε, we are done. Otherwise, change $\underline{T}_p$ and try again following the same steps from b to e.

Let $\underline{T}_p$ be the average packet service time. Since at equilibrium $(\lambda_1+\lambda_{M+1})$ of total composite arrivals generates packets of length T_o while the rest generates a packet of length T_r, the average packet service time is given by

$$\underline{T}_p = \frac{T_o \cdot (\lambda_1 + \lambda_{M+1}) + T_r \cdot \sum_{i=2}^{M} \lambda_i}{\lambda_T} \tag{4.8}$$

4.3 Packet Success Probability Bounds

Before starting the analysis, it should be noted that, when evaluating probability of packet success in CDMA unslotted ALOHA system, the random variation of the number of active users during a packet service time have to be taken into account. In [11] and [56], an efficient method to compute the probability of packet success has been proposed for hard decision decoding. However, since a soft decision for turbo decoding is considered here, the method in [11] cannot be applied to evaluate the probability of packet success for given packet generation statistics. Due to the difficulties in evaluating exact values, a lower and an upper bound is evaluated, each of which gives the corresponding lower and upper bound on the system throughput.

---

[1] Instead of finding the actual value of $p_s^{(i)}$, we find a lower and upper bound, which give the corresponding throughput bounds

4.3.1 Lower Bound on Packet Success Probability, $p_s(\lambda, \mu)$

The code performance can be related to SNIR, which is, in CDMA system, expressed in terms of the number of active terminals. In random access systems, such as unslotted ALOHA, however, the number of active terminals varies with time and, hence, the statistical property of the random fluctuation of active terminals should be examined first.

In Figure 4.2, one can safely assume by applying Burke's theorem that the packet arrival at each node is a Poisson process and by Jackson's theorem each node can be regarded as an independent queue, so that the composite offered traffic is simply a sum of the offered traffic to each node. Since the SNIR is governed by the total traffic, it is not needed to handle each node separately to evaluate SNIR fluctuation. Let the system state be the number of active interfering terminals (not including the desired one) at any given time during a packet transmission of the terminal under consideration. Let Δt be a small time duration, such that the state transition after Δt time lapse can be described as a birth-death process. Let λ and μ be the composite arrival rate given by (4.5) and the average departure rate given by the inverse of (4.8), respectively. Note that unslotted ALOHA systems can be regarded as $M/M/\infty$ queue for exponential service time distribution [13] or $M/G/\infty$ queue for general distributions. The latter fits to the system described in Section 4.1.1, where only two types of packet of length T_0 or T_r is used. From [63], the state transition matrix for such queue, as well as for $M/M/\infty$ queue, is given by [63]

$$\mathbf{P}_{t\to t+\Delta t} = [p_{ij}], \tag{4.9}$$

where

$$p_{ij} = p(k_{t+\Delta t} = j \mid k_t = i) = \begin{cases} \lambda \cdot \Delta t & \text{for } j = i+1 \\ 1-\lambda \cdot \Delta t - \mu \cdot i \cdot \Delta t & \text{for } j = i \\ \mu \cdot i \cdot \Delta t & \text{for } j = i-1 \\ 0 & \text{otherwise} \end{cases} \tag{4.10}$$

For a stationary Markov process with the transition matrix in (4.9), there exists a row vector **m**, such that $\mathbf{m} = \mathbf{m}\mathbf{P}_{t\to t+\Delta t}$, representing the steady-state distribution of system state. With (4.10), **m** is a vector whose element is the Poisson distribution given by

$$m_k = \frac{(\lambda/\mu)^k}{k!}\exp\left(-(\lambda/\mu)\right) \quad \text{for } k = 0,1,2,\ldots \tag{4.11}$$

Let $\mathbf{k}_j = (k_{j,\Delta t}, k_{j,2\Delta t}, \ldots, k_{j,T_j})$ denote a realization of state sequence in the packet duration T_j of the j^{th} attempt. Suppose that the base station has received packets from a terminal node up to i^{th} attempt and combined it with the previous packets to form a codeword of time span $T^{(i)} = T_1 + T_2 + \cdots + T_i$ and of effective code rate given by (4.1). Since in CDMA system the error performance depends on the number of interfering users, the conditional probability of packet success for given state sequence during the composite packet time $T^{(i)}$ can be defined as $p_s^{(i)}(\mathbf{k}_1, \mathbf{k}_2, \ldots, \mathbf{k}_i)$. However, it is very difficult to evaluate $p_s^{(i)}(\mathbf{k}_1, \mathbf{k}_2, \ldots, \mathbf{k}_i)$. Instead, it can be lower bounded by [60, 74];

$$p_s^{(i)}(\mathbf{k}_1, \mathbf{k}_2, \ldots, \mathbf{k}_i) \geq p_s^{(i)}(k_{\max}^{(i)}) \tag{4.12}$$

where $k^{(i)}_{\max}$ is defined as the largest element in the composite vector $[\mathbf{k}_1\ \mathbf{k}_2 \cdots \mathbf{k}_i]$; i.e. letting $k_{j,\max}$ be the largest element in $\mathbf{k}_j$,

$$k_{\max}^{(i)} \equiv \max_j\left(k_{j,\max}\right) = \max_j\left(\max_l k_{j,l\Delta t}\right).$$

$p_s^{(i)}(k)$ is the probability of packet success at i^{th} attempt, assuming the number of interfering users is the same k throughout the composite time interval $T^{(i)}$. As will be shown later, the evaluation of $p_s^{(i)}(k)$ is numerically feasible. With this bound, the average probability of packet success for given λ and μ can also be bounded by

$$p_s^{(i)}(\lambda,\mu) \geq \sum_k p_s^{(i)}(k) \cdot \Pr\{k_{\max}^{(i)} = k \mid \lambda,\mu\} \tag{4.13}$$

The probability mass function $\Pr\{k_{\max}^{(i)} = k \mid \lambda,\mu\}$ in (4.13) can be found by first evaluating the cumulative mass function

$$\Pr\{k_{\max}^{(i)} \leq k \mid \lambda,\mu\} \tag{4.14}$$

The time interval $T^{(i)}$ consists of i composite time intervals, T_1, T_2,..., T_i, each of which corresponds to the packet duration of the j^{th} attempt for $j = 1,2,\ldots,i$. Consecutive elements in $\mathbf{k}_j$ are correlated with each other since a state sequence $\mathbf{k}_j$ is Markov process described by the state transition matrix $\mathbf{P}_{t\to t+\Delta t}$ in (4.9). While, each state sequence $\mathbf{k}_j$, $j = 1,2,\ldots,i$ can be regarded independent of each other, as inter-attempt time interval between any two successive attempts is assumed large enough. Note also that for given λ and μ all $\mathbf{k}_j$ for $j = 1,2,\ldots,i$ are statistically identical as they come from the same Markov model defined by (4.9) and (4.10), except for their time span T_j.

Define $p_{k_{\max}}(k,T \mid \lambda,\mu)$ as the probability that a state sequence, which is drawn from a Markov process given by the state transition matrix $\mathbf{P}_{t\to t+\Delta t}$ with parameter λ and μ, has the largest state less than or equal to k in a time interval T; i.e.

$$p_{k_{\max}}(k,T \mid \lambda,\mu) = \Pr\{\text{The largest state in a time interval } T \leq k \mid \lambda,\mu\} \tag{4.15}$$

In particular, $\Pr\{k_{j,\max} \leq k \mid \lambda,\mu\} = p_{k_{\max}}(k,T_j \mid \lambda,\mu)$ for $j = 1,2,\ldots,i$. Since each state sequence $\mathbf{k}_j$, $j = 1,2,\ldots,i$ is independent of each other, the cummulative mass function can be expressed as a product form; i.e.

$$\Pr\{k_{\max}^{(i)} \le k \mid \lambda,\mu\} = \prod_{j=1}^{i} \Pr\{k_{j,\max} \le k \mid \lambda,\mu\} = \prod_{j=1}^{i} p_{k_{\max}}(k,T_j \mid \lambda,\mu) \qquad (4.16)$$

The probability $p_{k_{\max}}(k,T \mid \lambda,\mu)$ can be computed using the transition matrix $\mathbf{P}_{t\to t+\Delta t}$ and its steady-state distribution $\mathbf{m}$ for given λ and μ. As shown in Figure 4.3, all these sequences that have the largest state less than or equal to k in a time interval T lie in the shaded region. Therefore, the probability $p_{k_{\max}}(k,T \mid \lambda,\mu)$ can be found by enumerating all the state paths within this shaded region.

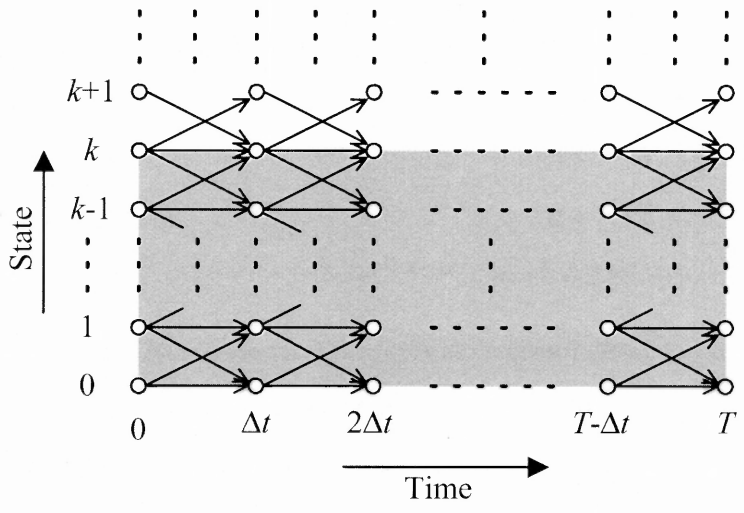

Figure 4.3 Trellis diagram for a Markov process. All the state sequences that have largest state less than or equal to k in a time interval T lie in the shaded region. We can find the probability $p_{k_{\max}}(k,T \mid \lambda,\mu)$ by enumerating the probability of all the state paths within this region.

Define $\mathbf{P}^{(k)}_{t\to t+\Delta t} = [p^{(k)}_{ij}]$ as the $(k+1)\times(k+1)$ principal sub-matrix of $\mathbf{P}_{t\to t+\Delta t} = [p_{ij}]$ such that $p^{(k)}_{ij} = p_{ij}$ for $i,j = 0,1,\ldots,k$. and $\mathbf{m}^{(k)} = [m_i^{(k)}]$ as the $1\times(k+1)$ row vector, which is the truncation of $\mathbf{m} = [m_i]$ such that $m_i^{(k)} = m_i$ for $i = 0,1,\ldots,k$. Let $\underline{\mathbf{m}}^{(k)}$ be the vector

obtained by enumerating all the state transitions for time interval T in the shaded region in Figure 4.3 (i.e. for $T/\Delta t$ transitions), then

$$\underline{\mathbf{m}}^{(k)} = [\underline{m}_i^{(k)}] = \mathbf{m}^{(k)} \cdot \left(\mathbf{P}_{t \to t+\Delta t}^{(k)}\right)^{T/\Delta t}, \tag{4.17}$$

whose i^{th} element is the probability of the state sequences that has a largest state less than or equal to k in a time interval T and is terminated at state i. Hence, the cumulative mass function, $p_{k_{\max}}(k, T \mid \lambda, \mu)$, can be found by summing up all the element of $\underline{\mathbf{m}}^{(k)}$; i.e.

$$p_{k_{\max}}(k, T \mid \lambda, \mu) = \sum_{i=0}^{k} \underline{m}_i^{(k)}. \tag{4.18}$$

Now, substituting (4.18) into (4.16) and taking derivative of (4.14) with respect to k, one can obtain the probability mass function $\Pr\{k_{\max}^{(i)} = k \mid \lambda, \mu\}$ needed for (4.13).

Note that $p_s^{(i)}(k)$ is the probability of packet success at i^{th} attempt assuming the number of interfering users is the same k throughout the composite time interval $T^{(i)}$. Since a codeword of the punctured turbo code of rate given by (4.1) is transmitted through the composite time $T^{(i)}$, $p_s^{(i)}(k)$ is just one minus the probability of codeword error evaluated at the SNIR corresponding to the number of interfering users, k, and the background noise power. For matched filter receiver, denoting $\gamma_{MF,AWGN}$ as the SNIR at its output of the receiver, $p_s^{(i)}(k)$ is simply given by

$$p_s^{(i)}(k) = 1 - p_{we}^{(i)}\left(\gamma_{MF,AWGN}\right) = 1 - p_{we}^{(i)}\left([\beta^{-1} + 2k/3N]^{-1}\right) \tag{4.19}$$

where β is the signal to background noise ratio, N is the bandwidth expansion factor (processing gain) of the CDMA system and k is the number of signals interfering with the desired signal. $p_{we}^{(i)}(\gamma)$ is the word error probability of the turbo code of rate given by

(4.1), evaluated at the SNIR of γ. Hence, for $p_{we}^{(i)}(\gamma)$, we can utilize the results of Chapter 2 (Figure 2.3). Together with the results of the previously computed probability mass function, we obtain the lower bound of (4.13).

4.3.2 An Upper Bound on $p_s(\lambda, \mu)$

Comparing to the lower bound, the upper bound on $p_s^{(i)}(\lambda,\mu)$ is not that meaningful since an upper bound on $p_{we}^{(i)}(\gamma)$ will actually be used, rather than itself. Nevertheless, the author provides an upper bound for $p_s^{(i)}(\lambda,\mu)$ using the upper bound on $p_{we}^{(i)}(\gamma)$ plotted in Figure 2.1, hoping to give an intuition on the steady-state system behavior.

Similar to the lower bound, an upper bound also can be found by

$$p_s^{(i)}(\mathbf{k}_1,\mathbf{k}_2,...,\mathbf{k}_i) \le p_s^{(i)}(k_{\min}^{(i)}) \tag{4.20}$$

with $k_{\min}^{(i)} \equiv \min_j(k_{j,\min}) = \min_j(\min_l k_{j,l\Delta t})$

However, to make the upper bound tighter, consider the following argument. Define $k_{mean}^{(i)}$ as the mean value of the composite vector [$\mathbf{k}_1$ $\mathbf{k}_2$ $\cdots$ $\mathbf{k}_i$], around which the state sequences randomly fluctuate. Note that when SNIR fluctuate with time, as in time varying fading channel, a word error rate is dominated by the symbols of which the SNIR is relatively small. In other word, the word error rate for AWGN channel with a certain SNIR is lower than that for time varying fading channel with the same value of average SNIR. We can extrapolate this situation to our case, in which the random fluctuation comes from the system load change, not from signal power change. In CDMA system SNIR is directly related to the number of active users. Hence, if the average SNIR roughly corresponds to $k_{mean}^{(i)}$, we can intuitively infer that the probability of packet success, $p_s^{(i)}(\mathbf{k}_1, \mathbf{k}_2,...., \mathbf{k}_i)$, is upper bounded by $p_s^{(i)}(k_{mean}^{(i)})$. Although this is just an

intuition, it is enough to give us a rough, but quite reasonable upper bound on the throughput performance of the system. Assuming that the PDF of $k^{(i)}_{mean}$ roughly corresponds to that of the system state distribution, which is given by Poisson distribution defined in (4.11), we have a rough upper bound, but tighter than that with (4.20), as follows.

$$\begin{aligned} p_s^{(i)}(\lambda,\mu) &\le \sum_k p_s^{(i)}(k)\cdot \Pr\{k^{(i)}_{mean}=k \mid \lambda,\mu\} \\ &\approx \sum_k p_s^{(i)}(k)\cdot \Pr\{k \mid \lambda,\mu\}^2 \\ &= \sum_k p_s^{(i)}(k)\cdot m_k \end{aligned} \tag{4.21}$$

where $\Pr\{k|\lambda,\mu\}$ is the probability that the system is in state k and m_k is the k^{th} element of the vector **m**. Note that the last line in (4.21) is the same form as the average probability of packet success for CDMA slotted ALOHA. Since a slotted ALOHA always perform better than an unslotted ALOHA for given offered traffic, $G = \lambda/\mu$, (4.21) can be regarded as an upper bound of CDMA unslotted ALOHA. As reported in [11], when applying CDMA to ALOHA, the performance difference between slotted and unslotted is not so big as in conventional ALOHA system, where the throughput difference is as big as 2:1.

---

[2] Preliminary experiments show the assumption is quite reasonable. Actually, the ensemble mean of the system state is exactly equal to $Ek^{(i)}_{mean}$, even though the second order statistic shows a small difference. Generally, $Var\ k^{(i)}_{mean} < Var\ k_t$ with k_t being the system state at a given time t. Hence we could approximate $\Pr\{k^{(i)}_{mean}|\lambda,\mu\}$ to $\Pr\{k|\lambda,\mu\}$.

4.3.3 Threshold Effect and Channel Load Sensing Protocol

In asynchronous CDMA system, MAI is the limiting factor on the performance. Thus, for given system parameters, such as processing gain and code rate, it is desirable to limit the number of active users, so as to ensure proper operation without system breakdown. This can be easily implemented with, for example, the preamble acknowledgement protocol as in random access in WCDMA system [17,18] or the Channel Load Sensing Protocol (CLSP) [57,59]. For convenience, the author consider the latter, where it is not needed to take into account the additional random fluctuation due to the preamble-only transmission. When applying channel load sensing protocol to a Poisson arrival model with composite offered traffic G_T, the system can be regarded as a *M/M/m* queue with finite value *m*, in which the state distribution is expressed by a truncated Poisson distribution [59]; i.e.

$$m_k = \frac{G_T^k / k!}{\sum_{n=0}^{K_{th}} G_T^n / n!} \quad \text{for } k = 0,1,\ldots,K_{\text{th}}. \tag{4.22}$$

where K_{th}, the threshold of truncation, is the maximally allowable number of active terminal nodes. With (4.22), the actual offered traffic is given by

$$G_{T,act} = \sum_{n=0}^{K_{th}} n \cdot m_n \tag{4.23}$$

[3]

To relate the throughput S to the composite offered traffic G_T, the same set of equation from (4.2) to (4.7) should be solved, but now G_T in (4.2) replaced with $G_{T,act}$. Similar to the previous discussion, λ_T and the corresponding $\mu = \lambda_T / G_{T,act}$ should be found by trial and error as described in Section 4.2.

---

[3] Note that for untruncated case ($K_{th} \to \infty$), $G_T = G_{T,act}$.

4.4 Numerical Results

The punctured turbo codes used here are the same as that in Chapter 2, i.e. a set of punctured turbo codes of input frame length 512 and code rate of 4/5, 2/3, 4/7, 1/2, 4/9, 2/5, 4/11 and 1/3. With the setup in Section II-B, we identify that $L_o = 512$, $L_r = 128$ and $M = 9$. The effective code rate at successive attempt is 1, 4/5, 2/3, 4/7, 1/2, 4/9, 2/5, 4/11 and 1/3, respectively.

Figure 4.4 shows the lower bounds on the average probability of packet success given by (4.13) and, in Figure 4.5, the two throughput bounds of CDMA unslotted ALOHA systems with hybrid type-II ARQ, each of which corresponds to the lower and upper bound on $p_s^{(i)}$. To compute $p_s^{(i)}(k)$ in (4.19), the results in Chapter 2 (Figure 2.3) was used for $p_{we}^{(i)}(\gamma)$. Although the lower and upper bounds are not so tight, especially when the offered traffic gets heavy, the results give us some insight into the system behavior. Figure 4.5 also plots, for comparison, the performance of unslotted ALOHA system without spreading (i.e. $(G_T)\cdot\exp(-2G_T)$), and the lower bounds of CDMA unslotted ALOHA with hybrid type-I ARQ using fixed rate of punctured turbo codes. Similar to the results with hybrid type-I ARQ in Chapter 2, the lower the code rate the higher the maximal channel efficiency could be obtained. Notice that when employing an efficient channel coding, such as turbo coding, to combat the MAIs, the CDMA unslotted ALOHA outperform the conventional ALOHA in packet throughput performance. Moreover, since CDMA system allows cell deployment with frequency utilization of 1, the overall channel efficiency can be higher, even when the degradation due to inter-cell interference is taken into consideration. Finally, as one may expect with the use of RCPT codes, hybrid type-II ARQ can automatically adjust the code rate so that the maximal throughput can be achieved with minimal channel usage. Figure 4.6 and 4.7 show the same plots as Figure 4.4 and 4.5 except for adding Channel Load Sensing Protocol, in which the normalized threshold α defined as K_{th}/N was set to 3.25. This is the system load that can be maximally supported by 1/3 rate turbo code, as shown in Figure 2.5.

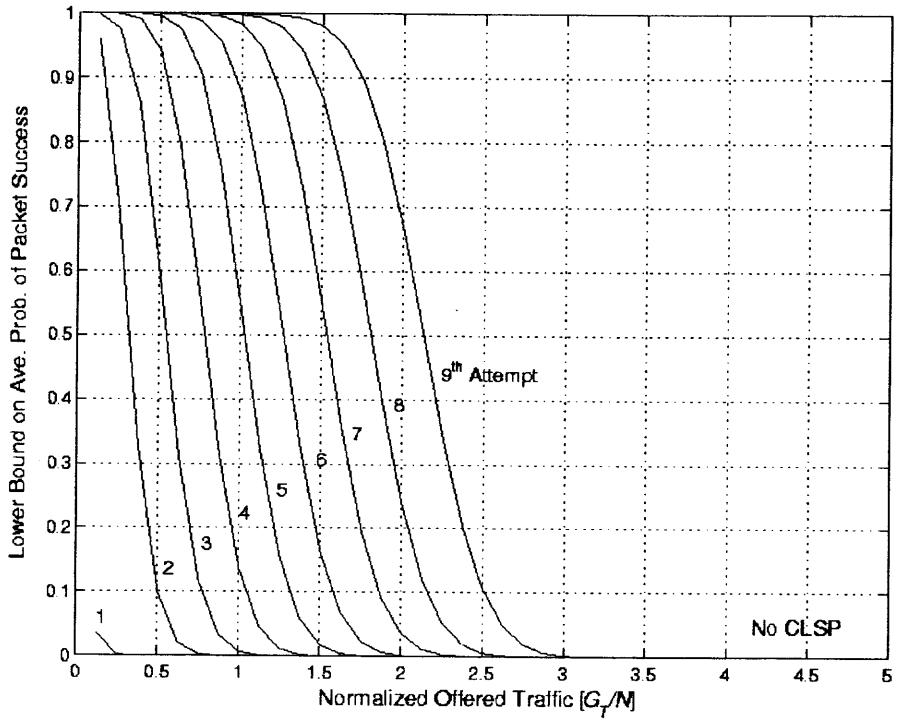

Figure 4.4 Lower bounds on the average probability of packet success at each attempt ($p_s^{(i)}(\lambda_T,\mu)$).

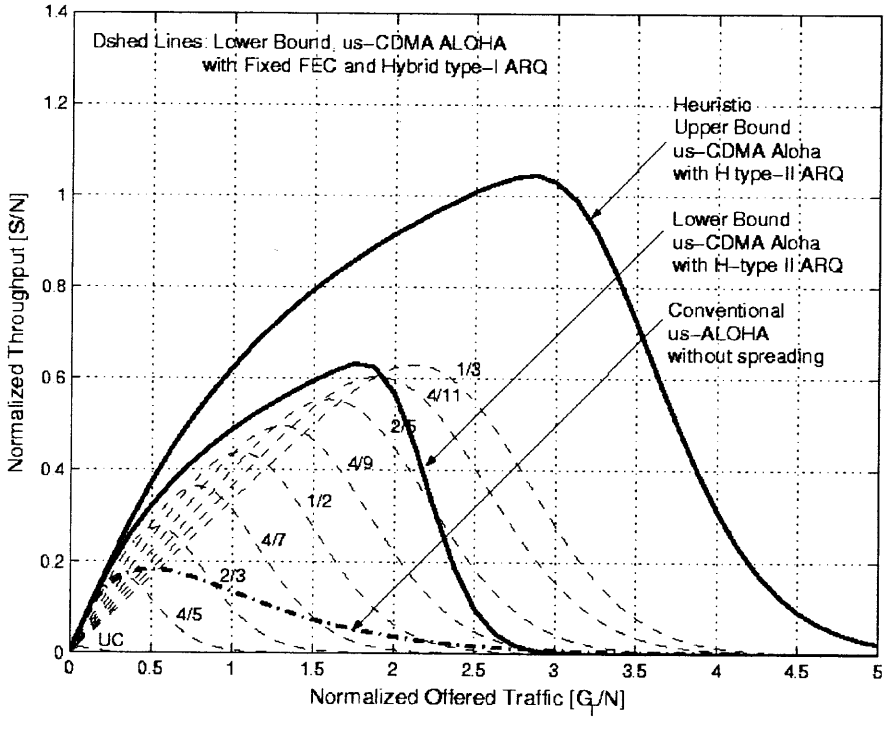

Figure 4.5 Throughput Bounds (Lower and Upper) of CDMA Unslotted ALOHA with Hybrid type-II ARQ using RCPT codes.

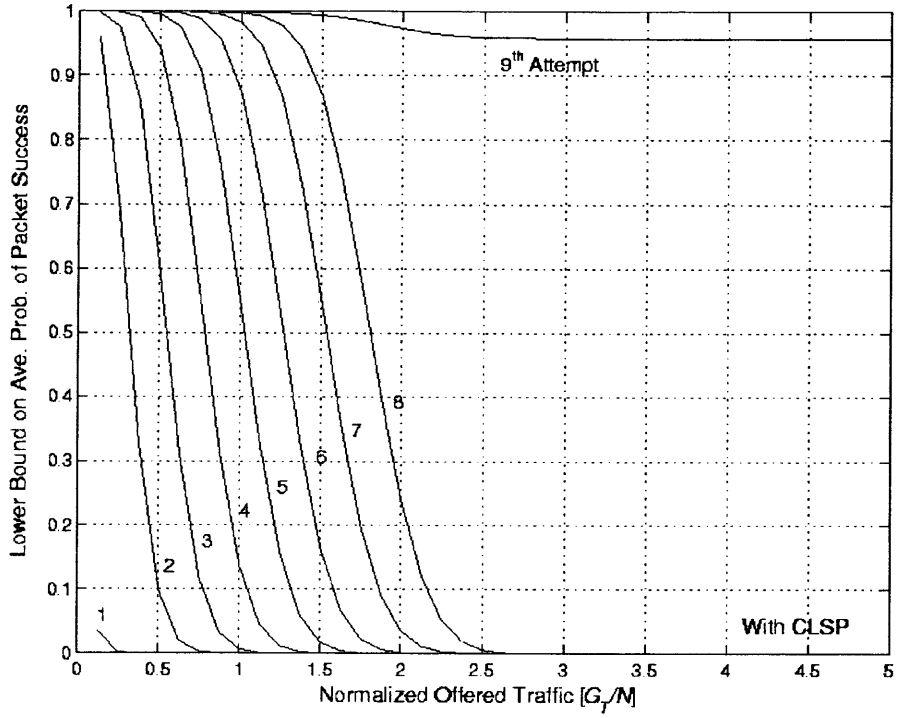

Figure 4.6 Lower bounds on the average probability of packet success at each attempt ($p_s^{(i)}(\lambda_T,\mu)$) with Channel Load Sensing ($\alpha = 3.25$).

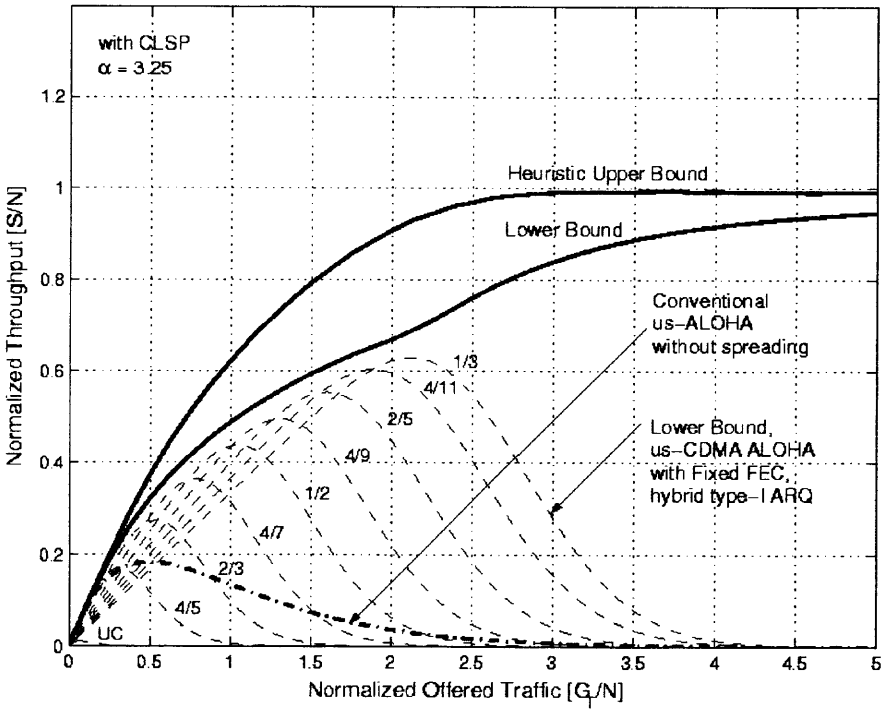

Figure 4.7 Throughput Bounds of CDMA Unslotted ALOHA with Channel Load Sensing Protocol ($\alpha = 3.25$).

Figure 4.8 depicts the throughput versus offered traffic curves with different values of thresholds. It shows that when the normalized threshold is less than 3.25, the throughput degradation at high traffic region is not so big, while it is catastrophic if the threshold exceeds 3.25. Thus, to ensure the proper system operation without system breakdown while keeping the channel efficiency maximized, the threshold should be carefully chosen according to the channel coding option of the system.

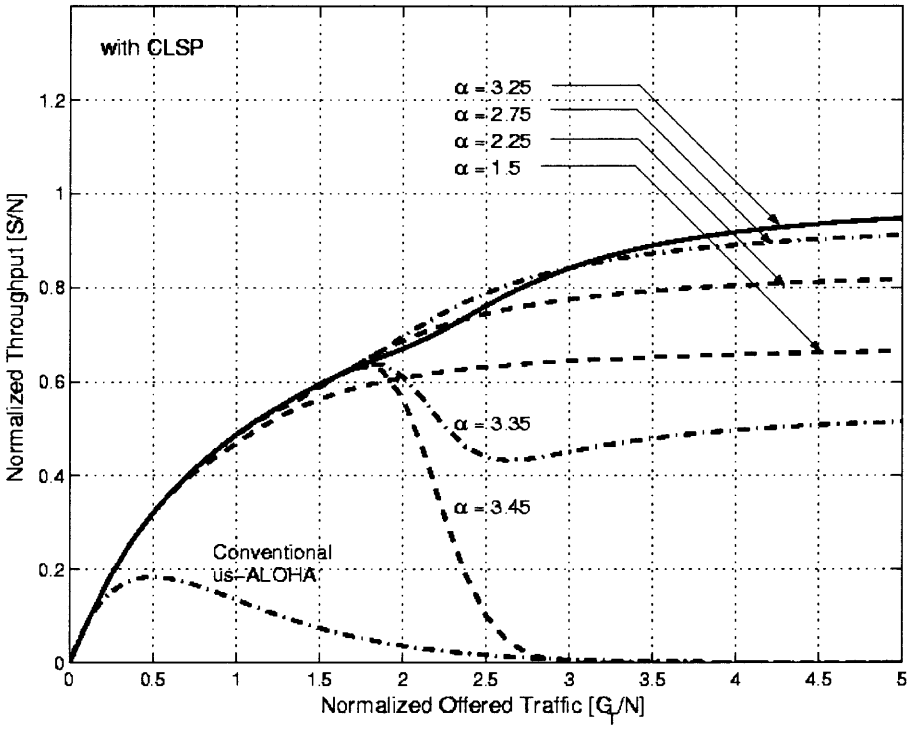

Figure 4.8 A Comparison of Throughput Bounds of CDMA Unslotted ALOHA with Channel Load Sensing Protocol, for various value of α.

4.5 Chapter Summary

CDMA unslotted ALOHA system is one of important candidate for packet data network, especially over cellular system with medium to large coverage area. The RACH protocol of WCDMA is very similar to CDMA unslotted ALOHA, except that the RACH

channel in WCDMA allows transmission at the predefined time offsets. However, since the offset time interval is much smaller than the packet duration (one tenth), it can be regarded as a modified version of CDMA unslotted ALOHA system. With this in mind, the author analyzed the throughput bound of CDMA based unslotted ALOHA system that employs hybrid type-II ARQ using rate compatible punctured turbo codes, which is a plausible scenario for packet data transmission over 3G Wireless or IEEE 802.11.a.

To analyze such system, the author introduced an expanded analytical model describing the equilibrium traffic flow of an ALOHA system with hybrid type-II ARQ. This model could be regarded as a network of queues so that Jackson and Burke's theorems could be applied to simplify the analysis. Assuming soft-decision decoding at receiver, the author also evaluated a lower and an upper bound on the probability of packet success. Then, with the expanded model and the packet success probability bound, the corresponding throughput bounds were obtained for given composite offered traffic. The author believes that the results shown in this Chapter can provide some insights into the CDMA based random access system behavior, especially when employing hybrid type-II ARQ.

CHAPTER 5

AN IMPLEMENTATION ISSUE: PARALLEL MAP ALGORITHM FOR LOW LATENCY TURBO DECODING

One of the problems in Turbo Code implementation is its decoding delay. In this chapter, the author proposes a parallel processing scheme for turbo decoding, which can be regarded as a blocked belief propagation algorithm. Since a convolutional code is used as a constituent code for turbo code, due to the recursive and iterative nature of the decoding algorithm the decoding delay may be unacceptable for present digital technology.

In the proposed blocked structure, each sub-block performs MAP decoding in parallel. However, unlike the previously proposed parallel scheme, where sub-block overlapping is used, it utilizes the forward and backward variables computed in the previous iteration to provide boundary distributions for each sub-block MAP decoder. The structure can be described as a coordinated belief propagation algorithm and is asymptotically optimal in the sense that the BER performance finally converges to the same as that of original turbo decoder. Although convergence of the belief propagation algorithm have not been proved yet, the simulation results show that the structure can converge in almost the same rate as that of original turbo decoding, provided that each sub-block has a reasonable length.

5.1 Decoding Delay in Turbo Codes

In turbo coding, convolutional codes are used as a constituent code in order to obtain a large coding gain and the decoding algorithm employs a type of recursive scheme, such as symbol-by-symbol MAP decoding [75,76] (also known as forward-backward algorithm) or its logarithmic versions [77] in which the variables are computed recursively. Moreover, since turbo decoding is an iterative algorithm, the decoding delay may not be acceptable.

Let $T_{codeword}$ be the time duration of a codeword and $T_{computation}$ be the decoding computation time. In convolutional codes, the decoding delay can be far less than $T_{codeword}$ if one uses a sliding window algorithm as described in [78]. While, since turbo code is a block code, the decoding delay cannot be less than $T_{codeword}$. For a block code, in which the decoding process can start only after the reception of an entire codeword, the decoding delay is the sum of $T_{codeword}$ and $T_{computation}$. To reduce the decoding delay in turbo decoding, one may use a short frame size code at the expense of performance degradation. This is a plausible option in low data rate systems because $T_{codeword}$ is the dominant factor in decoding delay. However, in high data rate systems, such as multi-mega bps, it may be required to reduce $T_{computation}$, which is dominant.

There are several approaches to reduce $T_{computation}$ in turbo decoding, including the parallel decoding schemes of [79], [80] and [81], in which multiple processors are used. In [79] and [80], the whole trellis stages are divided into multiple overlapped sub-blocks and the same MAP decoder as that of the regular turbo decoder is used for each sub-block. On the other hand, in [81], a sectionalized trellis is divided into sub-trellises, and multiple processors are used in parallel to compute the branch metrics in each sub-trellis[4].

This Chapter presents a parallel MAP algorithm in which, instead of using overlapping between neighbor sub-blocks, the forward and backward variables that were computed in the previous iteration is utilized as intermediate boundary distributions for each sub-block MAP decoder. In the structure of [79] and [80], each sub-block utilizes, in fact, only partial observations and hence it is possibly sub-optimal unless a reasonable overlapping depth is used, while the proposed scheme utilizes all the observations by message passing.

---

[4] This work may seem related to our work, but, in fact, it is totally different in principle

5.2 Forward-Backward Algorithm for Turbo Decoding

Consider a turbo code with two 1/2 rate systematic convolutional codes as its constituent code, whose simplified decoder structure is depicted in Figure 5.1. MAP 1 and 2 are the maximum a posteriori (MAP) decoders for constituent codes 1 and 2, respectively. One iteration of turbo decoding includes MAP 1, interleaving, MAP 2 and deinterleaving, in this order. MAP decoding includes the computation of forward variables, backward variables and the extrinsic part of the likelihood ratio.

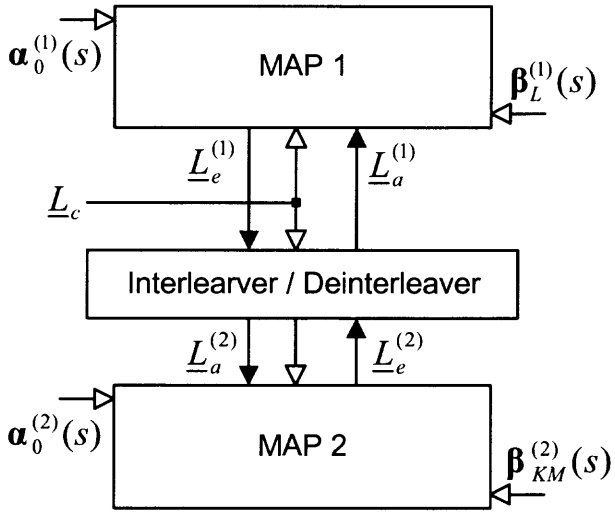

Figure 5.1 A simplified diagram of turbo decoder.

A problem with this structure is that MAP decoding is a recursive process and the entire decoding should be repeated many times (typically 5~10 iterations), causing a large computational decoding delay. Let $\alpha_j^{(i)}(s)$ and $\beta_j^{(i)}(s)$ be the forward and backward variables at the j^{th} trellis stage of state s of the i^{th} constituent code. For a detailed description of the turbo decoding algorithm and MAP decoding, see [75]. In MAP decoding, the whole forward and backward variables are computed recursively. For the former, starting from an initial distribution $\alpha_0^{(i)}(s)$, $\alpha_j^{(i)}(s)$ is computed recursively based on the distribution of the previous variable $\alpha_{j-1}^{(i)}(s)$ and the channel inputs for the j^{th}

trellis stage. Similarly, for the latter, starting from $\beta_L^{(i)}(s)$, $\beta_j^{(i)}(s)$ is computed from $\beta_{j+1}^{(i)}(s)$ and the related observations. Due to the iterative and recursive nature of the decoding algorithm, the decoding computation time can be very large.

To reduce the decoding time, a parallel MAP scheme was proposed in [80], where a whole L trellis stages is divided into K sub-blocks and processed in parallel. However, when implementing each sub-block MAP separately in parallel, appropriate boundary distributions are not available. Hence, in [80], overlapping between neighbor sub-blocks is used; i.e. k^{th} sub-block MAP decoder starts its forward recursion from $\alpha_{(k-1)M-d}^{(i)}(s)$ and the backward recursion from $\beta_{kM+d}^{(i)}(s)$, where d is an integer representing the overlapping depth. Therefore, each sub-block MAP contains a computation of $M = L/K + 2d$ trellises and requires the additional $2d$ computations for each sub-block to provide appropriate boundary distributions at $\alpha_{(k-1)M}^{(i)}(s)$ and $\beta_{kM}^{(i)}(s)$. Furthermore, the algorithm is necessarily sub-optimal unless it uses large overlapping. As a rule of thumb, this overlapping depth should be 5 to 7 times the constraint length of the constituent convolutional code, to provide valid state distribution and to ensure the code performance to some extent.

5.3 Parallel Turbo Decoding: Blocked Belief Propagation Algorithm

A turbo decoder that employs the proposed parallel scheme is shown in Figure 5.2. As in [80], the noisy codeword of a constituent convolutional code of length L is divided into K sub-blocks of length $M = L/K$ trellis stages. However, instead of using overlapping, the forward and backward variables that were computed in the previous iteration of the adjacent sub-blocks are used to provide appropriate boundary distributions for each sub-block MAP decoder; i.e. the k^{th} sub-block MAP decoder starts the forward recursion with $\hat{\alpha}_{(k-1)M}^{(i)}(s)$ and the backward recursion with $\hat{\beta}_{kM}^{(i)}(s)$, where $\hat{}$ represents the values were computed in the previous iteration. All sub-block MAP decoders perform the computation simultaneously, and hence, the proposed algorithm reduces the decoding

computation time exactly by a factor of K, provided that it requires the same number of iterations to converge as that of the regular turbo decoder. This will be discussed later in Section 5.5.

Parallel MAP decoding

The operation of the proposed parallel MAP decoder can be summarized as follows. For the k^{th} sub-block, use $\hat{\alpha}^{(i)}_{(k-1)M}(s)$ and $\hat{\beta}^{(i)}_{kM}(s)$ as initial distributions in the corresponding sub-block MAP recursion to compute $\alpha^{(i)}_{(k-1)M+1}(s)$, $\alpha^{(i)}_{(k-1)M+2}(s)$,..., $\alpha^{(i)}_{kM}(s)$ and $\beta^{(i)}_{kM-1}(s)$, $\beta^{(i)}_{kM-2}(s)$,..., $\beta^{(i)}_{(k-1)M}(s)$, recursively in that order. Then, use the resulting forward and backward variables and $\underline{L}_a{}^{(i)}_{(k-1)M+jk}$ to compute the extrinsic information $\underline{L}^{(i)}_{e,(k-1)M+j}$, for j=1,..,M. These computations are performed in parallel for all sub-block decoders. Finally, store the boundary distributions $\alpha^{(i)}_{kM}(s)$ and $\beta^{(i)}_{(k-1)M}(s)$ into memory to be used for the neighbor sub-blocks in the next iteration.

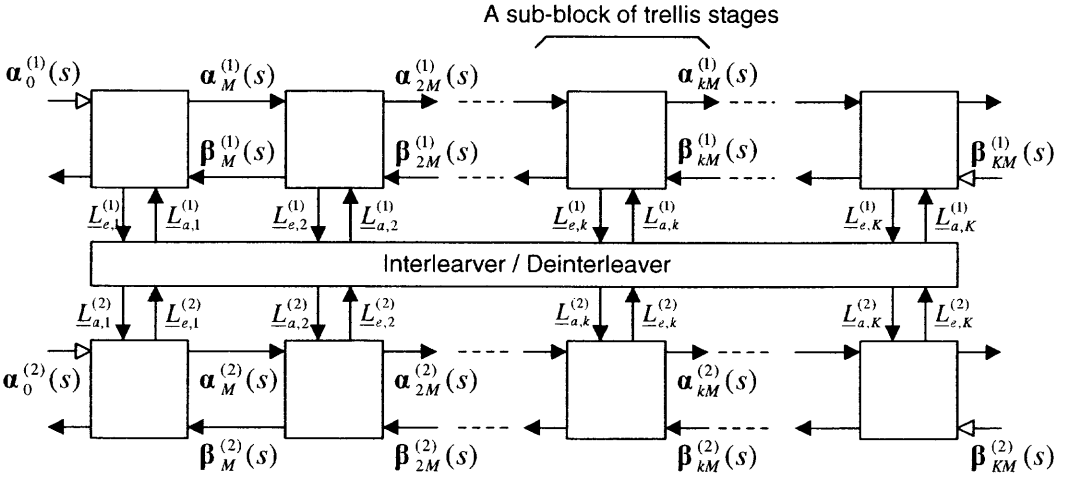

Figure 5.2 Turbo decoder with Blocked MAP. All the sub-block decoders, shown as a box, are implemented in parallel and perform the same operation; each of them starts forward-backward recursion with the boundary distributions computed in previous iteration.

It should be emphasized, as reported in [82-86], that the iterative turbo decoding can be described as a "Belief Propagation" algorithm, in which the likelihood ratios (beliefs) on the transmitted information bits are updated iteratively by exchanging information between nodes in a graph. Unfortunately, the convergence of the Belief Propagation algorithm for a loopy network[5] is not yet proven. However, as mentioned in [82], it inspires various other strategies for turbo decoding according to how the message passing in the graphical model is coordinated. In fact, immediate application of the belief propagation algorithm to the "hidden Markov chain", described in [82], results in our parallel MAP decoder with sub-block length M equal to 1. As in the belief propagation paradigm, the k^{th} sub-block decoder takes messages $\alpha_{(k-1)M}^{(i)}(s)$, $\beta_{kM}^{(i)}(s)$, i=1 or 2, from its neighbors and $\underline{L}_{a,k}^{(i)}$ from the other constituent decoder, produces updated information $\alpha_{kM}^{(i)}(s)$, $\beta_{(k-1)M}^{(i)}(s)$, $\underline{L}_{e,k}^{(i)}$ and sends them back to its neighbors. $\underline{L}_{a,k}^{(i)}$ and $\underline{L}_{e,k}^{(i)}$ denote $M\times 1$ vectors representing *a priori* and extrinsic information, respectively, of the k^{th} sub-block decoder in the i^{th} constituent code. For simplicity, the systematic part $\underline{L}_{c,k}^{(i)}$ was omtted in Figure 5.2. The white arrows in Figure 5.2 represent edge parameters that once initialized, remain fixed until the entire decoding is done. By the message passing between sub-blocks, each sub-block MAP decoder can utilize the whole observation to finally obtain optimal values on the likelihood ratios.

In [80], since each sub-block does not communicate with each other, the intermediate boundary distributions require additional neighborhood observations, which were provided by overlapping the sub-blocks. With the configuration in Figure 5.2, at least two advantages over the previous parallel MAP scheme in [79,80] can be obtained. First, there are no additional computations due to overlapping. Second, communicating with their neighbors, each sub-block MAP decoder can asymptotically converge to optimal values since information in one sub-block propagates through the whole network by message passing.

---

[5] As shown in [82], the graphical representation of turbo codes has many loops.

Initialization

Before proceeding with iterative decoding, the input messages to each sub-block decoder must be initialized properly. An example of the initialization of these variables is as follows.

1) Initialize permanently the edge boundary distributions

$$\alpha_0^{(i)}(s) = \beta_L^{(i)}(s) = \begin{cases} 1 & \text{for s} = 0 \\ 0 & \text{otherwise} \end{cases}.$$

2) Initialize temporally the intermediate boundary distributions $\alpha_{kM}^{(i)}(s) = \beta_{kM}^{(i)}(s) = 1/N_s$, for all s and k=1,..,K-1, where N_s is the number of states of the constituent convolutional code used, and store them into memory,.
3) Initialize the *a priori* likelihood ratios $\underline{L}_{a,k}^{(i)} = \mathbf{0}$, for k=1,2,..,K.

It was assumed that the constituent convolutional code starts and terminates at state zero with appropriate tail bits. The initialization in 2) was chosen for all intermediate boundary distributions since, when implemented in parallel, no priori information on the intermediate boundary distribution is available in the first iteration.

5.4 Simulation Results

In Figure 5.3, the bit error probabilities are plotted at each iteration step, by averaging over 1200 independent trials, each of which was simulated with sub-block lengths of 8, 16, 32, 128 and 8192, respectively. Since the overall block length was set to 8192 of information bits, the sub-block length of 8192 is equivalent to regular turbo decoding. At each trial, the interleaver was set at random. The simulations were performed with the Max-Log MAP algorithm.

Since the proposed parallel MAP algorithm is used to reduce computational delay, the convergence speed should also be taken into account. If the proposed algorithm requires more iterations than that required for the regular turbo decoder, the net delay

reduction may not be as much as we expected. In the figure, note the following. First, the final BER after convergence is almost the same as that of a regular turbo decoder. Second the longer the block length the faster the convergence. In this simulation, the performance with a sub-block length of 128 shows almost the same convergence speed as that of regular turbo decoding. This means that a delay reduction by a factor of $1/K$ can be obtained if one use a longer sub-block length than 128 for the turbo code used.

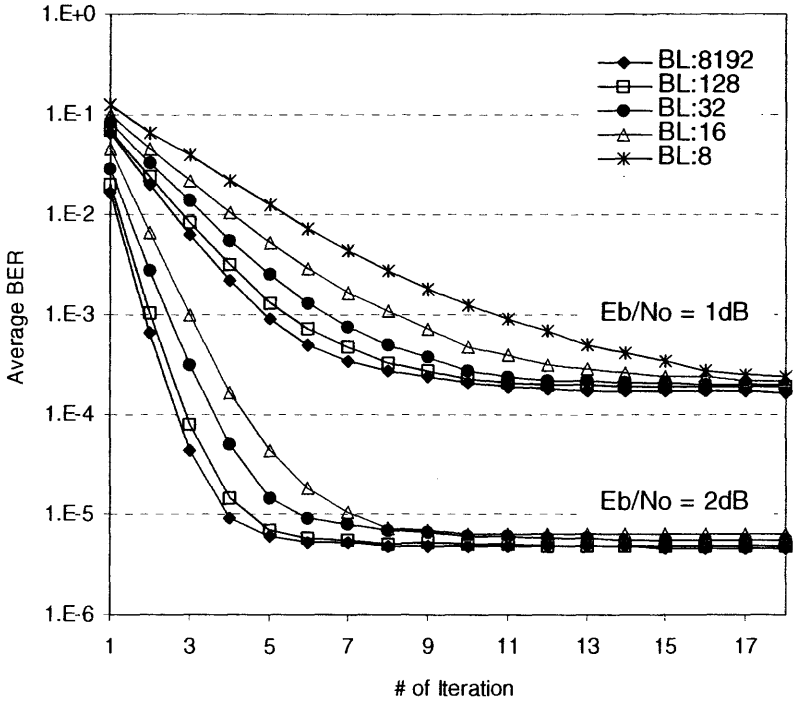

Figure 5.3 BER convergence of the blocked structure with sub-block length of 8, 16, 32, 128 and 8192 (equivalent to original turbo decoder) respectively. $E_b/N_0 = 1$.

The reason that the algorithm converge faster with longer sub-block is as follows. Although the convergence of the Belief Propagation algorithm for a loopy network is not yet proven, it can be intuitively inferred that a good initial boundary distribution would accelerate the convergence speed. Clearly, at the first iteration, the internal forward and backward variables computed in its early recursion of a sub-block MAP decoder will be

unreliable since, at initial iteration, no prior knowledge about the intermediate boundary distributions is available. However, if the sub-block length M is large enough, the values produced at the final recursion of each sub-block can be reliable enough. For example, for the k^{th} sub-block MAP of length M, the third forward variable, $\alpha_{kM+3}^{(i)}(s)$, can utilize only three observations, while $\alpha_{kM+M}^{(i)}(s)$ utilizes all the M observations that belongs to the k^{th} sub-block. Since the soft information is transferred through the recursive computation, even in the first iteration, quite reliable information on the boundary distributions can be obtained at the final recursion of a sub-block MAP decoding. The situation is similar to the sliding window algorithm for the decoding of convolutional codes, where the longer the trace back memory the better the performance we get.

5.5 Chapter Summary

In order to increase the decoding speed, the author propsed a parallel scheme of the forward-backward algorithm, where, instead of using overlaps as was previously suggested, the forward and backward variables computed at the adjacent sub-blocks in the previous iteration was used to provide appropriate boundary distributions to each sub-block MAP decoder. With the proposed algorithm, the computational decoding delay is divided exactly by M, the number of sub-block MAP processors. Simulation results show that the scheme asymptotically converges to the optimal performance in almost the same convergence rate as that of regular turbo decoder, provided that each sub-block is reasonably long. Compared to a regular turbo decoder, it requires only a small amount of additional memory, even though the algorithm employs multiple processors. Moreover, the modularity of the proposed algorithm makes hardware implementation easy; it is a concatenated structure of identical sub-block MAP decoders, all of which perform exactly the same operation as that of a regular MAP decoder.

CHAPTER 6

LINEAR MULTIUSER DETECTION IN RANDOM CDMA

The performance of LDD and MMSE detector is expressed in terms of the so-called 'near-far resistance', defined by a reciprocal of a diagonal component of inverse matrix. For random CDMA, the near far resistance is regarded as a random variable. Recently, many papers have dealt with the analysis of multiuser detectors for random spreading sequences. In most cases, however, these analyses derived only the expectations or bounds for the near-far resistance. Here, an approximate PDF of the near-far resistance is directly derived, based on Gaussian approximation of cross-correlation between any two of randomly generated spreading codes.

6.1 Introduction

Throughout the last decade, the linear multiuser detectors such as linear decorrelating detector [22-24] and MMSE detector [25,26] have been widely studied in various ways. The performances of those multiuser detectors were expressed in terms of reciprocal of diagonal components of inverse cross-correlation matrix, which is referred to as near-far resistance. In most cases, however, the performance analyses for those multiuser detectors have been performed for deterministic CDMA, in which it is assumed that the period of the spreading sequences is the same as the symbol interval and hence each component of the matrix is constant. In such case, the spreading sequence is said to be time-invariant.

On the other hand, in the currently commercialized or standardized CDMA systems, the performance has been analyzed for random CDMA system, where the periods of spreading sequences are much longer than the symbol interval. Although most multiuser detection schemes require short spreading sequence for reasonable complexity and practical point of view, the use of short spreading sequences does not necessarily

means that the analysis must be done for a specific set of spreading codes. There still exist many causes of the randomness of interference, even for the short spreading sequence system, such as random selection of spreading codes and/or random time delays. Considering these kinds of randomness, the author will call it, in general, random CDMA system, regardless of the type of spreading codes; short or long. With these reasons, each component of the cross-correlation matrix for random CDMA systems should be regarded as a random variable.

In more recent literatures [36-40], multiuser detectors have been considered for random CDMA system. In [36], the spectral efficiency of multiuser detectors has been analyzed for random spreading and provided with an average near-far resistance for various multiuser detectors. In [37-39], capacity of multiuser detector has been analyzed and compared with conventional matched filter receiver.

This chapter provides a direct approximation for the PDF of the near-far resistance of LDD and MMSE detector. Using this, the average BER performance for random spreading sequences can be obtained. For random CDMA signals, the statistical characterizations of each component of the inverse matrix are not tractable when the number of users is large. Therefore, based on the Gaussian approximation in [36,31,32], an approximate PDF of a near-far resistance for LDD and MMSE detector will be derived and used to obtain the average BER expression by taking expectation over the near-far resistance. Although the approach in this chapter is for random CDMA, even for deterministic CDMA system the cross-correlation has random nature due to the time variation of channel as well as the random assignment of spreading codes. Hence the results can also be interpreted as an expected BER performance in deterministic CDMA.[6]

---

[6] Even with short sequence system, due to the correlation property of PN sequences, one chip delay of a PN sequence can make the cross-correlation structure (an whole row of cross-correlation matrix) quite different. In this case we have to assume that the cross-correlation structure is random. And, we can calculate the expected BER by taking average over all possible set of cross-correlation. Clearly, the

6.2 Linear Multiuser Detectors

In this section, first, the operation and the performance of linear decorrelating detector and MMSE detector for time invariant CDMA signal will be briefly described. The Gaussian approximation will then be described in discrete time version to fit into our framework. Throughout this dissertation, base-band BPSK modulation and rectangular chip shaping will be assumed for simplicity.

6.2.1 Linear Decorrelating Detector (LDD)

As mentioned above, linear multiuser detectors have been generally analyzed for a set of "time-invariant" spreading sequences. Let $C = [c_1, c_2, \ldots, c_K]$ denote the spreading vector set of synchronous CDMA system with K users, where c_k is a sampled version of spreading code vector with length N chips. Assuming each of the spreading vectors is real and normalized to one, i.e. $c_k^T \cdot c_k = 1$ for all k, the cross-correlation matrix R, defined as $R = C^T \cdot C = [\rho_{ij}]$, is a positive definite matrix with each of the diagonal component ρ_{kk} equal to 1. LDD uses the inverse matrix R^{-1} to decouple the interferences in the correlator bank outputs. And the SNIR for the first user, conditioned on background noise variance σ_n^2, signal amplitude for the first user A_1 and given set of spreading sequences $\{c_k$ for $k = 1,2,\ldots,K\}$, is expressed as

$$SNIR_{LDD}(\sigma_n, A_1, \mathbf{c}_k \text{ for } k = 1,2,\ldots,K) = \frac{A_1}{\sigma_n \cdot \sqrt{[\mathbf{R}^{-1}]_{11}}} \tag{6.1}$$

---

expected BER for short spreading sequence system may be different from actually measured values if the cross-correlation does not change with time. However, the computation of the expected BER is exactly the same as that of the average BER for long spreading sequence system. In long spreading sequence system, it is expected that the average BER is quite close to the actual values even if the channel is time invariant.

The factor $1/\ [R^{-1}]_{11}$ is known as the near-far resistance of LDD. To simplify the expressions to be derived, we define X_{LDD} as square root of the near-far resistance.

$$X_{LDD} \equiv \frac{1}{\sqrt{[\mathbf{R}^{-1}]_{11}}} \tag{6.2}$$

which is a fixed value for deterministic CDMA. Another expression for the near-far resistance can be found in [20]. Dividing the $K \times K$ cross-correlation matrix into four block parts as

$$\mathbf{R} \equiv \mathbf{C}^T \cdot \mathbf{C} = \begin{pmatrix} \mathbf{c}_1^T \\ \overline{\mathbf{C}}_1^T \end{pmatrix} \cdot \begin{pmatrix} \mathbf{c}_1 & \overline{\mathbf{C}}_1 \end{pmatrix} = \begin{pmatrix} 1 & \mathbf{d}^T \\ \mathbf{d} & \overline{\mathbf{R}}_{11} \end{pmatrix} \tag{6.3}$$

where $\overline{\mathbf{C}}_1$ is the set of spreading vectors except for the first user. Then,

$$X_{LDD}^2 = \frac{1}{[\mathbf{R}^{-1}]_{11}} = 1 - \mathbf{d}^T \left[\overline{\mathbf{R}}_{11}\right]^{-1} \mathbf{d} = 1 - \alpha \tag{6.4}$$

where, using the definition in (3), it can be shown that

$$\alpha = \mathbf{c}_1^T \overline{\mathbf{C}}_1 \left(\overline{\mathbf{C}}_1^T \overline{\mathbf{C}}_1\right)^{-1} \overline{\mathbf{C}}_1^T \mathbf{c}_1 = \mathbf{c}_1^T \cdot P_{\overline{\mathbf{C}}_1}(\mathbf{c}_1) \tag{6.5}$$

$P_{\overline{C}_1}(\mathbf{c}_1)$ denotes the projection of $\mathbf{c}_1$ onto the space spanned by the vector set $\overline{\mathbf{C}}_1$. Note that α satisfies

$$0 \le \alpha \le |\mathbf{c}_1|^2 = 1 \tag{6.6}$$

6.2.2 Linear MMSE detector

While LDD uses the inverse cross-correlation matrix $\mathbf{R}^{-1}$, Linear MMSE multiuser detector uses the following matrix, instead of $\mathbf{R}^{-1}$ [25],

$$\mathbf{M} = (\mathbf{R} + \sigma_n^2 \mathbf{A}^{-2})^{-1} \tag{6.7}$$

Note that the decision variable of LDD is interference free if the inverse cross-correlation matrix exists while the output of MMSE multiuser detector contains both the noise and the interference. Without loss of generality, we will consider the decision variable of the first user. As described in [20], the decision variable of LMMSE detector for the first user can be expressed as

$$z_{1,MSE} = B_1 b_1 + \sum_{k=2}^{K} B_k b_k + \sigma_n \cdot n_1' \tag{6.8}$$

where B_k is the leakage coefficient for the k^{th} user, which quantifies the unresolved interference from the k^{th} user and is given by

$$B_k = A_k (\mathbf{MR})_{1k} \tag{6.9}$$

And n'_1 is a random variable, representing the noise enhancement, with mean zero and variance

$$Var(n_1') = (\mathbf{MRM})_{11} \tag{6.10}$$

When random spreading is used, the leakage coefficients and the noise enhancement are random variables.

6.3 LDD in Random CDMA

As mentioned in the previous section, the near-far resistance defined in (6.2) must be treated as a random variable in R-CDMA system. If the PDF of X_{LDD}, $f_{X_{LDD}}(x)$, is known, the first user's average BER for uncoded system is given by

$$P(\hat{b}_1 \neq b_1 \mid \sigma_n, A_1) = \int_x \mathrm{Q}\left(x \cdot \frac{A_1}{\sigma_n} \right) \cdot f_{X_{LDD}}(x) \cdot dx \tag{6.11}$$

where $Q(a) = \left(1/\sqrt{2\pi}\right) \int_a^\infty e^{-y^2/2} dy$.

6.3.1 Synchronous case

The near-far resistance $1/[\mathbf{R}^{-1}]_{11}$ for the user 1 can be expressed as $\det[\mathbf{R}]/Adj[\rho_{11}]$. With this expression, however, it is hard to evaluate the PDF of the near-far resistance X^2_{LDD}. However, assuming $\mathrm{E}|\rho_{ij}|^2 << 1$, we can use the following simple approximation, instead of the expression in (6.4).

$$X^2_{LDD,Sync} \approx 1 - \mathbf{d}^T \cdot \mathbf{d} = 1 - \sum_{k=2}^{K} \rho_{1k}^2 = 1 - Y_{LDD} \tag{6.12}$$

where we defined the random variable $Y_{LDD} = \sum_{k=2}^{K} \rho_{1k}^2$

The approximation in (6.12) is equivalent to setting $\overline{\mathbf{R}}_{11} \rightarrow \mathbf{I}_{K-1}$ in (6.3), where $\mathbf{I}_{K-1}$ is K-1×K-1 identity matrix, which can be interpreted as follows. The decorrelation is the projection of the received signal vector onto the vector orthogonal to all the spreading code vectors except for that of the user under consideration. With the approximation in (6.12), we have all other spreading sequences, except for that of the first user, are

orthogonal to each other. It means that all the other off-diagonal components in the cross-correlation matrix, except for those in the first row and the first column, are zero. As a results, $Adj[\rho_{11}] = 1$ and thus $X^2_{LDD,Sync} \approx \det[\mathbf{R}] = 1 - Y_{LDD}$.

With this approximation, the second term $\mathbf{d}^T \cdot \mathbf{d}$ in (6.12) may not satisfy the condition in (6.5); i.e. it may exceed one while the term $\alpha = \mathbf{d}^T \cdot [\overline{\mathbf{R}}_{11}]^{-1} \mathbf{d}$ defined in (6.3) and (6.4) is strictly non-negative value as noted in (6.5). However, for random spreading vectors with large N, each component in $\mathbf{d}$ will be small enough so that it is rare for $\mathbf{d}^T \cdot \mathbf{d}$ to exceed one. It was also seen from the simulation results that the PDF of Y_{LDD} converge fast to zero as $Y_{LDD} \to 1$. And we can neglect the probability that $Y_{LDD} > 1$ in the performance analysis discussed later.

Y_{LDD} is summation of K-1 terms of ρ_{Ik}^2, for each of which we can use the Gaussian approximation in (C.3). Therefore, the PDF of Y_{LDD} can be expressed as Chi-square distribution with K-1 degree of freedom, i.e.

$$f_{Y_{LDD}}(y) = \chi^2_{K-1}(y, \sigma_I^2) \equiv \left| \frac{1}{\sigma_I^2} \right| \cdot \frac{\left(y/\sigma_I^2\right)^{\frac{(K-1)-2}{2}} \cdot \exp\left(-\frac{y/\sigma_I^2}{2}\right)}{2^{(K-1)/2} \cdot \Gamma[(K-1)/2]} \tag{6.13}$$

where, $\sigma_I^2 = 1/N$ and the gamma function $\Gamma[a] = \int_0^\infty t^{a-1} e^{-t} dt$. Furthermore, since $X_{LDD,Sync}$ $\approx (1 - Y_{LDD})^{1/2}$, the PDF of $X_{LDD,Sync}$ is approximately expressed as

$$f_{X_{LDD,Sync}}(x) \approx 2x \cdot f_{Y_{LDD}}(1 - x^2) \quad \text{for } 0 < x < 1 \tag{6.14}$$

A comparison of simulated results with the approximated results is shown in Section 6.5.

6.3.2 Asynchronous case

While the asynchronous LDD has been first introduced in [23], where the use of time invariant spreading sequences was assumed, the scheme proposed in [89] is suitable more for our analysis since it can be easily extended to time-varying CDMA. Thus, the ideas of the previous subsection are applied to analyze the approximate performance of asynchronous LDD for random spreading sequences, using the model in [89][7]. With this model, the cross-correlation matrix of the spreading waveforms for one packet is given by,

$$\mathbf{R} = \begin{bmatrix} \mathbf{R}_0(0) & \mathbf{R}_0(-1) & \mathbf{0} & \mathbf{0} & \cdots & \mathbf{0} \\ \mathbf{R}_1(1) & \mathbf{R}_1(0) & \mathbf{R}_1(-1) & \mathbf{0} & \cdots & \vdots \\ \mathbf{0} & \mathbf{R}_2(1) & \mathbf{R}_2(0) & \mathbf{R}_2(-1) & & \vdots \\ \vdots & \vdots & & & & \vdots \\ \vdots & & \mathbf{R}_m(1) & \mathbf{R}_m(0) & \mathbf{R}_m(-1) & \vdots \\ \vdots & \vdots & & & & \vdots \\ \vdots & \vdots & & \mathbf{R}_{M-2}(1) & \mathbf{R}_{M-2}(0) & \mathbf{R}_{M-2}(-1) \\ \mathbf{0} & \cdots & & \mathbf{0} & \mathbf{R}_{M-1}(1) & \mathbf{R}_{M-1}(0) \end{bmatrix} \tag{6.15}$$

where m is bit index in a packet and M is the packet length. Each of the element matrix, $\mathbf{R}_m(h)$, h = -1,0,+1, is a $K \times K$ matrix (K is the number of users in the system). And each element in those matrixes is given by

$$[\mathbf{R}_m(h)]_{ij} = \int_{T_b} s_i^{m+h}(t-\tau_i) \cdot s_j^m(t-\tau_j) \cdot dt$$

---

[7] Seemingly, the model in [Ch2.25] is the same as [Ch2.3]. However, the underlying assumption is different from each other. In [Ch2.3] it was assumed that only the short code is used so that all the diagonal block components are all the same. On the other hand, in [Ch2.25], they did not assume the use of short codes considering the possible use of long codes

where $s^m_k(t)$ is the spreading waveform for mth bit of the user k, which is defined in the interval $[mT_b, (m+1)T_b]$. Assuming the users are numbered in the order of their time delays, such that $0<\tau_1<\tau_2<\cdots<\tau_K$, $\mathbf{R}_m(1)$ is an upper and $\mathbf{R}_m(-1)$ a lower triangular matrix with all the diagonal element equal to zero. Thus, each row and column in the right hand side of (6.15) contains only $2(K-1)$ non-zero interfering cross terms (two for each of the interfering users). It holds for every bit of every user in the packet, except for the first bit and last bit in the packet, where only one interfering cross term exists for each interfering user. However, assuming the packet size is large, the end effect will be ignored in the BER analysis.

Now, we apply the same idea as for synchronous LDD analysis, described in Section 6.3.1, to the asynchronous system model. First, we decompose the matrix $\mathbf{R}$ into four parts, as we did in (6.3), and replace the principal submatrix $\overline{\mathbf{R}}_{m\times K+k,m\times K+k}$ with $\mathbf{I}_{M\cdot K-1}$, for the sake of analysis. As described in Section 6.3.1, it is equivalent to setting all the off-diagonal components, except for the elements in the $(m\times K+k)^{\text{th}}$ row and column, to zeros. Then, the inverse diagonal component for mth bit of the user k is approximated as

$$\frac{1}{[\mathbf{R}]^{-1}_{m\times K+k,m\times K+k}} \approx 1-\sum_{l=1,l\neq k}^{K}\left[[\mathbf{R}_m(-1)]^2_{kl}+[\mathbf{R}_m(0)]^2_{kl}+[\mathbf{R}_m(+1)]^2_{kl}\right] \tag{6.16}$$

Since $\mathbf{R}_m(+1)$ and $\mathbf{R}_m(-1)$ are upper and lower triangular matrix, respectively, with all the diagonal element equal to zero, it can be shown that either $[\mathbf{R}_m(-1)]_{kl}$ or $[\mathbf{R}_m(+1)]_{kl}$ is zero. Hence, one of the three terms in the bracket in (6.16) is zero. To simplify the notation, we rewrite (6.16) as follows

$$X^2_{LDD,Async}=\frac{1}{[\mathbf{R}]^{-1}_{kk}}\approx 1-\sum_{l=1,l\neq k}^{K}\left[[\rho^L_{kl}]^2+[\rho^R_{kl}]^2\right]=1-\sum_{l=1,l\neq k}^{K}Z_l=1-Z_{LDD} \tag{6.17}$$

where, we omitted the bit index m for compact expression and replaced '$m\times K+k$' with 'k'. The superscript "L" and "R" indicate the interference from other asynchronous users in the left and right side of the user k's bit interval. Assuming the processing gain N is large enough, then $Z_{LDD}<1$.

For random spreading sequences, given the delay τ_k, for k=1,2,...,K, each term in the summand in (6.17) is independent. Denote $\tau_k = D_k + \delta_k$ with T_c=1, where D_k = 0,1,...,N-1 and $0 \le \delta_k < 1$. Using the Gaussian approximation described in Section 2.7, for the first user, the PDF of ρ^L_{1k} and ρ^R_{1k} conditioned on D_k and δ_k are given by

$$\rho^L_{1k}(D_k,\delta_k) \sim \mathcal{N}\left(0, \sigma^2_{1k,L}(D_k,\delta_k)\right) \quad \text{for } k = 2,3,...,K \tag{6.18.a}$$

$$\rho^R_{1k}(D_k,\delta_k) \sim \mathcal{N}\left(0, \sigma^2_{1k,R}(D_k,\delta_k)\right) \quad \text{for } k = 2,3,...,K \tag{6.18.b}$$

where $$\sigma^2_{1k,R}(D_k,\delta_k) = [(D_k+1)\cdot(1-\delta_k)^2 + D_k\cdot\delta_k^2]/N^2 \tag{6.19.a}$$

$$\sigma^2_{1k,L}(D_k,\delta_k) = [(N-D_k-1)\cdot(1-\delta_k)^2 + (N-D_k)\cdot\delta_k^2]/N^2 \tag{6.19.b}$$

With this Gaussian assumption, one can show that the r.v. $\rho^L_{1k} + \rho^R_{1k}$ has normal distribution with mean 0 and variance $2/3N$, by taking average of the variance on δ_k. This leads to the classical result of Standard Gaussian Approximation in [34].

Contrast to the synchronous case, the PDF of Z cannot be obtained easily because the ρ^L_{1k} and ρ^R_{1k} depend on the same random variables D_k and δ_k. Note that, given D_k and δ_k, ρ^L_{1k} and ρ^R_{1k} in (6.18) are conditionally independent of each other. Thus, from (6.18) and (6.19), the PDF and the characteristic function of Z_k conditioned on D_k and δ_k are given by

$$f_{Z_k}(z \mid D_k, \delta_k) = \chi_1^2\left(z, \sigma_{1k,L}^2(D_k, \delta_k)\right) * \chi_1^2\left(z, \sigma_{1k,R}^2(D_k, \delta_k)\right) \tag{6.20}$$

$$\Phi_{Z_k}(\omega \mid D_k, \delta_k) = \left(1 - j2\omega\sigma_{1k,L}^2(D_k, \delta_k)\right)^{-1/2} \cdot \left(1 - j2\omega\sigma_{1k,R}^2(D_k, \delta_k)\right)^{-1/2} \tag{6.21}$$

where * denotes the convolution operator and $\chi_M^2(z, \sigma^2)$ is chi-square distribution function with M degree of freedom, defined as in (6.13). Using (6.20) and (6.21), the marginal PDF of Z_k can be expressed as a mixture density function

$$f_{Z_k}(z) = \sum_{D_k=0}^{N-1} \frac{1}{N}\left[\int_0^1 \chi_1^2\left(z, \sigma_{1k,L}^2(D_k, \delta_k)\right) * \chi_1^2\left(z, \sigma_{1k,R}^2(D_k, \delta_k)\right) \cdot d\delta_k\right] \tag{6.22}$$

$$\Phi_{Z_k}(\omega) = \sum_{D_k=0}^{N-1} \frac{1}{N}\left[\int_0^1 \left[\left(1 - j2\omega\sigma_{1k,L}^2(D_k, \delta_k)\right) \cdot \left(1 - j2\omega\sigma_{1k,R}^2(D_k, \delta_k)\right)\right]^{-1/2} d\delta_k\right] \tag{6.23}$$

When the time delays are i.i.d., all the Z_k's are also identically distributed. Let $\Psi_Z(\omega)$ be the characteristic function of Z_k's; i.e. $\Phi_{Zi}(\omega) = \Psi_Z(\omega)$ for all i. Then, the characteristic function of Z_{LDD} is given by

$$\Phi_{Z_{LDD}}(\omega) = \prod_{k=2}^{K} \Phi_{Z_k}(\omega) = \left[\Psi_Z(\omega)\right]^{K-1} \tag{6.24}$$

Finally, the PDF of the near-far resistance of asynchronous LDD can be approximated to

$$f_{X_{LDD,Async}}(x) \approx 2x \cdot f_{Z_{LDD}}(1 - x^2) \tag{6.25}$$

where $f_{Z_{LDD}}(z) = (1/2\pi)\int_{-\infty}^{\infty} \Phi_{Z_{LDD}}(\omega) \cdot e^{-j\omega z} d\omega$. (6.26)

6.3.3 Simpler approximation

Since ρ^L_{1k} and ρ^R_{1k} depend on the random variables D_k and δ_k, the PDF of Z_k was treated as a mixture density described in (6.22). Now, to simplify the analysis, ρ^L_{1k} and ρ^R_{1k} are assumed to be i.i.d. random variables with the same Gaussian PDF, $\mathcal{N}(0, 1/3N)$. With this assumption, $\sigma^2_{1k,L}(D_k, \delta_k)$ and $\sigma^2_{1k,R}(D_k, \delta_k)$ in (6.18) can be replaced with $E[\sigma^2_{1k,L}(D_k, \delta_k)]$ and $E[\sigma^2_{1k,R}(D_k, \delta_k)]$[8], respectively, and the PDF of Z_{LDD} is simply approximated to a chi-square distribution with $2(K\text{-}1)$ degree of freedom, i.e.

$$f_{Z_{LDD}}(z) = \chi^2_{2(K-1)}(z, 1/3N) \tag{6.27}$$

With this simplification, the PDF of the near-far resistance X_{LDD} is obtained by (6.25) with $f_{Z_{LDD}}(z)$ given in (6.27).

6.3.4 Expected Near-far Resistance of LDD

Further insight into the performance of LDD for random spreading sequences can be obtained from the expectation of the near-far resistance. To satisfy the condition that the support of $f_X(x)$ is [0,1], z should be restricted in [0,1] since $X^2 \approx 1\text{-}Z$. And the expectation of Z should be calculated by integrating $z \cdot f_Z(z)$ from 0 to 1. However, the pdf of Z, $f_Z(z)$, developed here have non-zero value in the range [1,∞]. Nevertheless, since the values of $f_Z(z)$ in the range [1, ∞] are almost zero, $E[X^2_{LDD}]$ can be easily computed approximately by the expectation of Z_{LDD}. Given the PDF of Z_{LDD} as in (6.27), it can be easily computed as follows,

---

[8] See Appendix C for the drivation of $E[\sigma^2_{1k,L}(D_k, \delta_k)]$ and $E[\sigma^2_{1k,R}(D_k, \delta_k)]$

$$E\left[X^2_{LDD,Sync}\right] \approx 1 - E[Z_{LDD}]$$
$$= 1 - \int_0^{\infty} z \cdot f_Z(z) \cdot dz = 1 - \frac{2(K-1)}{3N} \tag{6.28}$$

Although Z_{LDD} should not exceed 1 in (6.17), we can compute $E[X^2_{LDD}]$ by (6.18), rather than by using $1-\int_0^1 z \cdot f_Z(z) \cdot dz$, since in a practical condition the PDF of Z_{LDD} converge fast to zero as $Z_{LDD} \rightarrow 1$, so that the contribution of $\int_1^{\infty} z \cdot f_Z(z) \cdot dz$ is negligible. Similarly, for synchronous systems,

$$E\left[X^2_{LDD,Async}\right] \approx 1 - E[Y_{LDD}] = 1 - \frac{(K-1)}{N} \tag{6.29}$$

The result for synchronous system is identical to the bound obtained in [20] for average near-far resistance of MMSE multiuser detector. For asynchronous systems, however, the result in this chapter differs in that there is an additional scaling factor of 1/3. The validity of our result in (6.28) is verified via simulation results in Section 6.5.

6.4 MMSE detector in Random CDMA

Since LDD output is interference free[9], it was enough to take only the noise enhancement into account in LDD analysis. At the output of the MMSE detector, however, there exist both the enhanced noise and the unresolved interference, so that it is required to take both into account. Using the Central limit theorem, we will assume in the derivation of MMSE detector performance that the unresolved interference is Gaussian, even when the spreading codes are deterministic. As it will be shown later, this assumption simplifies the derivation.

---

[9] When the inverse of the cross-correlation matrix exists.

As mentioned earlier in Section 6.3, when random spreading is used, the leakage coefficients B_k's and the noise enhancement of MMSE detector, n'_1, are random variables. To simplify the analysis of MMSE receiver, the same approch as in the previous section is employed; i.e. it is assumed that all the spreading code vectors of interfering users are orthogonal to each other such that $\overline{\mathbf{R}}_{11} \rightarrow \mathbf{I}_{K-1}$. With this assumption, simple expressions for B_1, B_k's and var(n'_1) can be obtained from (C.7), (C.9) and (C.11) in Appendix C, respectively

$$B_1 = A_1\Delta\left(1-\sum_{k=2}^{K}\frac{\rho_{1k}^2}{1+\sigma_n^2/A_k^2}\right) \tag{6.30.a}$$

$$B_k = A_k\Delta\left(\frac{\sigma_n^2}{A_k^2+\sigma_n^2}\right)\cdot\rho_{1k} \quad \text{for k = 2,3,...,K} \tag{6.30.b}$$

$$Var(n_1') = \Delta^2\cdot\left(1-\sum_{k=2}^{K}\left[\frac{1}{1+\sigma_n^2/A_k^2}+\frac{\sigma_n^2/A_k^2}{(1+\sigma_n^2/A_k^2)^2}\right]\rho_{1k}^2\right) \tag{6.31}$$

where, from (C.8), $\Delta^{-1} = \left(1+\frac{\sigma_n^2}{A_1^2}\right)-\sum_{k=2}^{K}\frac{\rho_{1k}^2}{1+\sigma_n^2/A_k^2}$.

It can be shown that (6.30-a), (6.30-b) and (6.31), in conjunction with the decision variable of MMSE detector shown in (6.8), lead to

$$SNIR_{MMSE} \approx \frac{B_1^2}{\sigma_n^2 Var(n'_1)+\sum_{k=2}^{K}B_k^2} = \frac{A_1^2}{\sigma_n^2}\left(1-\sum_{k=2}^{K}\frac{\rho_{1k}^2}{1+\sigma_n^2/A_k^2}\right) \tag{6.32}$$

Using the Central Limit Theorem, we apply the Gaussian approximation as in [33] to the second term in the right hand side of (6.8). Then, the bit error probability for uncoded system is obtained by taking averaging on (6.32) as follows

$$P_{e,LMMSE} = EQ\left(\sqrt{SNIR_{MMSE}}\right)$$

Comparing (6.12) with (6.32), the MMSE counterpart of $X^2_{LDD,Sync}$ can be defined as

$$X^2_{MMSE,Sync} \equiv \frac{SNIR_{MMSE}}{A_1^2/\sigma^2} \approx \left(1 - \sum_{k=2}^{K} \frac{\rho_{1k}^2}{1+\sigma_n^2/A_k^2}\right) \tag{6.33}$$

Although these results are only approximation, it can give us helpful insight into the property of LMMSE detector and, due to the simple structure of the expression, the PDF of the SNIR for LMMSE detector can be easily obtained. Similar to (6.12), we define a random variable Y_{MMSE} as

$$Y_{MMSE} = \sum_{k=2}^{K} \frac{\rho_{1k}^2}{1+\sigma_n^2/A_k^2} \tag{6.34}$$

In AWGN Channel with perfect power control, one can simply set $A_1 = A_2 = \cdots = A_K = A$. Since A/σ is constant, the same derivation as in the previous section for LDD can be used. Using the Gaussian approximation in Section 6.3, the PDF of Y_{MMSE} is simply approximated to a Chi-square distribution with K-1 degree of freedom, similar to (6.13);

$$f_{Y_{MMSE}}(y) = \chi^2_{K-1}\left(y, \frac{1}{N\cdot(1+\sigma_n^2/A^2)}\right) \tag{6.35}$$

And for synchronous CDMA system, the expected BER of LMMSE detector is given by

$$P_{e,LMMSE} = \int_0^1 Q\left(\frac{A}{\sigma_n}\cdot x\right)\cdot f_{X_{MMSE}}(x)\cdot dx \tag{6.36}$$

where $f_{X_{MMSE}}(x) \approx 2x \cdot f_Y(1-x^2)$. Also, similar to the analysis of LDD in asynchronous system and through the same derivation, the following is obtained for asynchronous system.

$$X^2_{MMSE,Async} = 1 - \sum_{k=2}^{K} \frac{\rho^2_{1k,L} + \rho^2_{1k,R}}{1+\sigma_n^2/A_k^2} = 1 - Z_{MMSE} \tag{6.37}$$

With the independent assumption on $\rho_{1k,L}$ and $\rho_{1k,R}$ and perfect power controlled condition, the PDF of Z_{MMSE} is given by

$$f_{Z_{MMSE}}(z) = \chi^2_{2(K-1)}\left(z, \frac{1}{3N\cdot(1+\sigma_n^2/A^2)}\right) \tag{6.38}$$

As defined in [20], the near-far resistance of LMMSE detector is expressed as the same form as that of LDD since it is defined with the assumption of infinite signal to background noise ratio. It is also true in our approach; as the signal to background noise ratio, A^2/σ^2_n, approaches infinity, the PDF in (6.38) approaches to that in (6.28).

Similar to the argument in Section 6.3.4, it also easy to show that the expectation of X^2_{MMSE} is given by

$$E\left[X^2_{MMSE}\right] \approx 1 - \frac{(K-1)}{N(1+\sigma_n^2/A^2)} \quad \text{for synchronous system} \tag{6.39}$$

$$E\left[X^2_{MMSE}\right] \approx 1 - \frac{2(K-1)}{3N(1+\sigma_n^2/A^2)} \quad \text{for asynchronous system} \tag{6.40}$$

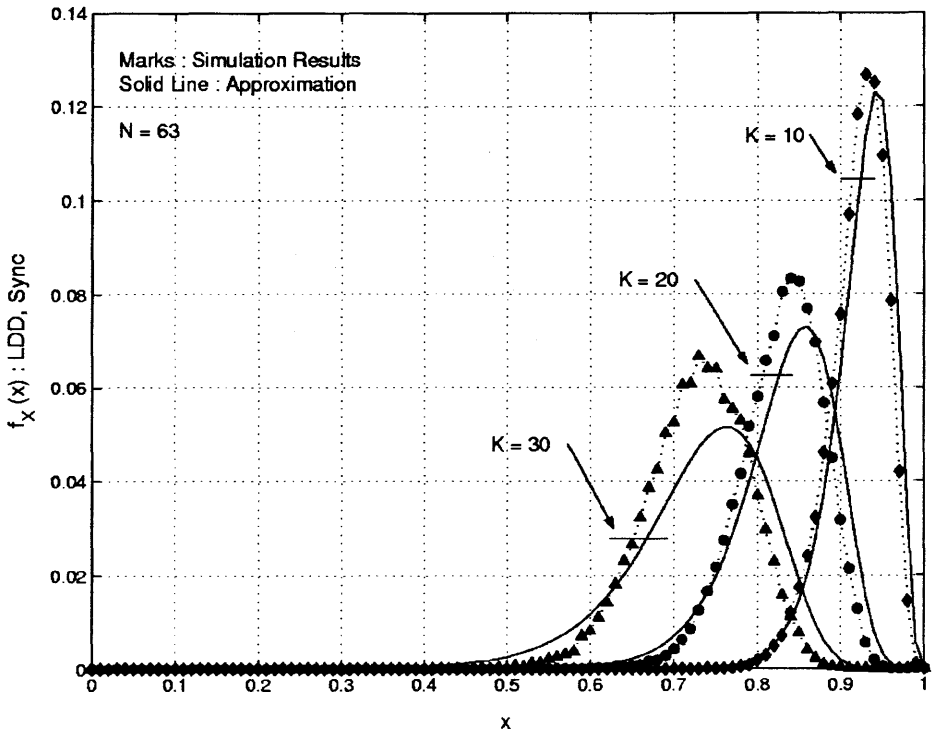

Figure 6.1 PDF of the near-far resistance for Synchronous LDD (N=63).

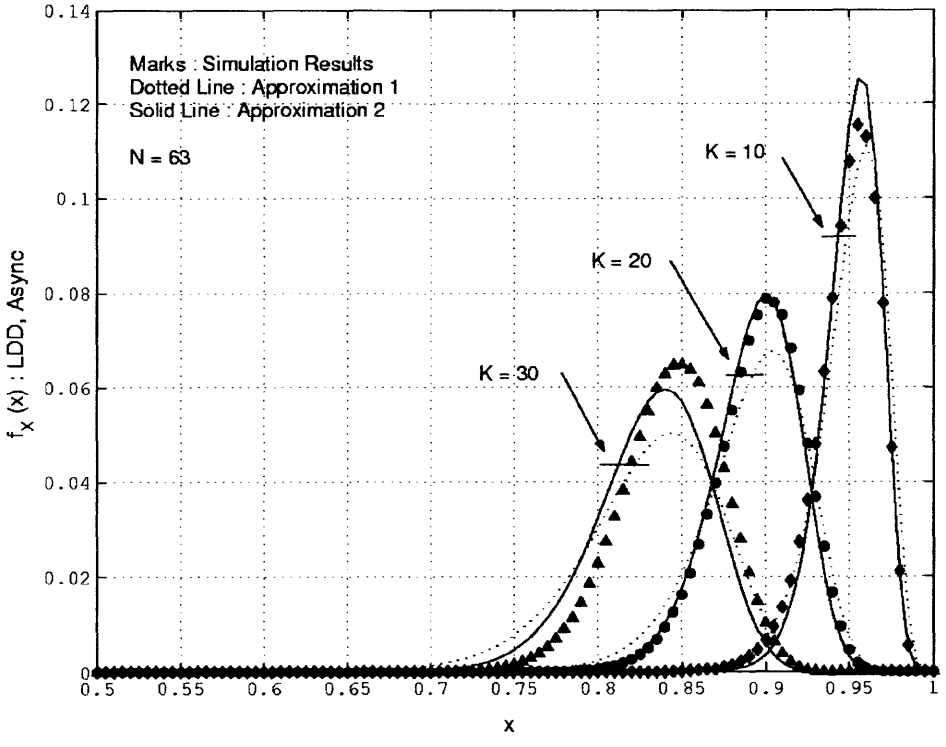

Figure 6.2 PDF of the near-far resistance for Asynchronous LDD (N=63).

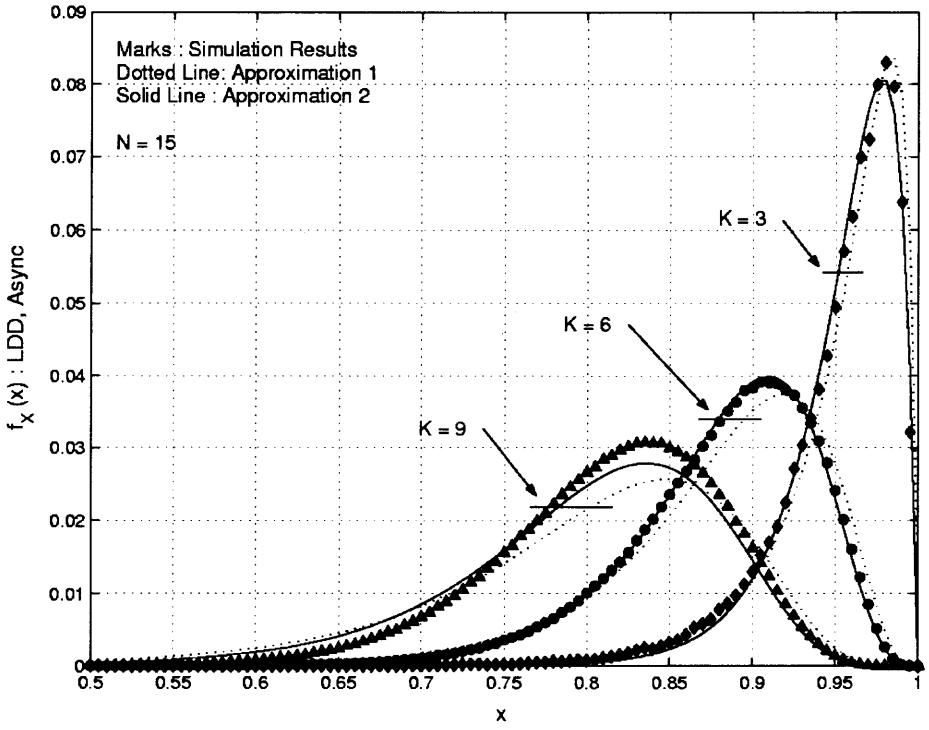

Figure 6.3 PDF of the near-far resistance for Asynchronous LDD (N=15).

6.5 Simulations and Numerical Results

In this Section, the approximate approach is verified by comparing with simulated results. The probability densities of the near-far resistance and the expected BER for uncoded system are compared with those of the simulated results. The results for the conventional detector and the single user bound are also shown for comparison. In all simulations, base-band BPSK signaling and AWGN channel were considered for simplicity.

Figure 6.1 shows a comparison of the PDF of near-far resistance of linear multiuser receivers. As noted in [20], the near-resistance of LMMSE receiver is expressed as the same form as that of LDD and, thus, only those of LDD are shown. Using processing gain N = 63 and K = 10, 20 and 30, Figure 6.1 shows a comparison of approximated analytical results for synchronous system, using (6.14), with the results obtained from the simulation. Figure 6.2 and 6.3 also compare the PDF obtained from the simulation with those obtained by approximate analysis for asynchronous system, using (6.25) with (6.26)

and with (6.27), termed Approx. 1 and Approx. 2, respectively. The parameters were set $N = 63$ and $K = 10$, 20 and 30 in Figure 6.2 and $N = 15$ and $K = 3$, 6 and 9 in Figure 6.3. The results for asynchronous system show that the latter (Approx.2) is closer than the former (Approx.1). This is an unexpected result because Approx.2 is a simpler approximation than Approx.1. The author believes that it is due to the Gaussian approximation in (6.18) and (6.19). As can be expected, the Gaussin approximation is not applicable to those cases where D_k is small in (6.18) and the contribution of these portion in (6.22) and (6.23) make Approx.1 more deviated from actual PDF. Although there are some deviations for both the approaches, one can say in general that the smaller the number of users (relative to the processing gain N) the closer the approximated results to the simulated values.

Figure 6.4 and 6.5 shows the BER performances in AWGN channel, each for the conventional matched filter detector, LDD, MMSE detector and single user bound, respectively. Assuming the perfectly power-controlled condition, the signal to background noise ratio (SbNR) were set to 10 dB for all the users, and the processing gain N was set to 63. The analytical BER is computed by (6.11), (6.25) and (6.27) for LDD and by (6.36), (6.25) and (6.35) for MMSE detector. The analytical BER of both LDD and MMSE detector appears to be fairly close to the simulated values. Figure 6.6 and 6.7 shows the same results for $N = 15$. Comparing with Figure 6.4 and 6.5 ($N = 63$), the approximation is not as close to the simulation results as that in the previous case shown in Figure 6.4 and 6.5.

As shown in the comparisons, the deviations from actual values grow as the number of user increases. These deviations are mainly due to the Gaussian approximation and the orthogonality assumption on the cross-correlation between interfering users. While the deviation caused by the Gaussian Approximation is negligible if the processing gain is large enough, the deviation due to the orthogonality assumption limits the applicability of the approximate approach. However, even with these deviations, the approximate approach derived in this chapter can be successfully applied provided that

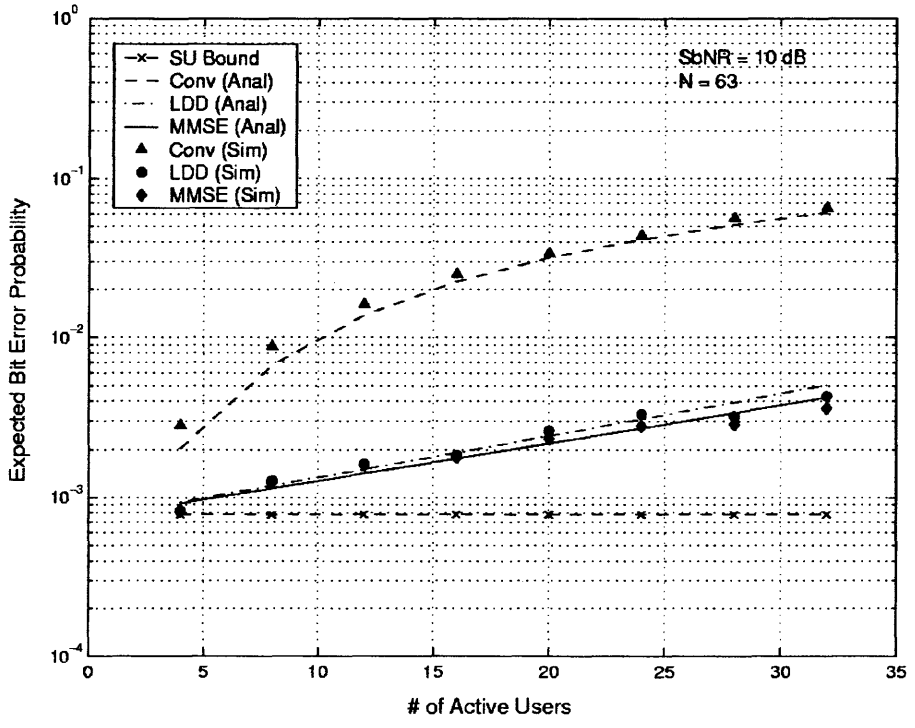

Figure 6.4 A Comparison of Average BER for Asynchronous CDMA (SNR_k = 10dB, N = 63).

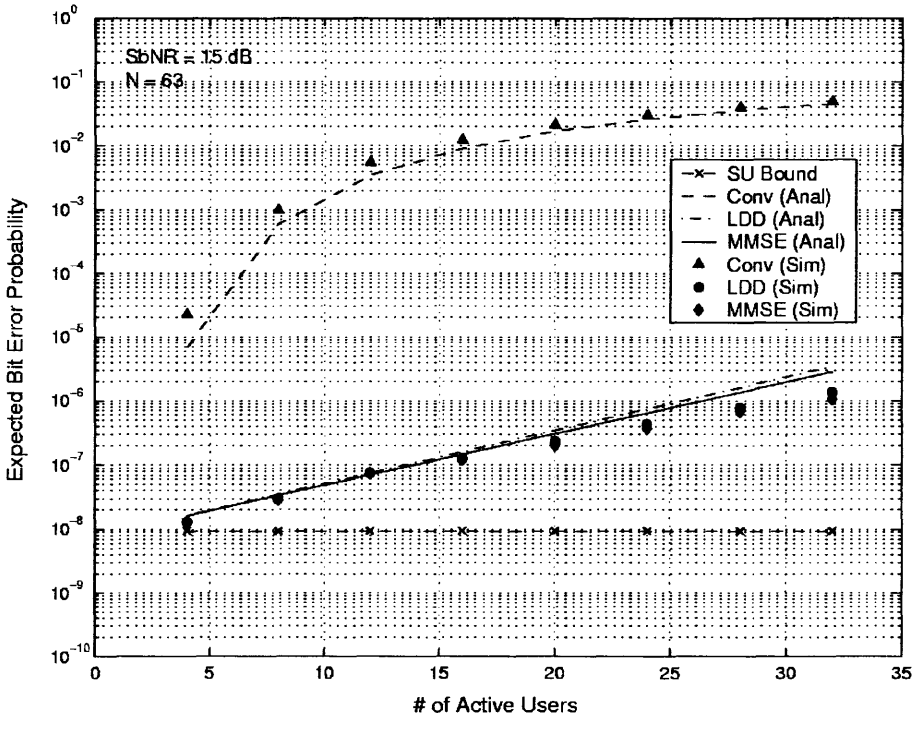

Figure 6.5 A Comparison of Average BER for Asynchronous CDMA (SNR_k = 15dB, N = 63).

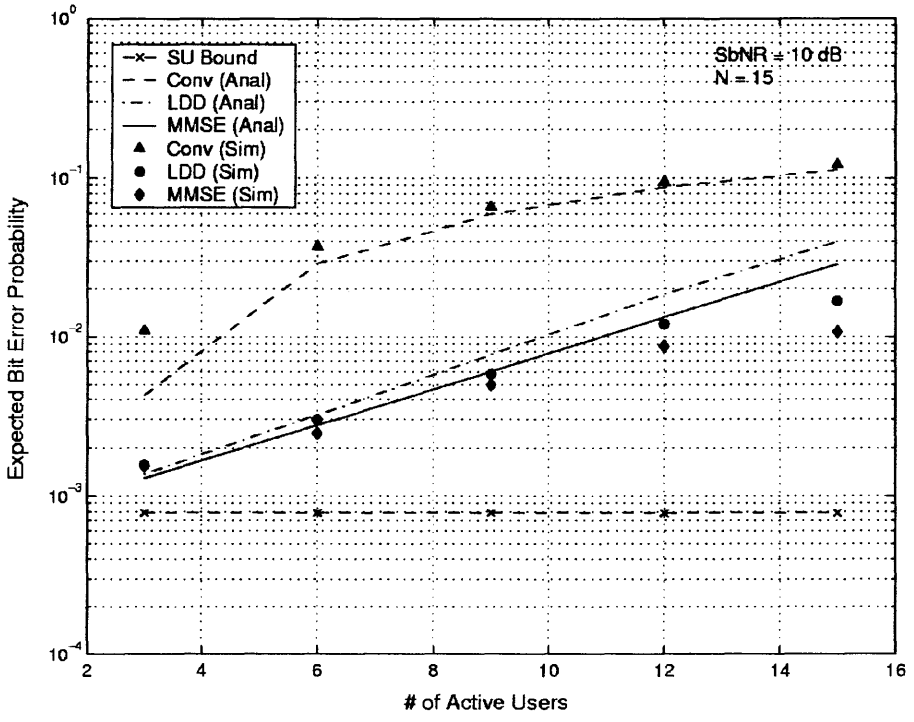

Figure 6.6 A Comparison of average BER for Asynchronous CDMA ($SNR_k = 10dB, N = 15$).

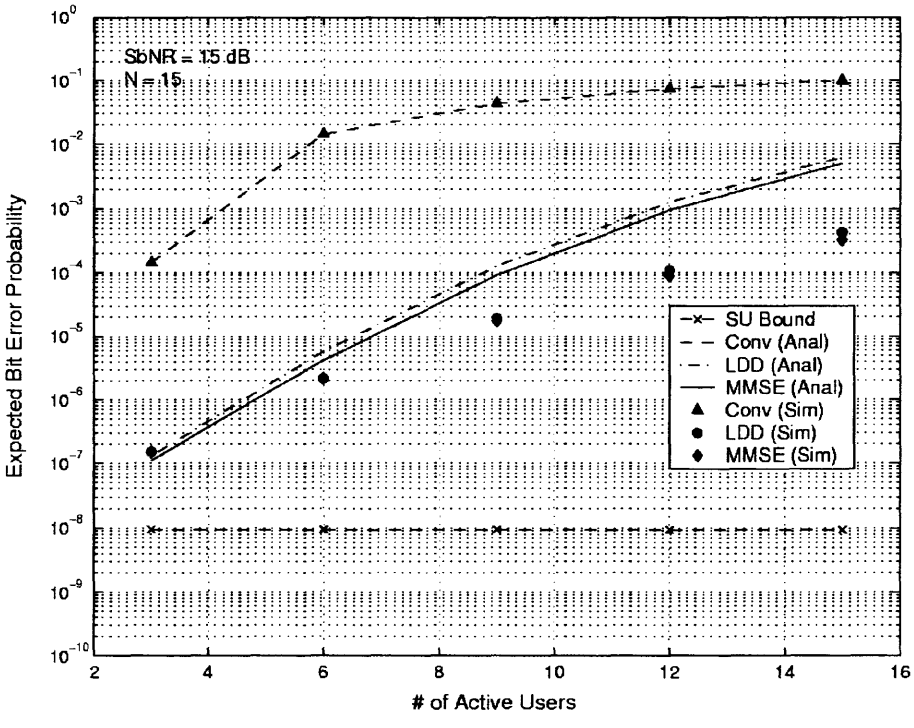

Figure 6.7 A Comparison of average BER for Asynchronous CDMA ($SNR_k = 15dB, N = 15$).

the processing gain is large enough, saying larger than 32, and the number of users is less than half the processing gain.

6.6 Chapter Summary

In this chapter, using the Gaussian approximation of a cross-correlation between the spreading waveforms, an approximate PDF of near-far resistance of LDD and MMSE detector was derived for random spreading waveforms. The simulation results show the validity of the approximate analysis. As can be inferred from (6.27) and (6.29) for LDD and from (6.38) and (6.39) for MMSE, for synchronous system, the PDF of the near-far resistance of LDD and its MMSE counterpart could be approximated as a reversed and shifted Chi-square distribution function with (K-1) degrees of freedom. For asynchronous system, the expression of the PDF is more complicated. However, a simpler but more accurate expression could be obtained when adding further but reasonable assumption that ρ^{L}_{1k} and ρ^{R}_{1k} are independent of each other. The pdf is then expressed in the same form as those for synchronous system; i.e. a reversed and shifted Chi-square distribution function with 2(K-1) degrees of freedom.

While the approach proposed in this chapter can be successfully applied when the number of users K is less than about half the processing gain $N/2$, it is not enough for heavily loaded wireless channel, where there are so many delayed replicas of original signal. Due to the autocorrelation property of PN sequences, these replicas can be regarded as independent interferers and, hence, the effective number of interfering signal become much larger than that of the actual number of system users.

CHAPTER 7

CONCLUSION

7.1 Contributions

In this dissertation, coded CDMA systems were reinvestigated in terms of packet data communications terminology. Contributions of the work can be summarized as follows.

- Using the improved union bound, the performance of turbo coded CDMA system with hybrid ARQ was evaluated in deterministic environment.
- A generalized analytical framework, named as Queuing Network Model, has been devised to analyze CDMA based ALOHA system that employs Hybrid type-II ARQ.
- The model was applied to CDMA slotted ALOHA with Packet Combining and the effectiveness of the model verified by comparing with simulation results.
- The throughput bounds of CDMA Unslotted ALOHA with hybrid type-II ARQ using RCPT codes were also investigated.
- As an implementation issue, an efficient parallel scheme for low latency turbo decoding has been proposed, based on Pearl's belief propagation algorithm.
- For linear multiuser receivers in random spreading environment, an approximate PDF of output SNIR of linear decorrelating detector and MMSE receiver was directly derived using Gaussian approximation. The resulting expressions are as simple as that of the conventional matched filter receiver and quite close when the number of users is less than half of the processing gain.

7.2 Remarks

Achievable Spectral Efficiency of Turbo coded CDMA: Apparently, due to the multiple access interferences, the CDMA system with only matched filter receiver is useless

without coding. Well-designed FEC coding and ARQ scheme is crucial in CDMA systems for packet data transmission. As shown numerically, using a turbo codes of rate 1/3, one can obtain a spectral efficiency around 1.1 bits/Hz/sec. By employing multiuser detection, the spectral efficiency could be even higher than 1.6 bits/Hz/sec.

MF vs. LMMSE receiver: The results in Ch.2 show that the spectral efficiency with linear MMSE receiver saturates at a code rate of about 4/5, i.e. does not improve further with lower rate coding, while, for matched filter receivers, better performance can be obtained with lower code rate. Theoretically, as the system load goes to infinity, the spectral efficiency of linear MMSE receiver converges to that of matched filter receiver. In practical situation, however, there exists a noticeable performance gap between the two receivers unless a very low rate code is used. Certainly, multiuser detections can improve the system capacity for given rate of coding options, but the efficiency can also be improved with lower rate channel coding, even without multiuser detection. As the number of users $K \rightarrow \infty$, the spectral efficiency of MMSE receiver converges to that of the conventional matched filter receiver. Hence we may consider lower rate turbo coding in favor of multiuser detection if the latter requires more complicated hardware than that needed for implementing lower rate channel coding/decoding.

Hybrid Type-II ARQ as a mean of decentralized Automatic Rate Adaptation: It is well known that Code Combining Hybrid type-II ARQ that uses RCPC or RCPT codes is a decentralized code rate adaptation. While, it was not generally recognized that Packet combining hybrid type-II ARQ can be regarded as a mean of decentralized Spreading factor adaptation. In connection oriented CDMA systems, the system resources, such as Power, Spreading factor and Code rate, can be controlled in centralized fashion to optimize the system utilities. While, in packet based cellular system or Ad hoc network, where traffic changes unpredictably and/or the transceivers know little about the entire system, decentralized resource control would be preferable to the centralized.

Effectiveness of our Analytical Framework: The results in Ch.5 verify the effectiveness of the analytical framework introduced in this dissertation, even with immediate retransmission.

CDMA ALOHA with variable length traffic: In most cases, fixed length traffic is not a practical assumption. For variable traffic length, there exists correlation between the nearby slots. To this case, one can extend the iterative procedure and the bounding technique introduced in Ch.4.2 to analyze CDMA unslotted ALOHA. The only difference is that for unslotted system the state transition occurs at any time while for slotted or slotted-offset ALOHA system transition occurs at slot boundaries.

APPENDIX A

PDF OF MF RECEIVER OUTPUT SNIR IN *L*-PATH FADING CHANNEL

In this appendix, the PDF of matched filter output SNIR is derived for L-path Rayleigh fading channel.

Consider a CDMA system that consists of K active users, all of which have the same number of multipath L. Assume that each path signal is independent and identically distributed with exponential distribution whose average per-path signal to background noise ratio, E_s/N_0, equals B/L, such that the total average E_s/N_0 is equal to B. That is, the PDF of the input signal to background noise ratio for the lth path of the kth user, $\beta_{k,l}$, can be expressed as

$$\beta_{k,l} \sim \frac{L}{B}\exp\left(-\frac{L\beta}{B}\right) \text{ for all } k, l. \tag{A.1}$$

To simplify the notation, let us combine the double index (k, l) into single index $i = 1,2,\ldots,KL$. Then, for the first path signal of the first user, which corresponds to $i = 1$, the SNIR at the output of a matched filter receiver, conditioned on β_i's $\forall i$, can be expressed as

$$\gamma_{MF} = \frac{\beta_1}{1+(1/3N)\sum_{i=2}^{KL}\beta_i} \tag{A.2}$$

Defining $\nu \equiv 1+\frac{1}{3N}\sum_{i=2}^{KL}\beta_i$, it is easy to show that the PDF of ν is given by

$$\nu \sim 3N \cdot \chi^2_{2(KL-1)}\left(3N(\nu-1), \frac{B}{2L}\right) \tag{A.3}$$

where the scaled chi-squared distribution function is defined as

$$\chi^2_M(y,\sigma_I^2) \equiv \left|\frac{1}{\sigma_I^2}\right| \cdot \frac{\left(y/\sigma_I^2\right)^{\frac{M-2}{2}} \cdot \exp\left(-y/2\sigma_I^2\right)}{2^{M/2} \cdot \Gamma[M/2]} \tag{A.4}$$

with the gamma function $\Gamma[a] = \int_0^\infty t^{a-1} e^{-t} dt$.

Using (A.2), (A.3) and (A.4), a closed form expression for the PDF of the SNIR at the matched filter (rake finger) output of the first path of the first user can be obtained as

$$f_{\gamma_{MF}}(\gamma) = \int_1^\infty v \cdot \frac{L}{B} \exp\left(-\frac{L}{B} v \cdot \gamma\right) \cdot \frac{3N}{\Omega} \cdot \chi^2_{2(KL-1)}\left(\frac{3N}{\Omega}(v-1), \frac{B}{2L}\right) \cdot dv \tag{A.5}$$

(2.7) is obtain by substituting (A.4) into (A.5) and performing integration.

APPENDIX B
DETAILS ON THE IMPROVED UNION BOUND

This appendix provides some detailed derivations of the improved union bound used in Chapter 2.

B.1 Derivation of (2.17.a) and (2.17.b)

Using Chernoff bound, one can obtain

$$\Pr\{D(\mathbf{y},\mathbf{x}_j) \geq t\} \leq e^{-ts} \cdot E[e^{sD(\mathbf{y},\mathbf{x}_j)}] = e^{-ts} \cdot \int_{\mathbf{y}} e^{sD(\mathbf{y},\mathbf{x}_j)} \cdot p(\mathbf{y} \mid \mathbf{x}_j) \cdot d\mathbf{y} \tag{B.1}$$

for any $s > 0$. Substituting (2.16) into (B.1) and noting that

$$p(\mathbf{y} \mid \mathbf{x}_j) = \prod_{n=0}^{N-1} p(y_n \mid x_{jn}),$$

(B.1) can be expressed as

$$\Pr\{D(\mathbf{y},\mathbf{x}_j) \geq t\} \leq e^{-ts} \cdot \prod_{n=0}^{N-1} \int_{y_n} [\psi(y_n)]^s [p(y_n \mid x_{jn})]^{1-s} \cdot dy_n \tag{B.2}$$

Since x_{jn} can have only two values (0 or 1), the integral $\int_{y_n} [\psi(y_n)]^s [p(y_n \mid x_{jn})]^{1-s} \cdot dy_n$ can also have only two values for any n. If the codeword $\mathbf{x}_j$ have weight d, then it has d ones and N-d zeros. Then, (B.2) becomes

$$\Pr\{D(\mathbf{y},\mathbf{x}_j) \geq t\} \leq e^{-ts} \cdot \left[\int_{-\infty}^{\infty} [\psi(y)]^s [p_1(y)]^{1-s} \cdot dy\right]^d \cdot \left[\int_{-\infty}^{\infty} [\psi(y)]^s [p_0(y)]^{1-s} \cdot dy\right]^{N-d} \tag{B.3}$$

For $\mathbf{x}_j = \mathbf{x}_0$ of which the Hamming weight d is zero, we have (2.17.a) with (2.18.a).

Similarly, using the Chernoff bound, for any $r < 0$ and $w < 0$

$$\Pr\{D(\mathbf{y},\mathbf{x}_j) - D(\mathbf{y},\mathbf{x}_0) < 0, D(\mathbf{y},\mathbf{x}_0) < t\} \le e^{-rt} \int_{\mathbf{y}} e^{rD(\mathbf{y},\mathbf{x}_0)} e^{w[D(\mathbf{y},\mathbf{x}_j)-D(\mathbf{y},\mathbf{x}_0)]} \cdot p(\mathbf{y} \mid \mathbf{x}_0) \cdot d\mathbf{y} \tag{B.4}$$

when using the fact that $E_0(\mathbf{x}_j^d) = \text{Event}\{D(\mathbf{y},\mathbf{x}_j) - D(\mathbf{y},\mathbf{x}_0) < 0\}$. Using the definition in (2.16) and assuming the Hamming weight of $\mathbf{x}_j$ is d, one can obtain (2.17.b) with (2.18.a) and (2.18.b).

B.2 Derivation of (2.22), (2.23) and (2.24)

For given s and r and noting that $g(\cdot)$ and $h(\cdot)$ depend on $\psi(y)$, the minimization of the right hand side of (2.19) is equivalent to maximization of (2.20) with respect to $\psi(y)$. Resorting to calculus of variation, $\psi(y)$ that maximize (2.20) should satisfy

$$-\frac{s}{s-r} \cdot \left(\delta \cdot h(r,w)^{-1} \cdot \frac{\partial h(r,w)}{\partial \psi} + (1-\delta) \cdot g(r)^{-1} \cdot \frac{\partial g(r)}{\partial \psi} \right) + \frac{r}{s-r} \cdot \left(g(s)^{-1} \cdot \frac{\partial g(s)}{\partial \psi} \right) = 0 \tag{B.5}$$

Or equivalently

$$\frac{rs}{s-r} \cdot \left(\delta \cdot h(r,w)^{-1} \cdot \psi^{r-1} p_0^{1-r+w} p_1^{-w} + (1-\delta) \cdot g(r)^{-1} \cdot \psi^{r-1} p_0^{1-r} \right) - \frac{rs}{s-r} \cdot \left(g(s)^{-1} \cdot \psi^{s-1} p_0^{1-s} \right) = 0 \tag{B.6}$$

which leads to the fact that the function $\psi(y)$ should be of the form of (2.22) with

$$k = \left((1-\delta)\cdot g(s)\cdot g(r)^{-1}\right)^{\frac{1}{s-r}} \tag{B.7.a}$$

$$\alpha = \frac{\delta}{1-\delta}\cdot\frac{g(r)}{h(r,w)} \tag{B.7.b}$$

Note that in (B.5) and (B.6), $h(r, w)$, $g(r)$ and $g(s)$ are in turn a function of $\psi(y)$. Therefore, to find $\psi(y)$ that maximize (2.20), the implicit equation (B.6) should be solved. However, instead of finding a closed form solution of (B.6), one can find the constant k and α that satisfy (B.7.a) and (B.7.b) by dynamic programming method. Nevertheless, as will be shown later, it is not needed to find k, as it will be cancelled out in (2.20). Thus, setting $k = 1$ and using (2.18.a) and (2.18.b) lead to

$$g(r)+\alpha\cdot h(r,w) = \int_{-\infty}^{\infty}\psi(y)^{r}\cdot p_0(y)^{1-r}\left[1+\alpha\cdot\left[\frac{p_1(y)}{p_0(y)}\right]^{-w}\right]dy \tag{B.8}$$

Substituting (2.22) into (B.8) and with $k = 1$, we have

$$\begin{aligned} g(r)+\alpha\cdot h(r,w) &= \int_{-\infty}^{\infty} p_0(y)^{s}\left(1+\alpha\left[\frac{p_1(y)}{p_0(y)}\right]^{-w}\right)^{\frac{s}{s-r}}\cdot p_0(y)^{1-s}dy \\ &= \int_{-\infty}^{\infty}\psi(y)^{s}\cdot p_0(y)^{1-s}dy \\ &= g(s) \end{aligned}$$

Equation (2.24) is obtained by substituting α·$h(r,w)$ in (2.23) into (B.7.b) to have $g(r)/g(s) = 1-\delta$. Thus, using (2.18.a), (2.18.b) and (2.22) with $k = 1$, it becomes (2.24).

APPENDIX C
GAUSSIAN APPROXIMATION

This appendix provides a detailed description of the Gaussian approximation used in Chapter 6, based on the random spreading assumption.

In Random CDMA, it is assumed that the spreading codes vary randomly from symbol to symbol and hence a cross-correlation between any two of random spreading code vectors is regarded as a random variable. As it will be shown here, it can be approximated by a Gaussian random variable with sufficiently large processing gain.

Let us define the random variable L as the number of chips having equal sign between any two of random spreading code vectors. Then, the pdf of L can be expressed as a binomial distribution function,

$$P_L(l) = \binom{N}{l} 2^{-N} \tag{C.1}$$

where $l \in \{0, 1, \ldots, N\}$. With $N \to \infty$, using DeMoivre-Laplace theorem [C11], the right hand side of (11) can be approximated by a Gaussian density function as follows.

$$P_L(l) \approx \frac{1}{\sqrt{2\pi(N/4)}} \exp\left(\frac{-[l-(N/2)]^2}{2 \cdot (N/4)} \right) = f_L(l) \tag{C.2}$$

Furthermore, the normalized cross-correlation ρ_{ij} between two of randomly generated spreading vector, c_i and c_j, can be expressed as $\rho_{ij} = c_i^T \cdot c_j = (2l-N)/N$. Using the approximation in (12), the PDF of ρ_{ij} can be approximated as follows

$$f_P(\rho) \approx \frac{N}{2} \cdot f_L\left(\frac{N(1+\rho)}{2}\right) = \frac{1}{\sqrt{2\pi/N}} \exp\left(-\rho^2 / [2/N]\right) = \mathcal{N}\left(0, \frac{1}{N}\right) \tag{C.3}$$

where, the index ij has been omitted for convenience and $\mathcal{N}(\alpha,\beta)$ indicates normal distribution function with mean α and variance β.

For asynchronous CDMA, let us consider a partial cross-correlation between $c_i(t)$ and $c_j(t)$ which are defined in $[0,T_b]$ and let τ_i and τ_j be their time delays. Setting $\tau_i = 0$, the partial cross-correlation between $c_i(t-\tau_i)$ and $c_j(t-\tau_i)$ can be expressed as

$$\rho_{ij}^0 = \int_{\tau_j}^{T_b} c_i(t) c_j(t-\tau_j) dt = \frac{T_c - \delta_j}{T_c} \cdot \mathbf{c}_i^T \cdot \mathbf{c}_j^{(D_j)} + \frac{\delta_j}{T_c} \cdot \mathbf{c}_i^T \cdot \mathbf{c}_j^{(D_j+1)} \tag{C.4}$$

where $\mathbf{c}_j^{(D)}$ is a code vector of $\mathbf{c}_j$ right-shifted by D and zero-padded. Since $\mathbf{c}_i^T \cdot \mathbf{c}_j^{(D)}$ is a sum of $(N\text{-}D)$ binary random variables normalized by the factor $1/N$, using the Gaussian approximation mentioned in (C.3), one can obtain

$$\mathbf{c}_i^T \cdot \mathbf{c}_j^{(D)} \sim \mathcal{N}\left(0, \frac{N-D}{N^2}\right) \tag{C.5}$$

Furthermore, due to the property of PN sequences, the cross-correlation, $\mathbf{c}_i^T \cdot \mathbf{c}_j^{(D)}$ and $\mathbf{c}_i^T \cdot \mathbf{c}_j^{(D+1)}$, can be regarded as independent variables. Therefore, given D_k and δ_k, the PDF of ρ^0_{ij} can be approximated by Gaussian random variable as follows.

$$\rho_{ij}^0(D_j, \delta_j) \sim \mathcal{N}\left(0, \sigma_{ij,0}^2(D_j, \delta_j)\right) \tag{C.6.a}$$

with $\sigma^2_{ij,0}(D_j,\delta_j)=[(D_j+1)\cdot(1-\delta_j)^2+D_j\cdot\delta_j^2]/N^2$ (C.6.b)

The same argument holds for $\rho^{-1}{}_{ij}$ as well.

$$\rho^{-1}_{ij}(D_j,\delta_j)\sim\mathcal{N}\left(0,\sigma^2_{ij,-1}(D_j,\delta_j)\right) \quad \text{(C.7.a)}$$

with $\sigma^2_{ij,-1}(D_j,\delta_j)=[(N-D_j-1)\cdot(1-\delta_j)^2+(N-D_j)\cdot\delta_j^2]/N^2$ (C.7.b)

For further simplification, $E[\sigma^2_{ij,0}(D_j,\ \delta_j)]$ can be used in (C.6.a), instead of $\sigma^2_{ij,0}(D_j,\ \delta_j)$. As will be shown in Chapter 3, this simplification leads quite accurate results while makes things much easier. When using $E[\sigma^2_{ij,0}(D_j,\ \delta_j)]$ in (6.18), the conditioning on D_j and δ_j can be dropped since $E[\sigma^2_{ij,0}(D_j,\ \delta_j)]$ is just constant values. Moreover, since $E[\sigma^2_{ij,0}(D_j,\ \delta_j)]$ = $E[\sigma^2_{ij,-1}(D_j,\ \delta_j)]$, the random variables $\rho^0{}_{ij}$ and $\rho^{-1}{}_{ij}$ are not only independent but also identically distributed. Then, $\rho^0{}_{ij}$ and $\rho^{-1}{}_{ij}$ are approximated to i.i.d. random variables with the same Gaussian distribution

REFERENCES

1. A. J. Viterbi, *CDMA: Principles of Spread Spectrum Communication*, Addison-Wesley, June 1995.

2. Telecom. Industry Association (TIA), *CDMA 2000 ITU-R RTT Candidate Submission*, 1998.

3. European Telecommunications Standards Institute (ETSI), *ETSI UMTS Terrestrial Radio Access (UTRA) ITU-R RTT Candidate Submission*, 1998.

4. *Association of Radio Industries and Businesses* (ARIB), *Japan's Proposal for Candidate Radio Transmission Technology on IMT-2000: W-CDMA*, 1998.

5. TTA, *Global CDMA I: Multi-band Direct Sequence CDMA System RTT System Description*, 1998.

6. TTA, *Global CDMA II for IMT-2000 RTT System Description*, 1998.

7. H. Holma and A. Toskala, *WCDMA for UMTS: Radio Access for Third Generation Mobile Communications*, John Wiley and Sons, 2001.

8. R. L. Pickholtz, D. L. Schilling and L. B. Milstein, "Theory of Spread-Spectrum Communications – A Tutorial", *IEEE Trans. On Comm.* Vol. COM-30, No.5, pp. 855-884, May 1982.

9. T. S. Rapparport, *Wireless Communications: Principles and Practice*, Prentice Hall, 1996.

10. R. Khan, "Advances in Packet Radio Technology", *Proc. IEEE*, Vol. 66, Nov. 1978.

11. K. Joseph and D. Raychaudhuri, "Throughput of Unslotted Direct-Sequence Spread-Spectrum Multiple-Access Channels with Block FEC Coding", *IEEE Trans. On Communications*, Vol. 41, No.9, pp. 1373-1378, Sep. 1993.

12. P. W. de Graaf and J. S. Lehnert, "Performance Comparison of a Slotted ALOHA DS/SSMA Network and a Multi-channel Narrow-Band Slotted ALOHA Network", *IEEE Trans. On Comm.* Vol. 46, No.4, pp. 544-552, Apr. 1998.

13. C. Berrou, A. Glavieux, and P. Thitimajshima, "Near Shannon-limit Error-Correction Coding and Decoding: Turbo-Codes", *Proc. Int. Communication Conf.* pp. 1064-1070. May 1993, Geneva, Switzerland.

14. C. Berrou and A. Glavieux, "Near Optimum Error Correcting Coding and Decoding: Turbo-Codes", *IEEE Trans. on Communication*, Vol. COM-44, No.10 pp. 1261-1271, Oct. 1996.

15. D. J. Costello Jr., J. Hagenauer, H. Imai and S. B. Wicker, "Application of Error Control coding", *IEEE Trans. on Information Theory*, vol. IT-44, pp. 2531-2560, Oct. 1998.

16. S. B. Wicker, *Error Control Systems for Digital Communication and Storage*, Prentice Hall, 1995.

17. S. S. Lim, Q. Cao, C. Demetrescu, D. J. Reader and J. Lin, "3rd Generation RACH Transmission – A Candidate", *Proc. Of VTC'99 Spring*, pp. 140-144.

18. G. Frank and R. Weber, "Random Access Scheme for the ETSI/UTRA WCDMA", *Proc. Of VTC'99 Spring*, pp. 1360-1364.

19. Vembu and A. J. Viterbi, "Two Different Philosophies in CDMA - Comparison", *Proc. IEEE Vehicular Technology Conf.*, April 28 - May 1. 1996, Atlanta, GA. pp. 869-873.

20. S. Verdu, *Multiuser Detection*, Cambridge University Press.

21. S. Verdu, "Minimum Probability of Error for Asynchronous Gaussian Multiple-Access Channels", *IEEE Trans. on Information Theory*, vol. IT-32, pp. 85-96, Jan. 1986.

22. R. Lupas and S. Verdu, "Linear Multiuser Detectors for Synchronous Code-Division Multiple-Access Channels", *IEEE Trans. on Information Theory*, vol. IT-35, pp. 123-136, Jan. 1989.

23. R. Lupas and S. Verdu, "Near-Far Resistance of Multiuser Detectors in Asynchronous Channels", *IEEE Trans. on Communication*, vol. COM-38, pp. 496-508, Apr. 1990.

24. A. Duel-Hellen, "Decorrelating Decision-Feedback Multiuser Detector for Synchronous Code-Division Multiple-Access Channel", *IEEE Trans. on Communication*, vol. COM-41 pp. 285-290, Feb. 1993.

25. U. Madhow and M. L. Honig, "MMSE Interference Suppression for Direct-Sequence Spread-Spectrum CDMA", *IEEE Trans. on Communication*, vol. COM-42, No. 12 pp. 3178-3188, Dec. 1994.

26. H. V. Poor and S. Verdu, "Probability of Error in MMSE Multiuser Detection", *IEEE Trans. on Info. Theory*, vol. 43 pp. 858-871, May. 1997.

27. M. Varanasi and B. Aazhang, "Multistage Detection in Asynchronous Code-Division Multiple-Access Communications", *IEEE Trans. on Communication*, vol. COM-38 No. 4, pp. 509-519, April. 1990.

28. M. Varanasi and B. Aazhang, "Near-Optimum Detection in Synchronous Code-Division Multiple-Access Systems", *IEEE Trans. on Communication*, vol. COM-39 No. 5, pp. 725-736, May. 1991.

29. A. J. Viterbi, "Very Low Rate Convolutional Code for Maximum Theoretical performance of Spread-Spectrum Multiple-Access Channels", *IEEE Journal on Selected Areas in Communications,* Vol. 8 No.4 pp. 641-649, May. 1990.

30. P. Patel and J. Holtzman, "Analysis of a Simple Successive Interference Cancellation Scheme in a DS/CDMA System", *IEEE Journal on Selected Areas in Communications*, vol. 12 No. 5, pp. 796-807, June. 1994.

31. S. Yoon and Y. Bar-Ness, "Performance Analysis of Random CDMA Linear Multiuser Detectors Using Gaussian Approximation", submitted to *IEEE Journal of Selected Areas in Communications*.

32. S. Yoon and Y. Bar-Ness, "An Approximate performance of Linear Decorrelating Detector for Dynamic CDMA", *Proc. ISSSTA'*2000 Sep 5-8. 2000, NJ.

33. M. B. Pursley and D. J. Taipale, "Error probabilities for Spread-Spectrum Packet Radio with Convolutional Codes and Viterbi Decoding", *IEEE Trans. On Comm.* Vol. 35, No.1, pp. 1-12, Jan. 1987.

34. J. S. Lehnert and M. B. Pursley, "Error Probability for Binary Direct-Sequence Spread-Spectrum Communications with Random Signature Sequences", *IEEE Trans. on Communication*, vol. COM-35 No.1 pp. 87-98, Jan. 1987.

35. R. K. Morrow, Jr. and J. S. Lehnert, "Packet Throughput in Slotted DS/SSMA Radio Systems with Random Signature Sequences", *IEEE Trans. On Comm.* Vol. 40, No.7, pp. 1223-1230, Jul. 1992.

36. S. Verdu and S. Shamai, "Spectral Efficiency of CDMA with Random Spreading", *IEEE Trans. on Info. Theory*, vol. 45 No.2 pp. 622-640, March. 1999.

37. D. N. C. Tse and S. V. Hanly, "Linear Multiuser Receivers: Effective Interference, Effective Bandwidth and User Capacity", *IEEE Trans. on Info. Theory*, Vol. 45 No.2 pp. 641-657, Mar. 1999.

38. D. N. C. Tse and O. Zeitouni, "Linear Multiuser Receivers in Random Environments", *IEEE Trans. on Information Theory*, Vol. 46 No.1 pp. 171-188, Jan. 2000.

39. Kiran and D. N. C. Tse, "Effective Interference and Effective Bandwidth of Linear Multiuser Receivers in Asynchronous CDMA Systems", *IEEE Trans. Information Theory*, Vol. 46, No.4, pp. 1426-1447, July 2000.

40. J. Zhang, E. K. P. Chong and D.N.C. Tse, "Output MAI Distributions of Linear MMSE Multiuser Receivers in DS-CDMA Systems", *IEEE Trans. Information Theory*, Vol. 47, No.3, pp. 1128-1144, March 2001.

41. T. M. Cover, *Elements in Information Theory*. John Wiley & Sons, Inc. 1991.

42. A. J. Viterbi, "Convolutional Codes and Their Performance in Communication Systems", *IEEE Trans. Comm.* Vol. COM-19, No.5, pp. 751-772, Oct. 1971.

43. T. M. Duman and M. Salehi, "New Performance Bounds for Turbo Codes", *IEEE Trans. on Communications*, Vol. 46 pp. 717-723, June 1998.

44. A. M. Viterbi and A .J. Viterbi, "Improved Union Bound on Linear Codes for Input-Binary AWGN Channel with Application to Turbo Codes", Proc. ISIT'1998 pp. 29, Cambridge, MA, Aug.16-21, 1998.

45. D. Divsalar and E. Biglieri, "Upper Bounds to Error Probabilities of Coded Systems over AWGN and Fading Channel", *Proc. of GlobeCom*'2000, Vol. 3, pp. 1605 –1610, San Francisco, CA.

46. I. Sason and S. Shamai, "On Improved Bounds on the Decoding Error Probability of Block Codes over Interleaved Fading Channel, with Application to Turbo-Like Codes", *IEEE Trans. on Info. Theory*, Vol. 47 pp. 2275-2299, Sep. 2001.

47. D. Divsalar, "A Simple Tight Bound on Error Probability of Block Codes with Application to Turbo Codes", *TMO Progress Report* 42-139, pp. 1-35, Nov. 1999.

48. R. G. Gallager, *Low Density Parity-Check Codes*, MIT Press, Cambridge, MA, 1963.

49. R. G. Gallager, "A Simple Derivation of Coding Theorem and Some Applications", *IEEE Trans. on Information Theory*, Vol. IT-11 pp. 3-18, Jan. 1965.

50. S. Benedetto and G. Montorsi, "Unveiling turbo codes: Some results on parallel concatenated coding scheme", *IEEE Trans. on Information Theory*, Vol. 42 pp. 409-428, March. 1996.

51. S. Benedetto and G. Montorsi, "Design of Parallel Concatenated Convolutional Codes", *IEEE Trans. on Info. Theory*, Vol. 44 No.5 pp. 591-600, May. 1998.

52. A. J. Viterbi, "Shannon Theory and Turbo Decoding", Shannon Day Presentation Material, May.18, 1998.

53. D. N. Rowitch, *Convolutional and Turbo Coded Multicarrier Direct Sequence CDMA, and Applications of Turbo Codes to Hybrid ARQ Communications Systems*, Ph.D. Dissertation, Univ. of California at San Diego, 1998.

54. D. Raychaudhuri, "Performance Analysis of Random Access Packet-Switched Code Division Multiple Access Systems", *IEEE Trans. On Comm.* Vol. 29, pp. 895-900, Jun. 1981.

55. K. Joseph and D. Raychaudhuri, "Stability Analysis of Asynchronous Random Access CDMA Systems", *Proc. GlobeComm'86*, pp. 48.1-48.1.7, Dec. 1986.

56. Abdelmonem and T. N. Saadawi, "Performance Analysis of Spread Spectrum Packet Radio Network with Channel Load Sensing", *IEEE Journal on Selected Areas in Communications*, Vol. 7, No.1, pp. 161-166, Jan. 1989.

57. M. Yin and V. O. K. Li, "Unslotted CDMA with Fixed Packet Lengths", *IEEE Journal on Selected Areas in Communications*, Vol. 8, No.4, pp. 529-541, May, 1990.

58. T. Sato, H. Okada, T. Yamazato, M. Katayama and A. Ogawa, "Throughput Analysis of DS/SSMA Unslotted ALOHA System with Fixed Packet Length", *IEEE Journal on Selected Areas in Communications*, Vol4, No.4, pp. 750-756, May, 1990.

59. D. J. Goodman, "Cellular Packet Communications", *IEEE Trans. On Comm.* Vol. 38, No.6, pp. 1272-1280, Aug. 1990.

60. A. Annamalai and V. K. Bhargava, "Throughput Performance of Slotted DS/CDMA ALOHA with Packet Combining over Generalized Fading Channels", *Electronics Letters*, Vol. 33, pp. 1195-1197, Sep. 1997.

61. A. M. Y. Bigloo, T. A. Gulliver and V. K. Bhargava, "Maximum-Likelihood Decoding and Code Combining for DS/SSMA Slotted ALOHA", *IEEE Trans. On Comm.* Vol. 45, pp. 1602-1612, Dec. 1997.

62. Y. Sun, "Network Diversity of Random Access Slotted CDMA Network", *Proc. Asilomar Conference '99*, pp. 1606-1610, Nov. 1999.

63. D. Bertsekas and R. Gallager, *Data Networks 2nd ed.*, Prentice Hall, 1992.

64. A. S. Barbulescu and S. S. Pietrobon, "Rate Compatible Turbo Codes", *Electronics Letters*, Vol. 31, pp. 535-534, Mar. 1995.

65. P. Jung and J. Plechinger, "Performance of Rate Compatible Punctured Turbo-Codes for Mobile Radio Applications", *Electronics Letters*, Vol. 33, pp. 2102-2103, Dec. 1997.

66. D. N. Rowitch and L. B. Milstein, "Rate Compatible Punctured Turbo (RCPT) codes in a Hybrid FEC/ARQ system", *Proc. Communications Theory Mini-Conf. Of GlobeCom*'97, pp. 55-59. Phoenix, AZ, Nov. 1997.

67. J. Hamorsky, U. Wachsmann, J. B. Huber and A. Cizmar, "Hybrid Automatic Repeat Request Scheme with Turbo Codes", *Proc. Of 1997 Int. Symposium on Turbo Codes*, pp. 247-250, Sep. 1997.

68. P. Jung, J.Plechinger, M. Doetsch, and F. M. Berens, "A Pragmatic Approach to Rate Compatible Puncture Turbo Codes for Mobile Radio Applications", Int. Conf. on Advances in Comm. and Control, Jun. 1997, Corfu, Greece.

69. J. Li and H. Imai, "Performance of Hybrid-ARQ Protocols with Rate Compatible Turbo Codes", *Proc. Of 1997 Int. Symposium on Turbo Codes*, pp. 188-191, Sep. 1997.

70. D. N. Rowitch and L. B. Milstein, "On the Performance of Hybrid FEC/ARQ Systems Using Rate Compatible Punctured Turbo (RCPT) Codes", *IEEE Trans. On Comm.* Vol. 48, No.6 pp. 948-959, June. 2000.

71. R. Mantha and F. R. Kschischang, "A Capacity-Approaching Hybrid ARQ Scheme Using Turbo Codes", *Proc. GlobeCom*'99, pp. 2341-2345.

72. J. Hagenauer, "Rate-Compatible Punctured Convolutional Codes (RCPC Codes) and Their Applications", *IEEE Trans. On Comm.* Vol. 36, pp. 389-400, Dec. 1988.

73. L. R. Lugand, D. J. Costello and R. H. Deng, "Parity Retransmission Hybrid ARQ Using Rate 1/2 Convolutional Codes on a Nonstationary Channel", *IEEE Trans. on Communication*, vol. COM-37 No.7 pp. 755-765, July. 1989.

74. S. Kallel and D. Haccoun, "Generalized Type II Hybrid ARQ Scheme Using Punctured Convolutional Coding", *IEEE Trans. on Communication*, vol. COM-38 No.11 pp. 1938-1946, Nov. 1990.

75. J. Hagenauer, E. Offer and L. Papke, "Iterative Decoding of Binary Block and Convolutional Codes", *IEEE Trans. on Information Theory*, vol. IT-42, No.2 pp. 429-445, March. 1996.

76. L. Bahl, J. Cocke, F. Jelinek and J. Raviv, "Optimal decoding of linear codes for minimizing symbol error rate", *IEEE Trans. on Information Theory*, pp. 284-287, March. 1974.

77. P. Robertson, E. Villebrun and P. Hoeher, "A Comprison of Optimal and Sub-optimal Decoding Algorithms Operating in the Log Domain", *Proc. of Int. Conf. on Communications*'95, pp. 1009-1013, June 1995, Seattle, WA.

78. A. J. Viterbi, "An Intuitive Justification and a Simplified Implementation of the MAP Decoder for Convolutional Codes", *IEEE Journal on Selected Areas in Communications*, Vol. 16, No.2 pp. 260-264. Feb. 1998.

79. S. A. Barbulescu, *Iterative Decoding of Turbo Codes and Other Concatenated Codes*, Ph.D. dissertation, University of South Austrailia, pp. 23-24, Feb. 1996.

80. J. Hsu and C. Wang, "A Parallel Decoding Scheme for Turbo Codes", ISCAS'98 4:445-448, June 1998.

81. Y. Lin, S. Lin and M. Fossorier, "MAP Algorithm for Decoding Linear Block Codes Based On Sectionalized Trellis Diagrams", *GlobeCom'98*, Sydney, Australia, Nov. 1998.

82. R. J. McEliece, D. J. C. MacKay and J-F. Cheng, "Turbo Decoding as an Instance of Pearl's Belief Propagation Algorithm", *IEEE Journal on Selected Areas in Communications*, Vol. 16, No.2 pp. 140-152. Feb. 1998.

83. B. J. Frey and F. R. Kschischang, "Probability Propagation and Iterative Decoding", *Proc. Allerton Conference on Communication, Control and Computing* 1996, Urbana-Champaign, IL.

84. B. J. Frey and D. J. C. Mackay, "A Revolution: Belief Propagation in Graphs with Cycles", *Neural Information processing Systems Conference*, Denver Colorado, Dec. 1997.

85. F. R. Kschischang and B. Frey, "Iterative Decoding of Compound Codes by Probability Propagation in Graphical Models", *IEEE Journal on Selected Areas in Communications*, Vol. 16, No.1 pp. 1-11. Jan. 1998.

86. B. Frey, *Graphical Model for Machine Learning and Digital Communication*, MIT Press, Cambridge, MA, 1998.

87. J. Hagenauer and P. Hoeher, "A Viterbi algorithm with soft-decision outputs and its applications," Proc. of GLOBECOM '89, pp. 47.1.1-47.1.7. Dallas, TX.

88. U. Madhow and M. L. Honig, "On the Average Near-far Resistance for MMSE detection of direct sequence CDMA signals with random spreading", *IEEE Trans. on Info. Theory*, Vol. 45 No.6 pp. 2039-2045, Sep. 1999.

89. F. Zheng and S. K. Barton, "Near-Far Resistant Detection of CDMA Signals via Isolation Bit Insertion", *IEEE Trans. on Communication*, vol. COM-43 No. 2/3/4, pp. 1313-1317, Feb/March/April. 1995.

90. S. Yoon and Y. Bar-Ness, "Analysis of CDMA Slotted ALOHA with Packet Combining Using Queuing Network Models", submitted to IEEE Comm. Letters.

91. S. Yoon and Y. Bar-Ness, "Throughput Analysis of Turbo-Coded CDMA Communication Systems", *VTC* 02s, pp. 1462-1466, Birmingham, AL. 2002.

92. S. Yoon and Y. Bar-Ness, "Packet Data Communications over Coded CDMA Part I: Achievable Spectral Efficiency of CDMA Systems with Turbo Codes and Multiuser Detections", to be submitted to *IEEE Trans. on Wireless Comm.*

93. S. Yoon and Y. Bar-Ness, "Packet Data Communications over Coded CDMA Part II: Throughput Bound of CDMA Unslotted ALOHA with Hybrid Type-II ARQ using Rate Compatible Punctured Turbo Codes", to be submitted to *IEEE Trans. on Wireless Comm.*